

Ingemar Bengtsson

## SPHERICAL SYMMETRY AND BLACK HOLES

2012

These are notes for some lectures on spherically symmetric spacetimes—a nice subject since it is possible to go into great detail about the phenomena of gravitational collapse and black holes, at the expense of not saying anything connected to gravitational radiation.

The contents:

- Our spacetimes—the general spherically symmetric line element
- The Vaidya solution—a first encounter with collapse and censorship
- Equilibrium states—static spacetimes and Killing horizons
- Optical and hyperbolic geometry—some geometrical ideas
- What is the matter—stress-energy tensors and cold stars
- The Tolman-Bondi solution—a second encounter with collapse
- The Gödel spacetime—added by special request

The lectures stopped when the term did, meaning that the discussion of the Tolman-Bondi solution stops abruptly somewhere halfway through.

## OUR SPACETIMES

### *The Ansatz*

A spacetime is spherically symmetric if it admits an  $SO(3)$  group of isometries. In particular every point will lie on some round sphere, on which the rotation group acts transitively, which means that one can go from any point on the sphere to any other point by means of a rotation. The spheres can degenerate to single points, being fixed points around which the rotations take place. Any point in flat space is the fixed point for some rotation group, but in the more typical cases the rotation group is unique and there is at most one fixed point. There may be none: a cylinder is invariant under rotations, but the circles along which the rotation takes place do not have a centre anywhere on the cylinder.

A round sphere of radius  $r$  has the metric

$$d\gamma^2 = r^2 d\Omega^2 = r^2 (d\theta^2 + \sin^2 \theta d\phi^2) . \quad (1)$$

We use a coordinate system that fails at two antipodal points on the sphere, but this is of no consequence since all points on the sphere are equivalent. There are three linearly independent Killing vectors on the sphere. In these coordinates they are

$$L_1 = -\sin \phi \partial_\theta - \cot \theta \cos \phi \partial_\phi , \quad L_2 = \cos \phi \partial_\theta - \cot \theta \sin \phi \partial_\phi , \quad L_3 = \partial_\phi . \quad (2)$$

We have already fallen into the habit of regarding vector fields as differential operators in some coordinate basis. It is readily checked that  $[L_1, L_2] = -L_3$  and cyclically, that is these vector fields close to the Lie algebra of  $SO(3)$ .

In addition to the angular coordinates there will be two coordinates telling us which sphere we are on. Since rotations do not take us out of a given sphere the spacetime Killing vectors are given by the previous expressions. We now require that the spacetime metric be left invariant by rotation in the sense that, for any linear combination  $\vec{\xi}$  of the Killing vectors,

$$\mathcal{L}_{\vec{\xi}} g_{ab} = \xi^c \partial_c g_{ab} + \partial_a \xi^c g_{cb} + \partial_b \xi^c g_{ac} = 0 . \quad (3)$$

Working through this requirement one sees that the metric splits in two blocks,

$$ds^2 = g_{AB}dx^A dx^B + r^2 d\Omega , \quad (4)$$

where  $g_{AB}$  is some 1+1 dimensional metric whose components are independent of the angles. Since the function  $r$  may depend on  $x^0$  and  $x^1$  this is sometimes referred to as a warped product metric. We refer to  $r$  as the area radius of the round spheres, since their areas will be equal to  $4\pi r^2$  — regardless of whether  $r$  is the proper distance to the centre or not, and indeed regardless of whether the spheres do have a centre or not.

The area radius  $r$  has an invariant meaning, and so has

$$||\nabla r||^2 = g^{ab}\nabla_a r \nabla_b r . \quad (5)$$

This can be used to define the Misner-Sharp mass function  $m$  through

$$m = \frac{r}{2} \left( 1 - g^{ab}\nabla_a r \nabla_b r \right) \quad \Leftrightarrow \quad g^{ab}\nabla_a r \nabla_b r = 1 - \frac{2m}{r} . \quad (6)$$

The function  $m$  is constant on each round sphere, and is supposed to represent the active gravitational mass inside it. It is in fact a special case of something known as Hawking's quasi-local mass. In relativity theory it is very hard to come up with a definition of the amount of energy contained within a closed surface, because energy can be transported across the surface by gravitational waves in a way that defies local description. This difficulty can be ignored for round spheres in a spherically symmetric spacetimes, which is why the Misner-Sharp mass makes perfect sense within this context.

The question now arises whether the gradient of  $r$  is non-zero. An everywhere constant  $r$  is certainly possible, and there are interesting spacetimes—such as the Nariai solution of Einstein's equations including a cosmological constant—for which this happens, but for the moment we simply assume that  $\nabla_a r \neq 0$ . It is then possible to use  $r$  as a local coordinate on the 1+1 dimensional part, and we do so from now until further notice. This means then that

$$g^{rr} = 1 - \frac{2m}{r} . \quad (7)$$

Eq. (6), on the other hand, holds in every coordinate system.

The metric on any two dimensional space can always be written on diagonal form, and then it is

$$ds^2 = -e^{2\beta} \left(1 - \frac{2m}{r}\right) dt^2 + \frac{dr^2}{1 - \frac{2m}{r}} + r^2 d\Omega^2 . \quad (8)$$

Here  $\beta = \beta(t, r)$  and  $m = m(t, r)$  are two arbitrary functions, and  $d\Omega^2$  is the metric on a unit sphere. Any spherically symmetric metric can be brought to this form, provided only that the gradient of the area radius of the round spheres is non-vanishing. The function  $\beta$  can be changed by reparametrizations of  $t$ , and unlike  $m$  it does not have an invariant meaning. Hypersurfaces of constant  $t$  do have a meaning, as we will see.

### *Some special cases*

It can now be checked (very simply if one uses a computer algebra system) that the Ricci tensor vanishes if and only if

$$m = M = \text{constant} \quad \text{and} \quad \beta = \beta(t) . \quad (9)$$

We can set  $\beta = 0$  by means of a reparametrization of the coordinate  $t$ , and we have arrived at the Schwarzschild solution, which admits the extra Killing vector  $\xi = \partial_t$ . Incidentally we have also proved Birkhoff's theorem:<sup>1</sup> Every spherically symmetric solution of Einstein's vacuum equations admits an extra symmetry, and is in fact static for values of  $r$  large enough to ensure that  $\xi$  is timelike. And the solution is unique, given  $M$  which has an interpretation as the total energy of the configuration. On the one hand this is surprising. It means that spherically symmetric oscillations of a round star leave absolutely no gravitational imprint outside the star. On the other hand this is expected, since a similar statement is true in Newtonian gravity due to the special properties of the inverse square force. Einstein's theory shares the absence of monopole radiation with Maxwell's, but other gravity theories may behave differently in this respect.

Adding a cosmological constant or an electromagnetic field is not enough to change the conclusion. All that happens is that the mass function becomes

---

<sup>1</sup>J. T. Jebsen, *Über die allgemeinem kugelsymmetrischen Lösungen der Einsteinschen Gravitationsgleichungen im Vakuum*, Ark. Mat. Astr. Fys. **15** N:o 18 (1921).

$$m(r) = M - \frac{e^2}{2r} + \frac{\lambda r^3}{6} . \quad (10)$$

This is interestingly different from the Schwarzschild case, but the solution remains static when  $r > 2m$ .

These spacetimes have metrics of the form

$$ds^2 = -V(r)dt^2 + \frac{dr^2}{V(r)} + r^2 (d\theta^2 + \sin^2 \phi) . \quad (11)$$

Interestingly, whatever the function  $V(r)$  may be, the area radius now has an alternative interpretation. A radial null geodesics obeys the equation

$$V(r)\dot{t}^2 = \frac{\dot{r}^2}{V(r)} , \quad (12)$$

where the dot denotes differentiation with respect to an affine parameter along the geodesic. Because the solution is static there is a conserved energy

$$E = \xi_a \dot{x}^a = -V(r)\dot{t} , \quad (13)$$

where  $\xi = \partial_t$  is the static Killing vector. Combining these equations we see that

$$\dot{r} = \pm V(r)\dot{t} = \mp E = \text{constant} . \quad (14)$$

In this special case the area radius equals the affine parameter up to a constant, which means that the area radius itself is also an affine parameter along the congruence of radial null geodesics.<sup>2</sup>

#### *Flamm's surface and Marolf's surface*

To ensure that we have understood the Schwarzschild solution correctly we recall its Penrose diagram. It captures the causal structure of the complete Schwarzschild solution, but badly distorts its geometry.

To rectify this it is good to keep Flamm's paraboloid in mind. This is a two dimensional slice through the Schwarzschild spacetime obtained by

---

<sup>2</sup>T. Jacobson, *When is  $g_{tt}g_{rr} = -1$ ?*, Class. Quant. Grav. **24** (2007) 5717.

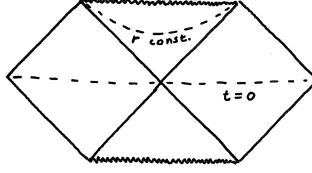


Figure 1: The Penrose diagram of the completed Schwarzschild manifold. Each point is a round sphere and radial light rays slope 45 degrees. Two interesting hypersurfaces are marked.

choosing  $t = 0$  and  $\theta = \pi/2$ , so that we look at an equatorial plane with the intrinsic metric

$$ds^2 = \frac{dr^2}{V(r)} + r^2 d\phi^2, \quad V(r) = 1 - \frac{2M}{r}. \quad (15)$$

This geometry can be embedded as a surface of revolution in flat space, and one obtains Flamm's paraboloid.<sup>3</sup> Note also that a surface defined by  $r = \text{constant} < 2M$  and  $\theta = \pi/2$  is an infinite cylinder of constant cross section. The symmetry under translations in  $t$  is now a symmetry of space. The radius of the cylinders decrease as time evolves, and the solution is not static in this region.

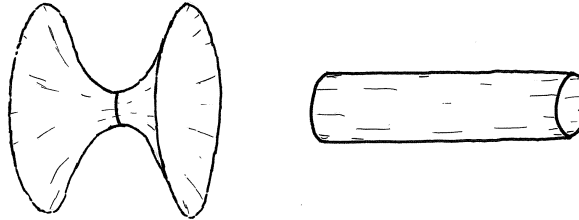


Figure 2: Flamm's paraboloid (at  $t = 0$ ) with the event horizon marked, and an infinite cylinder at  $r = \text{constant} < 2M$ .

We can also choose one point from each sphere, say at the North Pole ( $\theta = 0$ ), and consider the  $1 + 1$  dimensional metric

---

<sup>3</sup>L. Flamm, *Beiträge zur Einsteinschen Gravitationstheorie*, Physik. Z. **17** (1916) 448.

$$ds^2 = -V(r)dt^2 + \frac{dr^2}{V(r)} , \quad V(r) = 1 - \frac{2M}{r} . \quad (16)$$

To visualize this curved geometry we can try to embed it into a flat 2+1 dimensional Minkowski space. Although this idea is an old one, it seems that the resulting picture appeared in the literature only quite recently.

We will describe Minkowski space with its inertial coordinates  $(T, X, Y)$ . The intrinsic coordinates on our surface will be  $t$  and  $r$ , and we must ensure that it is invariant under translations in  $t$ . In the region where  $X^2 > T^2$  we therefore define an embedded surface by the parametric equations

$$T = \rho(r) \sinh \frac{t}{aM} , \quad X = \rho(r) \cosh \frac{t}{aM} , \quad Y = Y(r) . \quad (17)$$

The constant  $a$  and the functions  $\rho$  and  $Y$  are to be determined. The intrinsic metric becomes

$$ds^2 = -dT^2 + dX^2 + dY^2 = -\frac{\rho^2}{a^2 M^2} dt^2 + (\rho'^2 + Y'^2) dr^2 . \quad (18)$$

We make the choice

$$\rho = aM\sqrt{V(r)} \quad \Rightarrow \quad ds^2 = -V(r)dt^2 + \left( \frac{a^2 M^4}{r^4 V(r)} + Y'^2 \right) dr^2 . \quad (19)$$

Next we choose

$$Y'^2 = \frac{1}{1 - \frac{2M}{r}} \left( 1 - \frac{a^2 M^4}{r^4} \right) \quad \Rightarrow \quad ds^2 = -V(r)dt^2 + \frac{dr^2}{V(r)} . \quad (20)$$

The metric on the surface now takes the desired form. It remains to choose the constant  $a$  so that the surface is smooth, and to check that it can be joined smoothly to the surface one constructs, using a very similar calculation, in the region  $T^2 > X^2$ . After having considered the formula we set

$$a = 4 \quad \Rightarrow \quad Y(r) = \int_{2M}^r \sqrt{1 + \frac{2M}{r} + \frac{4M^2}{r^2} + \frac{8M^4}{r^4}} dr . \quad (21)$$



Figure 3: Marolf's surface in Minkowski space. On the right the event horizon appears as two intersecting straight lines.

A computer will now draw the surface for us. This is a metrically correct picture of the geometry that is conformally distorted by the Penrose diagram.<sup>4</sup>

Inspection reveals an everywhere regular surface. The singularity at  $r = 0$  seems to have disappeared. It is still there though. To see what happens we look at the curve that forms the intersection of the surface with the plane  $X = 0$ . It turns out that this is a curve whose acceleration grows with proper time, in such a way that it reaches infinite values of  $Y$  and  $T$  in a finite amount of proper time. In other words, the singularity is there, but it sits at conformal infinity.

Marolf's surface probably does not teach us much about the Schwarzschild solution, but it does tell us something about Minkowski space: it contains timelike curves that go to infinity in a finite parameter time. A simpler example of this behaviour can be found by looking at the timelike curves

$$X^n - T^n = k^2, \quad n > 1. \quad (22)$$

If  $n = 2$  this is a hyperbola along which the acceleration measured in the particle's rest frame is constant. In general we can parametrize the curve by setting

$$X = \sigma, \quad T = (\sigma^n - k^2)^{\frac{1}{n}}. \quad (23)$$

The parameter is some function  $\sigma(\tau)$  of the proper time  $\tau$ . We have

$$d\tau = \sqrt{T'^2 - X'^2} d\sigma, \quad (24)$$

---

<sup>4</sup>D. Marolf, *Spacetime embedding diagrams for black holes*, Gen. Rel. Grav. **31** 919, 1999.



where a dot and a prime means means differentiation with respect to  $\tau$  and  $\sigma$ , respectively. The amount of proper time it takes to go to an infinite value of  $X$  is then

$$\Delta\tau = \int_{\sigma_0}^{\infty} \sqrt{\sigma^{2n-2}(\sigma^n - k^2)^{\frac{2-2n}{n}} - 1} d\sigma = \int_{\sigma_0}^{\infty} \sqrt{(1 - k^2\sigma^{-n})^{\frac{2-2n}{2}} - 1} d\sigma . \quad (25)$$

By means of a Taylor expansion we see that this integral converges to a finite value if and only if  $n > 2$ . It would be unpleasant to follow such a curve though because its proper acceleration diverges as it approaches infinity. In fact, it would be as unpleasant as free fall into the Schwarzschild singularity. (Besides which, the acceleration integrated along the curve would be infinite, so no actual rocket can do this.<sup>5</sup>)

This behaviour is typical of Lorentzian spacetimes: there are curves that reach the edge of the manifold at finite values of their affine parameters. But Minkowski space does not contain any geodesics with this property, and is therefore said to be a geodesically complete manifold. This is not true of the Schwarzschild solution since geodesics will disappear into the singularity, and therefore observers in free fall can vanish in finite time. We minimize this problem when we include all four regions of the Penrose diagram, but we cannot completely cure it.

### *Null and double null coordinates*

The coordinate system that we devised has the difficulty that it fails whenever the gradient of  $r$  is lightlike (at  $r = 2m$ ). There are many ways to remedy this. The problem lies in coordinatizing the  $1 + 1$  dimensional quotient space. Now it is well known that any two dimensional space is conformally flat. In the Lorentzian case we see this if we use a coordinate system consisting of some parameters along the two distinct families of null geodesics that necessarily exist. Since the vectors  $\partial_u$  and  $\partial_v$  point along these geodesics and are null, it must be possible to bring the metric to the form

---

<sup>5</sup>S. K. Chakrabarti, R. Geroch, and C.-b. Liang, *Timelike curves of limited acceleration in general relativity*, J. Math. Phys. **24** (1983) 597.

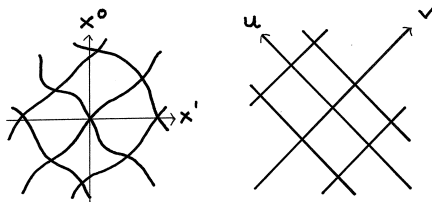


Figure 4: Why every two dimensional Lorentzian manifold is conformally flat: two null rays pass through every point, and can be made into coordinate lines.

$$ds^2 = -\Omega(\tilde{u}, \tilde{v})d\tilde{u}d\tilde{v} , \quad (26)$$

for some choice of a non-vanishing function  $\Omega$ . Doing this for the Schwarzschild solution leads to the well known Kruskal coordinate system, which has the advantage that it covers the whole of spacetime, but the disadvantage that it is somewhat awkward to use. Of course double null coordinates are also used in constructing Penrose diagrams, but then one simply ignores the cumbersome conformal factor  $\Omega$ .

For many purposes it is enough to go only half way, and let the area radius  $r$  stay as a coordinate. We know that radial null geodesics are described by

$$\frac{dt}{dr} = -\frac{e^{-\beta}}{1 - \frac{2m}{r}} , \quad (27)$$

where we settled for ingoing geodesics. In general this differential equation may be a hard nut to crack. We know however that there will be an integration constant  $v$  labelling the different geodesics, and we can use this label as one of our coordinates. We will trade the coordinate  $t$  for  $v$ , which is referred to as “advanced time”. Thus—whether we can solve the equation or not—we can perform the coordinate transformation

$$dv = dt + e^{-\beta} \frac{dr}{1 - \frac{2m}{r}} . \quad (28)$$

Then  $v$  is constant along every ingoing radial null geodesic. The metric takes the Eddington-Finkelstein form

$$ds^2 = -e^{2\beta} \left(1 - \frac{2m}{r}\right) dv^2 + 2e^\beta dvdr + r^2(d\theta^2 + \sin^2 \theta d\phi^2) . \quad (29)$$

Here  $\beta$  and  $m$  are some functions of  $v$  and  $r$ . This is an alternative expression of the most general spherically symmetric line element.

The spacetime described by these coordinates is manifestly regular at  $r = 2m$  so we are now allowed to extend the range of the coordinate  $r$  to cover the entire interval  $(0, \infty)$ . In the Schwarzschild case spacetime remains geodesically incomplete not only because of the singularity but also because outgoing null geodesics will appear seemingly out of nowhere for finite values of their affine parameters; in effect we are covering only two out of four regions of the Penrose diagram. A coordinate system using “retarded time”, labelling outgoing null geodesics, can be used to deal with this, but then the ingoing null geodesics will be incomplete. This we get around by using several overlapping coordinate patches, but there is still a problem with the special round sphere at  $r = 2m$ ,  $t = 0$ . This is more difficult to handle because  $\nabla_a r = 0$  there (as is evident from Fig. 2), and the coordinate  $r$  fails.

Explicitly the retarded time  $u$  labelling ingoing geodesics obeys

$$du = dt - e^{-\beta} \frac{dr}{1 - \frac{2m}{r}} . \quad (30)$$

We can get rid of  $r$  as a coordinate by using both  $u$  and  $v$ , but this does not immediately solve the problem. In fact it gets worse again, because

$$ds^2 = -e^{2\beta} \left(1 - \frac{2m}{r}\right) dudv . \quad (31)$$

This is ill-behaved at  $r = 2m$ . A possible cure is to relabel the geodesics,

$$u = u(\tilde{u}) , \quad v = v(\tilde{v}) . \quad (32)$$

Using  $\tilde{u}$  and  $\tilde{v}$  as coordinates we obtain

$$ds^2 = -e^{2\beta} \left(1 - \frac{2m}{r}\right) \frac{du}{d\tilde{u}} \frac{dv}{d\tilde{v}} d\tilde{u} d\tilde{v} . \quad (33)$$

The idea is to choose the functions  $u(\tilde{u})$  and  $v(\tilde{v})$  so that the conformal factor becomes non-zero in the region of interest. But in order to even begin playing this game we must know the function  $r = r(u, v)$ .

In order to see how things work out we concentrate on the interesting special case

$$ds^2 = -V(r)dt^2 + \frac{dr^2}{V(r)} + r^2 (d\theta^2 + \sin^2 \theta d\phi^2) . \quad (34)$$

Advanced and retarded time are now given by

$$v = t + \int^r \frac{dr}{V(r)} \equiv t + r_* , \quad u = t - \int^r \frac{dr}{V} \equiv t - r_* . \quad (35)$$

Here we introduced the Regge-Wheeler tortoise coordinate  $r_*$ . We will meet it again later on. In the Schwarzschild case it is given by

$$r_* = \int^r \frac{dr}{V(r)} = \int^r \frac{r dr}{r - 2M} = r + 2M \ln \left| \frac{r}{2M} - 1 \right| . \quad (36)$$

We note that  $r_* \rightarrow -\infty$  as  $r$  approaches  $2M$ , nicely cancelling the divergence in the coordinate  $t$ . This completes the transformation to Eddington-Finkelstein coordinates.

We choose to introduce the double null coordinates directly. In order to bring the metric into the desired form (26) we must solve the equations

$$\Omega \frac{\partial \tilde{u}}{\partial t} \frac{\partial \tilde{v}}{\partial t} = V(r) , \quad \frac{\partial \tilde{u}}{\partial r} \frac{\partial \tilde{v}}{\partial t} + \frac{\partial \tilde{u}}{\partial t} \frac{\partial \tilde{v}}{\partial r} = 0 , \quad \Omega \frac{\partial \tilde{u}}{\partial r} \frac{\partial \tilde{v}}{\partial r} = -\frac{1}{V(r)} . \quad (37)$$

Given that the function  $\Omega$  is at our disposal, the equations are easy to solve. This is so because they can be separated by setting  $\tilde{u}(r, t) = f(r)g(t)$ , and similarly for  $v(r, t)$ . A solution is

$$\tilde{u} = -e^{-ct} e^c \int^r \frac{dr}{V} = -e^{-cu} , \quad \tilde{v} = e^{ct} e^c \int^r \frac{dr}{V} = e^{cv} . \quad (38)$$

We now have the functions (32) explicitly, except that the integration constant  $c$  remains to be determined. If we can choose it so that the conformal factor

$$\Omega = -\frac{V(r)}{c^2 \tilde{u} \tilde{v}} = \frac{V(r)}{c^2} e^{-2c \int^r \frac{dr}{V}} \quad (39)$$

is non-vanishing in the region of interest, then we are done. For the Schwarzschild case we have

$$V(r) e^{-2c \int^r \frac{dr}{V}} = \frac{r - 2M}{r} e^{-2cr - 4cM \ln \left| \frac{r}{2M} - 1 \right|} , \quad (40)$$

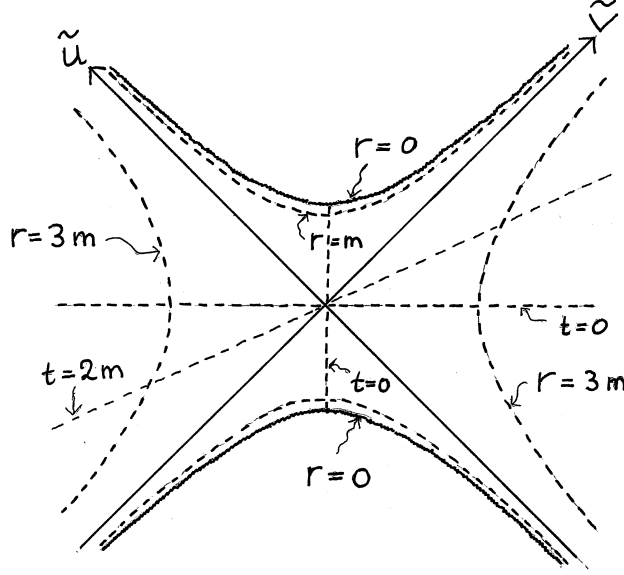


Figure 5: The Kruskal coordinate system.

so the appropriate choice is

$$c = \frac{1}{4M} \quad \Rightarrow \quad \Omega = \frac{32M^3}{r} e^{-\frac{r}{2M}} > 0 . \quad (41)$$

We have succeeded. This is the famous Kruskal coordinate system, whose origin is located at the troublesome sphere where  $\nabla_a r = 0$ . If we let  $\tilde{u}$  and  $\tilde{v}$  run from  $-\infty$  to  $\infty$  the manifold becomes maximally extended, and if any geodesic vanishes at finite parameter time it does so because it hits the singularity. An obvious drawback of the Kruskal-Szekeres coordinates is that the function  $r = r(\tilde{u}, \tilde{v})$  occurs explicitly in the metric—and the definition of  $r$  is now given in the highly implicit form

$$\left(1 - \frac{r}{2m}\right) e^{\frac{r}{2m}} = \tilde{u}\tilde{v} . \quad (42)$$

In this coordinate plane the singularity occurs as the two branches of the hyperbola  $\tilde{u}\tilde{v} = 1$ . Lines of constant  $t$  are given by

$$\frac{\tilde{v}}{\tilde{u}} = \pm e^{\frac{t}{2m}} , \quad (43)$$

where the sign depends on which of the four quadrants we are in.

*The hypersurface  $r = 2m$*

Since the Eddington-Finkelstein coordinates cover at least a part of the hypersurface  $r = 2m$  we can use them to try to see what is special about it. Why did it cause trouble in the original Ansatz (8)? From the definition of the mass function in eq. (6) we know that the gradient of the area radius becomes null at this hypersurface. To make the meaning of this property more clear we look at the equations for radial null geodesics, that is to say null geodesics emitted orthogonally to the round spheres that foliate the hypersurface. In Eddington-Finkelstein coordinates radial null geodesics obey

$$e^\beta \dot{v} \left( 2\dot{r} - e^\beta \left( 1 - \frac{2m}{r} \right) \dot{v} \right) = 0 , \quad (44)$$

where the dot means differentiation with respect to an affine parameter. The equation  $\dot{v} = 0$  takes care of the ingoing congruence. The outgoing congruence obeys

$$\frac{dr}{dv} = \frac{e^\beta(r - 2m)}{2r} . \quad (45)$$

Since  $r$  measures the area of a round sphere we see that a wave front emitted at  $r = 2m$  will, at least momentarily, keep its area constant. If emitted at  $r < 2m$  both the ingoing and the outgoing wavefronts are shrinking in area, at least momentarily. A sphere that behaves in this odd fashion is said to be trapped. The hypersurface therefore bounds the region where the round spheres are trapped, and it is itself foliated by round spheres that are marginally trapped, in the sense that the expansion of the outgoing congruence vanishes. The occurrence of trapped surfaces is in fact the hallmark of irreversible gravitational collapse—they are a key ingredient of Penrose's first singularity theorem.

Is our hypersurface timelike or spacelike? To see this we compute its normal vector

$$n_a = \nabla_a(r - 2m) = (1 - 2m_{,r})\nabla_a r - 2m_{,v}\nabla_a v . \quad (46)$$

where we use the comma notation for partial derivatives. Its norm, evaluated at  $r = 2m$ , is

$$n^2 = g^{ab}n_a n_b = -4e^{-\beta}m_{,v}(1 - 2m_{,r}) . \quad (47)$$

We see that the hypersurface can be timelike or spacelike depending on the mass function. In the Einstein case  $m_{,v} = 0$  it is a null hypersurface, and an outgoing null congruence emitted by one of the round spheres will stay within this null hypersurface. This is then an event horizon, dividing a part of spacetime from which signals can be sent to infinity from a region from which it is impossible to do so.

Now we know why the hypersurface  $r = 2m$  is special, but we still do not know why an important coordinate system fails there. However, the reason will be revealed shortly.

#### *The Kodama vector field*

To the area radius  $r$  and the Misner-Sharp mass  $m$  we can add one more invariantly defined structure in any spherically symmetric spacetime such that the gradient of  $r$  is non-zero. This is a vector field  $\xi$  which is orthogonal to the round spheres, and goes along the lines of constant  $r$  in the orthogonal complement of the spheres. It may or may not be a Killing vector, but at least the surfaces of transitivity keep their area as we move along it. In equations it obeys

$$\xi^a \nabla_a r = 0 \quad \Leftrightarrow \quad dr(\xi) = 0 . \quad (48)$$

For a reason that will appear presently it is normalized by

$$||\xi||^2 = -g^{ab}\nabla_a r \nabla_b r = -1 + \frac{2m}{r} . \quad (49)$$

With this normalization the vector field is referred to as the Kodama vector field. In the usual coordinates it is simply

$$\xi = e^{-\beta} \partial_t . \quad (50)$$

It is timelike in the region where  $r > 2m$ , null at  $r = 2m$ , and spacelike when  $r < 2m$ .

Again in the usual coordinates we compute that

$$\begin{aligned} \mathcal{L}_\xi g_{ab} = & \frac{2m_{,t}}{r} \left( e^\beta \nabla_a t \nabla_b t + \frac{e^{-\beta}}{(1 - \frac{2m}{r})^2} \nabla_a r \nabla_b r \right) + \\ & + 2\beta_{,r} e^\beta \left( 1 - \frac{2m}{r} \right) \nabla_{(a} t \nabla_{b)} r . \end{aligned} \quad (51)$$

(The round brackets around the indices denote symmetrization.) The Kodama vector is a Killing vector if

$$m = m(r) \quad \text{and} \quad \beta = \beta(t) . \quad (52)$$

In particular this is so in the Einstein case. One possible formulation of Birkhoff's theorem is that the Kodama vector becomes a Killing vector if the Ricci tensor vanishes. It remains a Killing vector also in the Reissner-Nordström-de Sitter spacetime.

In every case it follows that

$$\nabla_a \xi^a = \frac{1}{2} g^{ab} \mathcal{L}_\xi g_{ab} = 0 . \quad (53)$$

But more is true. If one defines the vector

$$K^a = G^{ab} \xi_b = 8\pi T^{ab} \xi_b , \quad (54)$$

one can show that spherical symmetry together with Einstein's equations imply that

$$\nabla_a K^a = \nabla_a (G^{ab} \xi_b) = G^{ab} \nabla_a \xi_b = \frac{1}{2} G^{ab} \mathcal{L}_\xi g_{ab} = 0 . \quad (55)$$

Of course the last step needs a detailed examination, and it works at all only because of the particular normalization of the Kodama vector. The result is interesting because it means that the Kodama vector field defines a conserved energy flux for spherically symmetric systems.<sup>6</sup> This is a little surprising, since one might have expected that a timelike Killing vector was needed for this.

---

<sup>6</sup>H. Kodama, *Conserved energy flux for the spherically symmetric system and the back-reaction problem in the black hole evaporation*, Prog. Theor. Phys. **63** (1980) 1217.



A question that can be asked of any vector field is whether it is hypersurface forming, that is whether there exist functions  $F$  and  $\tau$  such that

$$\xi_a = -F \nabla_a \tau . \quad (56)$$

If so the equation  $\tau = \text{constant}$  defines a hypersurface everywhere orthogonal to the vector field. This is a non-trivial property in general. According to Frobenius' theorem the condition that it holds is

$$\xi_{[a} \nabla_b \xi_{c]} = 0 , \quad (57)$$

where the square brackets denote anti-symmetrization. In two dimensions this holds for every vector field. Because the Kodama vector field is confined to the two dimensional orthogonal complement of the spheres it is always hypersurface orthogonal, and the functions  $F$  and  $\tau$  must exist. When the Kodama vector is timelike, the function  $F$  can be chosen to be a positive function, and we can refer to  $\tau$  as the Kodama time. In the usual coordinate system we get

$$\xi_a = -e^\beta \left( 1 - \frac{2m}{r} \right) \nabla_a t . \quad (58)$$

Hence the coordinate  $t$  is the Kodama time. It is not uniquely singled out by this requirement since we are free to reparametrize  $t$  with a monotone function  $t(\tau)$ . Hypersurfaces of constant  $t$  will coincide with hypersurfaces of constant  $\tau$ . These hypersurfaces do have an invariant meaning.

In particular, we now see that a coordinate system using the Kodama time  $t$  as one of the coordinates will encounter a problem at the hypersurface  $r = 2m$ , because the Kodama vector field becomes null there. This is the reason why the coordinate  $t$  cannot be used globally.

### *An application to Friedmann models*

Since it was somehow obvious from the original form (8) of the metric that hypersurfaces of constant  $t$  are quite special our results on the Kodama vector field may seem somewhat meagre. But note that the same logic can be applied regardless of the coordinate system used. Let us consider the closed Friedmann model, with the metric

$$ds^2 = a^2(-d\eta^2 + d\chi^2 + \sin^2 \chi d\Omega^2) , \quad a = a(\eta) . \quad (59)$$

We have chosen coordinates so that it is easy to see what radial null geodesics do: they move along lines sloping 45 degrees in the  $\eta - \chi$  plane. At constant  $\eta$  space is a round 3-sphere. This is evidently spherically symmetric, and indeed spherically symmetric around every point since it is a homogeneous space. We will focus on rotations leaving the North Pole at  $\chi = 0$  invariant.

We immediately derive the area radius and the Misner-Sharp mass:

$$r = a \sin \chi \quad (60)$$

$$m = \frac{r}{2}(1 - g^{ab}\nabla_a r \nabla_b r) = \frac{a}{2} \left(1 + \frac{\dot{a}^2}{a}\right) \sin^3 \chi , \quad (61)$$

where the dot means differentiation with respect to  $\eta$ . Let us now impose Einstein's equations. It is known that we get a solution with matter describing a homogeneous cloud of freely falling galaxies if

$$a = \frac{a_m}{2}(1 + \cos \eta) . \quad (62)$$

Here  $a_m$  is the radius of the Universe at the moment of maximal expansion, which in our coordinates occurs at  $\eta = 0$ . Using this solution in our expression for the Misner-Sharp mass gives

$$m = \frac{a_m}{2} \sin^3 \chi . \quad (63)$$

This is time independent, which means that galaxies do not cross the constant  $r$  hypersurfaces.

The Kodama vector field can be identified as

$$\xi = \frac{1}{a} \left( \cos \chi \partial_\eta - \frac{\dot{a}}{a} \sin \chi \partial_\chi \right) \quad \Leftrightarrow \quad \xi_a = -a \cos \chi \nabla_a \eta - \dot{a} \sin \chi \nabla_a \chi . \quad (64)$$

To find the Kodama time function  $t$  we must be able to express  $\xi_a$  as  $-F \nabla_a t$  for some positive function  $F$ . If we make the Ansatz  $t = f(\eta) \cos \chi$  we will arrive at the differential equation

$$\frac{df}{f} = -\frac{a}{\dot{a}} d\eta . \quad (65)$$

This is easy to solve in the Einstein case (62). We obtain

$$t = \frac{a_m}{2}(1 - \cos \eta) \cos \chi \quad (66)$$

$$\xi_a = -F \nabla_a t = -\frac{\dot{a}}{a_m - a} \nabla_a t , \quad (67)$$

and the function  $F$  is positive in the collapsing phase  $\eta > 0$ . The hypersurfaces of constant Kodama time  $t$  are spacelike only when  $r < 2m$ , as expected. Expressing the metric explicitly in terms of the coordinates  $r$  and  $t$  is in principle possible, but it would be hard to express the function  $\beta = \beta(t, x)$  in eq. (8) in explicit form.

#### Exercises:

- Are there spacelike geodesics that terminate at the Schwarzschild singularity? Can all spacelike separated points be connected by spacelike geodesics?
- Introduce double null coordinates for the Reissner-Nordström space-time.
- Check the steps in the derivation of the Kodama time for the Friedmann model, and sketch the constant  $t$  hypersurfaces on a conformal diagram.

## THE VAIDYA SOLUTION

### *Synge's method*

The Irish relativist Synge invented a method to solve Einstein's equations going as follows. To solve

$$G_{ab} = 8\pi T_{ab} , \quad (68)$$

rewrite as

$$T_{ab} = \frac{1}{8\pi} G_{ab} , \quad (69)$$

choose any metric tensor  $g_{ab}$ , compute its Einstein tensor  $G_{ab}$ , and read off the stress-energy tensor  $T_{ab}$  from eq. (69). The result is a solution of eq. (68). To avoid any misunderstanding, Synge meant this as a joke (and he did not predict dark matter). A stress-energy tensor computed in this way is not likely to obey any of the positivity conditions that are necessary for it to qualify as physical.

Very occasionally the method works though. As our input metric we choose a spherically symmetric metric in Eddington-Finkelstein coordinates, and specialize it to

$$ds^2 = - \left( 1 - \frac{2m(v)}{r} \right) dv^2 + 2dvdr + r^2 d\theta^2 + r^2 \sin^2 \theta d\phi^2 . \quad (70)$$

We then arrive at

$$T_{ab} = \frac{\dot{m}}{4\pi r^2} l_a l_b , \quad (71)$$

where the dot now means differentiation with respect to  $v$  and  $l_a$  is the inwards directed null vector field

$$l_a = -\nabla_a v \quad \Leftrightarrow \quad l^a \partial_a = -\partial_r . \quad (72)$$

Provided that  $\dot{m} \geq 0$  this is a perfectly respectable stress-energy tensor, which happens to be traceless. It describes a shell of incoherent electromagnetic radiation or null dust, coming in from past null infinity. The spacetime itself is called the Vaidya solution.

This is an interesting toy model of gravitational collapse. The rate at which matter comes in is at our disposal, and we choose to set  $m = 0$  when  $v < 0$ , then let  $m$  grow at some rate that suits us, until it reaches some finite value  $M$  at some later moment in advanced time—although to ensure that the solution be asymptotically flat to the future it is enough if the total mass remains finite. Alternatively we could start from a Schwarzschild black hole, and add a Vaidya region to model black hole accretion, but we will not pursue this.

With our choice the solution becomes divided into an initial flat region, a Vaidya region, and a final Schwarzschild region created by infall of radiation into a flat spacetime. There are pitfalls along the way: the radiation density will go to infinity at the origin. This is known as a shell focusing singularity. The geometry itself also misbehaves. The Kretschmann scalar—one of the scalar functions one can construct out of the curvature tensor—is

$$R_{abcd}R^{abcd} = \frac{48m^2}{r^6} . \quad (73)$$

Hence the geometry is singular at  $r = 0$ . The question arises whether this is due to the fact that we assumed exact spherical symmetry, or whether the singularity will be present also if the initial data are changed so that they are only approximatively spherically symmetric.

### *Cosmic censorship*

The singularity theorems—due mainly to work by Penrose, Hawking, and Geroch—state that if there exists a trapped surface in a solution of Einstein’s equations, the solution will be geodesically incomplete to the future provided that the stress-energy tensor obeys a suitable positivity condition. A trapped surface is a closed surface (in practice, a sphere) such that both of the two orthogonal congruences of future directed null geodesics that emanate from the surface are convergent when they leave the surface. For a closed surface in Minkowski space the outgoing congruence would be divergent, i.e. outgoing wavefronts are increasing their areas, so there are no trapped surfaces in Minkowski space. On the other hand we already know that a general spherical symmetric spacetime will have round trapped spheres at  $r < 2m$ . The thing to observe is that the trapped surface condition comes

in the form of an inequality, which means that it will be valid also for small perturbations away from the initial data that contain them. Hence the singularities found in spherically symmetric models are not just artefacts of the special symmetry. Geodesically incomplete means that there are geodesics (null or timelike) that disappear at a finite value of their affine parameters in an irreparable way, that is to say that it is impossible to find an extended spacetime free of this difficulty. More precisely, the theorems show that it is not possible to isometrically embed the solution as a subset of a larger geodesically complete manifold. Note that the restriction to geodesics is important, since Minkowski space contains incomplete curves—and Minkowski space certainly should count as regular. It is expected that the incomplete geodesics will encounter regions of diverging curvature when they disappear, but this does not follow from the theorems.

Strong censorship states that no observations of a future singularity can be made, that is to say that no future directed timelike or null curves emerge from them. In effect this means that a generic spacetime is globally hyperbolic, and fully determined by initial data on a spacelike Cauchy hypersurface. Weak censorship states that no observations of a future singularity can be made close to infinity in a generic asymptotically flat spacetime, that is to say that they occur only inside the event horizon that bounds the region that can be seen from infinity. In effect a black hole forms around the singularity, so that astronomers cannot see it. Observable singularities are called naked, and would wreak havoc with the predictive power of general relativity if they occur.

These formulations are vague, in particular the meaning of the word “generic” is not specified. It is known, for instance, that the Reissner-Nordström solution contains locally naked singularities, but there are arguments to show that this part of the solution is unstable against perturbations. The formulations can be improved, but they will remain vague until the cosmic censorship hypothesis is either proved or disproved. This will probably take a long time, and meanwhile black hole physics rests on an unproved conjecture. One can try to argue that astronomers would have alerted theoreticians that naked singularities are out there—if they were.

We want to know if the singularity in the Vaidya solution is naked or not. Note at the outset that if it is, this will not count as a serious failure of cosmic censorship, but will be blamed on the matter model, which gives a poor description of real world electromagnetic fields when the density becomes

very high. Nevertheless we will learn that the standard energy conditions imposed on  $T_{ab}$  are not in themselves enough to ensure cosmic censorship.

*The singularity: naked or not?*

To investigate whether the Vaidya singularity is naked we study radially directed null geodesics; they obey

$$\dot{x}^2 = \dot{v} \left( 2\dot{r} - \left( 1 - \frac{2m}{r} \right) \dot{v} \right) = 0 . \quad (74)$$

The ingoing congruence is described by

$$v = \text{constant} , \quad r = \tau_0 - \tau , \quad (75)$$

where  $\tau$  is an affine parameter along the ray.

Since the Eddington-Finkelstein coordinates are perfectly adapted to the study of the Vaidya solution we will draw pictures directly in the  $v$ - $r$ -plane. This is quite confusing at first, since the ingoing null geodesics will be parallel with the  $r$ -axis in the diagrams. It is not too hard to get used to though.

To investigate the singularity we need the outgoing congruence, whose equation is

$$\frac{dv}{dr} = \frac{2}{1 - \frac{2m}{r}} . \quad (76)$$

To solve it we must specify the mass function  $m(v)$ , but to begin with it is enough to observe that the forwards light cones are pointing towards decreasing  $r$  as soon as  $r < 2m$ . This means that if there are any signals coming out from the singularity they must come from a single point in the  $v$ - $r$ -diagram, namely  $(r, v) = (0, 0)$ . We can use a variant of Synge's method to investigate whether they do.<sup>7</sup>

We rewrite the geodesic equation as

$$2\frac{dr}{dv} = 1 - \frac{2m}{r} \quad \Leftrightarrow \quad m(v) = \frac{r}{2} \left( 1 - 2\frac{dr}{dv} \right) . \quad (77)$$

---

<sup>7</sup>Y. Kuroda, *Naked singularities in the Vaidya solution*, Prog. Theor. Phys. **72** (1984) 63.

Let us assume that, for small  $v$ , the outgoing geodesic is given by

$$r = \beta v^a, \quad \beta > 0, \quad a > 0. \quad (78)$$

Clearly a geodesic that starts at  $r = 0$  and goes into the region with positive  $r$ -values must behave like this, with a positive coefficient  $\beta$ , to leading order in  $v$ . We find that

$$m(v) = \frac{1}{2}\beta v^a(1 - 2\beta a v^{a-1}). \quad (79)$$

There are now three cases to investigate.

First the case when the mass function grows very slowly in the initial stages. Then

$$a > 1 : \quad m(v) \sim \frac{\beta}{2}v^a. \quad (80)$$

There are geodesics coming out of the singularity, and hence the singularity is at least locally naked. The next case is

$$a = 1 : \quad m(v) = \frac{1}{2}\beta(1 - 2\beta)v \equiv \mu v. \quad (81)$$

Since we insist that  $\dot{m} > 0$  we must set  $0 < \beta < 1/2$ , and we find that there is a locally naked singularity provided that

$$m(v) = \mu v, \quad \mu \leq \frac{1}{16}. \quad (82)$$

Finally we have the case when the mass starts out growing quickly:

$$0 < a < 1 : \quad m(v) \sim -a\beta^2 v^{2a-1}. \quad (83)$$

But this is not allowed: the assumption that outgoing geodesics exist leads to a contradiction with the condition that  $m(v)$  be a positive function. The conclusion is that there are no outgoing geodesics, and hence no naked singularity, in this case.

Although convenient, Synge's method is not needed to show this. A more systematic approach is to rewrite eq. (76) as an autonomous system of ordinary differential equations, namely



$$\frac{dv}{d\sigma} = 2r \ , \quad \frac{dr}{d\sigma} = r - 2m(v) \ . \quad (84)$$

We are now interested in the phase portrait in the  $r$ - $v$ -plane, especially in the neighbourhood of the obvious fixed point at the origin. (Recall that  $m(0) = 0$ .) We linearize around the fixed point, using the definition

$$\lim_{v \rightarrow 0_+} \frac{m(v)}{v} = \mu \ . \quad (85)$$

This gives the linear system

$$\begin{pmatrix} \dot{v} \\ \dot{r} \end{pmatrix} = \begin{pmatrix} 0 & 2 \\ -2\mu & 1 \end{pmatrix} \begin{pmatrix} v \\ r \end{pmatrix} \ . \quad (86)$$

The eigenvalues of the matrix are

$$\lambda_{\pm} = \frac{1}{2} \left( 1 \pm \sqrt{1 - 16\mu} \right) \ , \quad (87)$$

with the eigenvectors

$$\begin{pmatrix} 1 \\ \lambda_{\pm} \end{pmatrix} \sim \begin{pmatrix} \lambda_{\mp} \\ 2\mu \end{pmatrix} \ . \quad (88)$$

As long as  $\mu \leq 1/16$  the eigenvalues are real, the fixed point is a source, and a whole set of geodesics are coming out of it. If on the other hand  $\mu > 1/16$  the eigenvalues are complex, the fixed point is a center, and nothing comes out of it. We will come back to this way of doing the analysis later (see Fig. 8); anyway the conclusion is the same as before.

Whether this is a serious (partial) failure of cosmic censorship is a question we will have to think about. But so far we have addressed the issue of strong cosmic censorship only. A locally naked singularity may still be hidden behind an event horizon so that weak cosmic censorship holds. This is a more difficult question. To answer it we must specify the mass function and solve eq. (76) for the outgoing geodesics also far from the fixed point. In fact, depending on the mass function all three possibilities occur: naked, locally but not globally naked, and clothed.

### *The Penrose diagram*

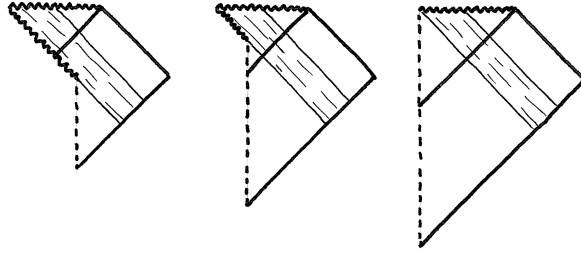


Figure 6: Possible Penrose diagrams for the Vaidya solution. Matter comes in in the dashed region. The singularity may be naked or clothed.

To draw the Penrose diagram we begin with the question how to draw the singularity. It will always have a spacelike part, because a radial null geodesic cannot come out from it anywhere in the region where  $r < 2m$  since it must decrease its value of  $r$  as it goes. But radial null geodesics can come out of the point where  $(r, v) = (0, 0)$ , if it is locally naked. Whenever this is the case the singularity will have a null part in the diagram. It cannot appear as a timelike line in the diagram because at fixed values of the angular coordinates only one incoming null geodesic can hit this point. So we have to draw the singularity either as a spacelike line or as a null line meeting a spacelike line. See Fig. 6.

At this point you may have become nervous. I came close to saying that the singularity “sits at  $r = 0$ ”, and this cannot be quite right since this is outside the range of our coordinates. There are no such points in the spacetime manifold. But it is still true that the singularity has acquired some structure and one can in fact talk, in a meaningful way, of spacelike, timelike, or null singularities. To do this strictly one can define the “points” of the singularity as equivalence classes of those curves that are leaving the spacetime manifold. Effectively this is what we just did.

To complete our Penrose diagram we must locate the event horizon. We cannot do this unless we first figure out the global behaviour of the outgoing null geodesics, and we cannot do this unless we first specify the mass function. We leave this open for now. In principle the null part of the singularity can be hidden behind the event horizon and then the locally naked singularity is clothed globally; in the self-similar case that we study below this never happens, but for more general choices of the mass function all three possibilities occur. See Fig. 6 once more.

When there are no global naked singularities a part of flat spacetime will be inside the event horizon. This flat region is the intersection of the interiors of a backwards (the inner boundary of the shell) and a forwards (the event horizon) light cone. In other words it is a causal diamond, and can be drawn without conformal distortion—the singularity sits at the top of the diamond and is situated at finite timelike distance from any point on the axis. Now consider the time an observer can spend within this causal diamond, which is the flat part of the interior of the black hole. This time will grow the larger the mass, and the faster it comes in. Then the observer will live longer inside the black hole, but if she follows the central world line in the diagram she will never notice—until she is suddenly killed.

This makes perfect sense, once one realizes that the event horizon is an “upside down” concept. Its location is not determined by what has happened, it is determined by what will happen. In particular its area grows quickly in Minkowski space, its rate of growth drops when the incoming radiation crosses it, and then the area stays constant in the Schwarzschild region.

### *Self-similar collapse*

To locate the event horizon we must specify the mass function  $m(v)$ , since it enters the equation for an outgoing null geodesic. A simple choice of the mass function, allowing us to actually solve for the outgoing geodesics, is

$$m = \mu v , \tag{89}$$

where  $\mu$  is a positive constant. We already know that the singularity is locally naked if  $\mu \leq 1/16$ . The linear mass function is distinguished since the Vaidya solution then admits the homothetic Killing field

$$\eta = v\partial_v + r\partial_r \quad \Rightarrow \quad \mathcal{L}_\eta g_{ab} = 2g_{ab} . \tag{90}$$

A homothety means that if you scale things up, everything remains the same. Self-similar spacetimes are rather special, and it is somewhat dangerous to draw general conclusions from them. But the extra symmetry leads to soluble equations, and this is irresistible.

It is useful to introduce the dimensionless variable

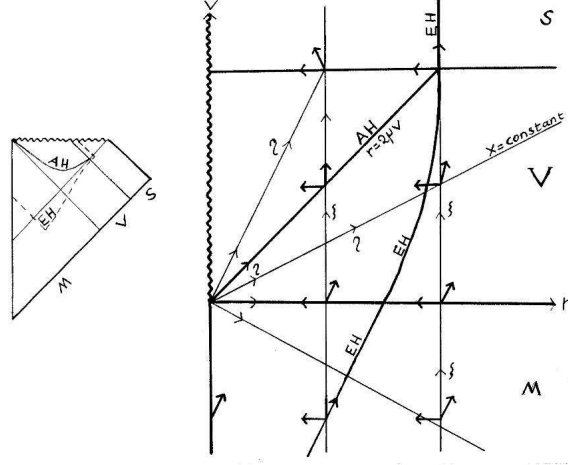


Figure 7: Since we use Eddington-Finkelstein coordinates for all calculations we use a  $v - r$ -diagram for visualization. The picture is for  $\mu = 1/2$  (a clothed singularity) and includes the homothetic Killing and the Kodama vector fields, selected future light cones, the event horizon EH, and the hypersurface  $r = 2m$ .

$$x = \frac{v}{r}, \quad \mathcal{L}_\eta x = 0. \quad (91)$$

For the Vaidya solution we note that

$$\eta^2 = 2\mu vr \left( \left( x - \frac{1}{4\mu} \right)^2 + \frac{1}{\mu^2} \left( \mu - \frac{1}{16} \right) \right). \quad (92)$$

The homothetic Killing vector is spacelike in the entire Vaidya region provided that  $\mu > 1/16$ , that is whenever the solution is free of locally naked singularities. In the Minkowski region it is timelike, and in the Schwarzschild region it does not exist.

By arrangement the mass is supposed to grow from 0 to some arbitrary  $M > 0$ , so that the Vaidya region is

$$0 < v < \frac{M}{\mu}. \quad (93)$$

In the coordinate system we use the metric is continuous at the boundaries of the Vaidya region, but its derivatives are not. Moreover the stress-energy

tensor is discontinuous there. Still there are no problems with the geodesic equation. Outgoing null geodesics are coming into the Vaidya region with a slope (in the  $v - r$ -diagram) equal to 2. A null geodesic leaves the Vaidya region with a slope equal to

$$\frac{dv}{dr}|_{v=M/\mu} = \frac{2}{1 - \frac{2M}{r}} . \quad (94)$$

The slope is vertical if it hits the boundary of the Schwarzschild region at  $r = 2M$ , which is where the event horizon is located. If it hits the boundary at larger  $r$ -values it will eventually disappear to infinity, and if it hits at smaller  $r$ -values it will fall back into the singularity, never to be seen by an observer outside the black hole. In the Vaidya region we must solve equation

$$\frac{dv}{dr} = \frac{2}{1 - \frac{2\mu v}{r}} . \quad (95)$$

The question is where null geodesics emerging into Schwarzschild at  $r = 2M$  come from. From the singularity, or from the flat region?

### *Outgoing geodesics*

Because we imposed self-similarity the problem of finding the path of the null geodesics has been reduced to that of solving the linear system (86). But the information we need can be obtained in a different way.<sup>8</sup> The right hand side of eq. (95) is a homogeneous function, which means that the equation can be solved by separation of variables if we rewrite it in terms of the dimensionless variable  $x = v/r$ . After a minor calculation we obtain

$$r \frac{dx}{dr} = \frac{1}{8\mu} \frac{(4\mu x - 1)^2 + 16\mu - 1}{1 - 2\mu x} . \quad (96)$$

This is easy to solve. Note by the way that

$$\frac{d^2v}{dr^2} = \frac{1}{16r} \left( \frac{dv}{dr} \right)^3 \left( (4\mu x - 1)^2 + 16\mu - 1 \right) . \quad (97)$$

---

<sup>8</sup>A. Papapetrou, *Formation of a singularity and causality*, in N. Dadhich et al. (eds): *A Random Walk in Relativity and Cosmology*, Wiley 1985.

The sign of the second derivative can be read off from here, so between eqs. (95) and (97) it is easy to see the qualitative behaviour of  $v(r)$  in a  $v-r$ -diagram. In particular, note that

$$x = \frac{1}{2\mu} \quad \Leftrightarrow \quad \frac{dv}{dr} = \infty . \quad (98)$$

This tells us where the solution curves become vertical in a  $v-r$ -diagram—or, if you like, where the round spheres become marginally trapped.

The equation to be solved is

$$\frac{dr}{r} = \frac{8\mu(1-2\mu x)dx}{(4\mu x-1)^2 + 16\mu - 1} . \quad (99)$$

Depending on whether the denominator on the right hand side can vanish or not the analysis splits into three cases:

- i*:  $\mu > 1/16$
- ii*:  $\mu = 1/16$
- iii*:  $\mu < 1/16$  .

We deal with them in turn.

The condition in case *i* ensures that first and second derivatives have the same sign everywhere. The solution is

$$r = u \frac{\exp \left[ \frac{1}{\sqrt{16\mu-1}} \arctan \frac{4\mu x-1}{\sqrt{16\mu-1}} \right]}{\sqrt{(4\mu x-1)^2 + 16\mu - 1}} , \quad (100)$$

where  $u$  is an integration constant. When sketching the curves it is helpful to observe that the curve becomes vertical at  $x = 1/2\mu$ , which is precisely our hypersurface  $r = 2m$ .

Now we can trace the event horizon back through the Vaidya region. The geodesic belongs to the horizon provided it emerges into the Schwarzschild region at  $r = 2M$  and  $x = 1/2\mu$ , which means that the constant  $u$  has to take the value

$$u = 8M\sqrt{\mu} \exp \left[ -\frac{1}{\sqrt{16\mu-1}} \arctan \frac{1}{\sqrt{16\mu-1}} \right] . \quad (101)$$

But then this particular geodesic crosses the boundary to the flat region ( $x = 0$ ) at

$$r_0 = 2M \exp \left[ -\frac{2 \arctan \frac{1}{\sqrt{16\mu-1}}}{\sqrt{16\mu-1}} \right] > 0 . \quad (102)$$

The geodesics that rule the event horizon, as well as all the geodesics that escape to infinity, come from the flat region. As long as  $\mu > 1/16$  the singularity at  $r = 0$  is indeed invisible from outside the black hole. This case is illustrated in Fig. 7.

In case *ii*,  $\mu = 1/16$ , the second order polynomial in eq. (96) has a double root. The equation is

$$r \frac{dx}{dr} = \frac{(x-4)^2}{8-x} , \quad (103)$$

with the special solution

$$x = 4 . \quad (104)$$

The remaining solutions are given by

$$r = u \frac{\exp[-\frac{4}{x-4}]}{x-4} . \quad (105)$$

Curves  $v(r)$  lying above the special solution become tangent to it as they approach the origin. See Fig. 8.

In the  $v - r$ -diagram the origin will not have a well defined light cone, rather there will be a whole set of null geodesics emerging. Those that cross the apparent horizon at  $v = 8r$  will end up at the singularity—they all have vertical slope at the apparent horizon—but the others will escape to infinity. Null geodesics emerging into Schwarzschild to the right of the line  $v = 4r$  enter the Vaidya region at some finite value of  $r > 0$ , and hence they come from the flat region. If the Vaidya region were continued to all positive  $v$  the line  $x = 4$  would be the event horizon (ignoring the singular nature of  $\mathcal{J}$  in this infinite mass spacetime), and then the locally naked singularity would be visible on the horizon, but not outside it. When the solution is matched to Schwarzschild the event horizon “jumps”, and the singularity is most definitely globally naked; the lightlike hypersurface defined by  $x = 4$

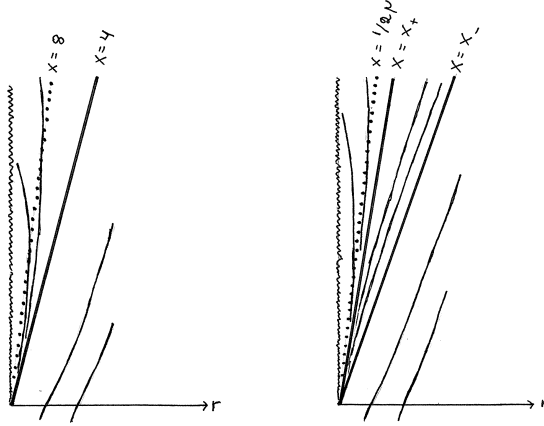


Figure 8: Cases *ii* and *iii*. Geodesics to the right of a special solution necessarily end at infinity. This includes all geodesics emerging from the flat region. Geodesics that cross  $r = 2m$  (the dotted line) are sucked into the singularity. Whether a geodesic emerging from the origin escapes to infinity depends on whether it reaches the Schwarzschild region before it crosses the dotted line.

remains as a Cauchy horizon beyond which the future cannot be predicted from the past, because we do not know what comes out of the singularity.

In case *iii*, a slowly growing mass, the second order polynomial in the numerator has two distinct roots  $x_{\pm}$ . The equation is

$$r \frac{dx}{dr} = \frac{2\mu(x - x_+)(x - x_-)}{1 - 2\mu x}. \quad (106)$$

There are two special solutions

$$x = x_{\pm} = \frac{1}{4\mu} \left( 1 \pm \sqrt{1 - 16\mu} \right). \quad (107)$$

For values of  $x$  in between  $x_-$  and  $x_+$  the second derivative in eq. (97) is negative. There will be two special solutions appearing as straight lines in the  $v - r$ -diagram. The singularity is globally naked already in the pure Vaidya case, and it emerges very clearly that there is a whole set of geodesics coming out of the “point”  $(r, v) = (0, 0)$ , which is why it appears as a null line in the Penrose diagram.



*Is cosmic censorship in doubt?*

We have observed a failure of cosmic censorship in the Vaidya model. We now know for a fact that the ingredients giving rise to singularities—in particular inequalities imposed on the Ricci tensor via energy inequalities—do not suffice to cover them up. However, this outcome is not a disaster. We can try to blame it on spherical symmetry, which is a non-generic situation. We can also try to blame it on the matter model, which is not physically realistic at high densities. Indeed, because a singularity in the form of infinite dust density would occur also in a flat background, its nakedness is usually dismissed as a pathology of the matter model rather than as a threat to cosmic censorship.

Let us go back to Fig. 6 once more. It is important that each point in the Penrose diagram is a sphere—except the dotted line which describes the spatial origin. The null part of the singularity is created as the incoming matter shells converge to that point. Such a singularity is referred to as a shell focusing singularity. According to our model the story ends there, but in the real world something else would happen—the shells might continue through there in a collisionless manner, or they would rebound inelastically. Hence our description there is quite suspect. The spacelike part of the singularity—if you like, the part that was successfully censored—is a different story. There the matter shells remain spherical shells, and the problem is that due to spacetime curvature the areas of the spheres are shrinking to zero.

If we reflect on our results we might reason as follows: in a fixed flat spacetime the collapse would lead to a singular mass density visible from afar. When the backreaction on the metric is taken into account the strong cosmic censor hides this singularity—but only provided the departure from flat space is strong enough. Intuitively this is a very reasonable conclusion, and it rather supports the idea that there is a mechanism that tends to hide singularities.

This ends our analysis of naked and clothed singularities in the self-similar Vaidya solution. In a way this was a simpler version of the next model, the Tolman-Bondi model, which is in itself a toy model of spherically symmetric gravitational collapse with “reasonable” matter. At the end of this path stands a theorem, due to Christodoulou, which supports cosmic censorship—but then the restriction to spherical symmetry in itself defines a toy model of the real thing, so this does not settle the question.

Exercises:

- Show that the null dust matter model can be derived by averaging a suitable electromagnetic stress-energy tensor, or in more technical terms that it comes from the eikonal approximation of a massless scalar field.
- Show that it is impossible to diagonalize the stress-energy tensor of the Vaidya solution by means of Lorentz transformations.

## EQUILIBRIUM STATES

### *Einstein's theorem*

Einstein proved that the only static and asymptotically flat solution of the Einstein vacuum equation on a spacetime of topology  $\mathbf{R}^4$  is, in fact, flat Minkowski space itself.<sup>9</sup> The proof is simple. The assumptions imply that one can find a coordinate system such that the metric is independent of a time coordinate  $t$ . The spacetime is then said to be stationary. It is static if we add the extra assumption that the metric is invariant under the reflection  $t \rightarrow -t$ , or equivalently if we demand that the Killing vector field  $\partial_t$  be hypersurface orthogonal. A static spacetime therefore splits naturally into space and time, while a non-static stationary solution (Kerr) does not.

We have arrived at the static Ansatz

$$ds^2 = -N^2 dt^2 + h_{ab} dx^a dx^b, \quad (108)$$

where  $x^a$  are coordinates on the spacelike hypersurfaces orthogonal to the Killing field, while  $h_{ab}$  and  $N$  are independent of the coordinate  $t$ . Asymptotic flatness requires that the coordinate system can be chosen so that

$$N \rightarrow 1 \quad \text{and} \quad h_{ab} \rightarrow \delta_{ab} \quad (109)$$

at large distances.

Next one writes the Einstein equations for this Ansatz. The result is

$$R_{tt} = -N h^{ab} \nabla_a^{(3)} \nabla_b^{(3)} N = 0 \quad (110)$$

$$R_{ab} = R_{ab}^{(3)} + \frac{1}{N} \nabla_a^{(3)} \nabla_b^{(3)} N, \quad (111)$$

where  $\nabla_a^{(3)}$  is the Levi-Civita derivative defined by the spatial metric. But the first equation here is the Laplace equation, and since we are assuming that  $N \rightarrow 1$  at infinity we must have  $N = 1$  everywhere. The second equation

---

<sup>9</sup>A. Einstein, *Demonstration of the non-existence of gravitational fields with a non-vanishing total mass free of singularities*, Univ. Nac. Tucumán Rev. **A2** (1941) 5.

then says that the spatial Ricci tensor vanishes, which—given that space has only 3 dimensions—implies that space is flat. QED.

An extension of the argument shows that Minkowski space is the only stationary solution of Einstein's vacuum equations with topology  $\mathbf{R}^4$ . The Schwarzschild metric is not a counterexample to the theorem since it is static only outside the null hypersurface at  $r = 2M$ . Its topology is not that of  $\mathbf{R}^4$ . A negative value of  $M$  would not help since there is a curvature singularity at  $r = 0$ , and again the spatial topology is not that of  $\mathbf{R}^3$ . For both positive and negative values of  $M$  the topology of the static region is that of an  $\mathbf{R}^4$  from which an infinite cylinder surrounding a coordinate axis has been removed.

### *Some more coordinate systems for the Schwarzschild spacetime*

The Schwarzschild solution is important enough to deserve having its portrait drawn in several ways. We start in Schwarzschild coordinates,

$$ds^2 = -V(r)dt^2 + \frac{dr^2}{V(r)} + r^2(d\theta^2 + \sin^2\theta d\phi^2), \quad V(r) = 1 - \frac{2M}{r}. \quad (112)$$

We are willing to contemplate an  $r$ -dependent shift of the time coordinate, as well as a reparametrization of the radial coordinate,

$$\tau = t + f(r), \quad r = r(\rho), \quad (113)$$

where  $r(\rho)$  is a monotone function. We begin with the time shift. The result is

$$ds^2 = -V(r)d\tau^2 + 2V(r)f'd\tau dr + \left(\frac{1}{V(r)} - V(r)f'^2\right)dr^2 + r^2(d\theta^2 + \sin^2\theta d\phi^2). \quad (114)$$

Then we reparametrize the radial coordinate, and try to arrange things so that the spatial metric becomes conformally flat, which means that it should equal a flat metric up to a factor. That is, when  $\tau = \text{constant}$  we want

$$ds^2 = \psi^4(d\rho^2 + \rho^2(d\theta^2 + \sin^2\theta d\phi^2)) = \psi^4(dx^2 + dy^2 + dz^2), \quad (115)$$

where  $\psi$  is some function of the spatial coordinates (and the exponent is chosen for later convenience). In the second step we introduced Cartesian coordinates through

$$\rho^2 = x^2 + y^2 + z^2 . \quad (116)$$

Examining the factor in front of the sphere metric we see that

$$\psi^4 \rho^2 = r^2 \quad \Rightarrow \quad \psi = \sqrt{\frac{r}{\rho}} . \quad (117)$$

Our task is then accomplished if

$$f'^2 = \frac{1}{V(r)^2} \left( 1 - \frac{r^2 V(r)}{\rho^2 r'^2} \right) . \quad (118)$$

This leaves us with many options.

To begin with, let us not employ the time shift at all. Then we have  $f = 0$ , and a differential equation for  $r(\rho)$ . Skipping lightly past the details, the solution gives

$$ds^2 = - \left( \frac{1 - \frac{m}{2\rho}}{1 + \frac{m}{2\rho}} \right)^2 dt^2 + \left( 1 + \frac{m}{2\rho} \right)^4 (dx^2 + dy^2 + dz^2) . \quad (119)$$

This is the isotropic coordinate system. The troublesome hypersurface  $r = 2M$  is now at  $\rho = M/2$ . But notice that the spatial metric is regular all the way down to  $\rho = 0$ . In fact the metric has a reflection symmetry under

$$\rho \rightarrow \frac{M^2}{4\rho} . \quad (120)$$

Hence this coordinate system covers regions I and III of the full spacetime (see Fig. 1). There is one asymptotic region at  $\rho \rightarrow \infty$ , and another at  $\rho \rightarrow 0$ . Finally it is worth noticing—for reasons that would take us outside spherical symmetry if we went into them—that the conformal factor  $\psi$  is the fourth power of a solution of the flat space Laplace equation.

With the time shift there are many possibilities. A simple choice for the radial coordinate is given by the constant shift

$$r = r(\rho) = \rho + \rho_0 . \quad (121)$$

This gives

$$V^2 f'^2 = \frac{1}{\rho^2} (2\rho(m - \rho_0) + \rho_0(2m - \rho_0)) . \quad (122)$$

The Schwarzschild metric takes the form

$$ds^2 = -\frac{\rho + \rho_0 - 2m}{\rho + \rho_0} d\tau^2 + \frac{2}{\rho} \sqrt{2\rho(m - \rho_0) + \rho_0(2m - \rho_0)} d\tau d\rho + \\ + \left(1 + \frac{\rho_0}{\rho}\right)^2 (dx^2 + dy^2 + dz^2) .$$

In fact we do not need to change the radial coordinate at all. Gullstrand, who was a redoubtable opponent of relativity theory in its early days, used the choice  $\rho_0 = 0$ ,  $r = \rho$ , and obtained the metric in the form

$$ds^2 = -\left(1 - \frac{2m}{r}\right) d\tau^2 + 2\sqrt{\frac{2m}{r}} d\tau dr + dx^2 + dy^2 + dz^2 . \quad (123)$$

The range of the coordinate  $r$  can now be extended to all positive values. This metric tensor remains well behaved at  $r = 2m$ , and we are covering regions I and II of the full spacetime. The spatial geometry of the hypersurfaces  $\tau = \text{constant}$  is that of a flat Euclidean space with its origin deleted, since they touch the spacetime singularity there. It is still true that

$$g^{ab} \nabla_a r \nabla_b r = V(r) , \quad (124)$$

and that this goes negative when  $r < 2m$ . Thus the hypersurfaces  $r = \text{constant}$  are spacelike when  $r < 2m$ . One problem with this form of the metric is that it approaches the flat metric at infinity rather slowly. A metric is said to be asymptotically flat if there exists a Cartesian coordinate system “close to infinity”, such that

$$g_{ab} - \eta_{ab} = o\left(\frac{1}{r}\right) . \quad (125)$$

The Schwarzschild and isotropic coordinate systems pass this test, but Gullstrand's does not. Actually there is a hierarchy of increasingly refined definitions of “asymptotically flat”, but we do not go into this here.

Another simple choice for the radial coordinate is  $\rho_0 = M$ , which gives

$$ds^2 = -\frac{\rho - M}{\rho + M}d\tau^2 + \frac{2M}{\rho}d\tau d\rho + \left(1 + \frac{M}{\rho}\right)^2(dx^2 + dy^2 + dz^2) . \quad (126)$$

The spatial geometry is now curved, albeit conformal to a flat space with its origin deleted. At constant  $\tau$

$$ds^2 = \left(1 + \frac{M}{\rho}\right)^2(d\rho^2 + \rho^2(d\theta^2 + \sin^2\theta d\phi^2)) . \quad (127)$$

When  $\rho \rightarrow 0$ —that is to say when  $r \rightarrow M$ , which is well inside the  $r = 2M$  hypersurface—the spatial geometry approaches that of a very long cylinder with constant circumference. In fact the spatial geometry resembles a trumpet, so this is called a trumpet slice through the Schwarzschild spacetime. The coordinate system fails when  $\rho = 0$  but it does have other advantages. Notably the metric now has the fall-off property (125). Moreover numerical relativists prefer to avoid the neighbourhood of the singularity if this is at all possible, so for them it is enough to cover the solution down to  $r = M$ .

In a quite different vein, there is the Kerr-Schild coordinate system. It starts with the metric in Eddington-Finkelstein coordinates, eq. (29) with  $\beta = 0$  and  $m = M$ , and sets

$$v = t + r . \quad (128)$$

Note that this time coordinate is not at all similar to the usual Schwarzschild time coordinate  $t$ . This gives

$$ds^2 = -(dt + dr)(dt - dr) + r^2(d\theta^2 + \sin^2\theta d\phi^2) + \frac{2M}{r}(dt + dr)^2 . \quad (129)$$

We then introduce Cartesian coordinates so that  $rdr = x_idx_i$ , and a four vector

$$l_a = \left(1, \frac{x}{r}, \frac{y}{r}, \frac{z}{r}\right) . \quad (130)$$

This allows us to express the metric in the remarkable form

$$g_{ab} = \eta_{ab} + \frac{2M}{r} l_a l_b , \quad g^{ab} = \eta^{ab} + \frac{2M}{r} l^a l^b , \quad (131)$$

where

$$l^a = \eta^{ab} l_b = g^{ab} l_b , \quad l_a l^a = 0 . \quad (132)$$

As the name of this coordinate system suggests, other interesting spacetime metrics—including the Kerr solution—can be expressed in a similar form, of course with a more involved definition of the null “vector”  $l_a$ .

### *Reissner-Nordström-de Sitter*

To get further examples of spacetimes with a static region we complicate the theory a little by admitting either an electromagnetic field, a cosmological constant, or both. The examples we are interested in are spherically symmetric metrics of the special form

$$\begin{aligned} ds^2 &= -V(r)dt^2 + \frac{dr^2}{V(r)} + r^2(d\theta^2 + \sin^2\theta d\phi^2) = \\ &= -V(r)dv^2 \pm 2dvdr + r^2(d\theta^2 + \sin^2\theta d\phi^2) . \end{aligned} \quad (133)$$

The metric is given in both the diagonal and the Eddington-Finkelstein form (ingoing or outgoing depending on the sign). They are interesting because there is an extra Killing vector

$$\xi = \partial_t = \partial_v , \quad \xi^2 = -V(r) . \quad (134)$$

The solution is static where  $V > 0$ , and there are hypersurfaces where the Killing vector becomes null whenever  $V = 0$ . I will refer to these hypersurfaces as “horizons”.

To begin with we add a positive cosmological constant to the vacuum equation, in which case we have the solution

$$V(r) = 1 - \frac{\lambda}{3} r^2 . \quad (135)$$



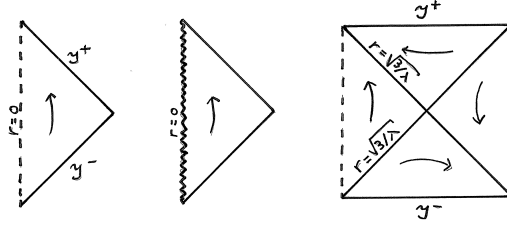


Figure 9: Minkowski space, negative mass Schwarzschild, and de Sitter space. Infinity is denoted with a script I. It is null or spacelike depending on whether  $\lambda = 0$  or  $\lambda > 0$ . The arrow points in the direction of the Killing vector field  $\partial_t$ .

This gives the de Sitter metric, and closer inspection shows that it has as many linearly independent Killing vectors as Minkowski space itself. Its spatial topology is that of a 3-sphere—which is a one parameter family of 2-spheres with two points at the ends. A horizontal slice of the Penrose diagram ends at two dashed lines representing the North and South poles of the 3-sphere. Our coordinate system is centred at one of the poles. Because of the positive cosmological constant conformal infinity has changed from a light cone at infinity to a pair of spacelike hypersurfaces. There is a horizon at  $r = \sqrt{3/\lambda}$  called the cosmological horizon, which is the boundary of the region that can ever be observed by an observer sitting at the origin of our coordinates. Any observer would be surrounded by a similar horizon. Evidently one can say much more about this interesting spacetime.<sup>10</sup> For now the observation that de Sitter space is not globally static will have to suffice.

Next we look at the Reissner-Nordström-de Sitter spacetime, for which

$$V(r) = 1 - \frac{2M}{r} + \frac{e^2}{r^2} - \frac{\lambda r^2}{3} = \frac{1}{r^2} \left( r^2 - 2Mr + e^2 - \frac{\lambda}{3} r^4 \right). \quad (136)$$

With this choice of  $V(r)$  the metric (133) is a solution of the Einstein-Maxwell equations. The parameter  $e$  is an integration constant arising when the Maxwell equations are solved, and equals the electric charge as evaluated by a surface integral at infinity. Still there is no charged matter anywhere.

---

<sup>10</sup>I. Bengtsson and S. Holst, *De Sitter space and spatial topology*, Class. Quant. Grav. **16** 3735, 1999.

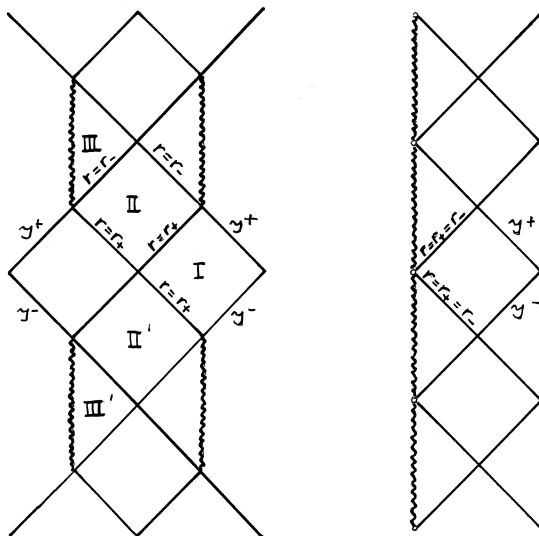


Figure 10: The Reissner-Nordström spacetime to the left, and the extremal Reissner-Nordström to the right.  $\lambda = 0$ . Ingoing Eddington-Finkelstein coordinates cover regions I, II, and III, while outgoing Eddington-Finkelstein coordinates cover regions I, II', and III'.

I will go through these spacetimes very quickly, trusting that you have encountered them before this. We begin with the case  $\lambda = 0$ . Then

$$V(r) = \frac{1}{r^2}(r - r_+)(r - r_-) , \quad r_{\pm} = M \pm \sqrt{M^2 - e^2} . \quad (137)$$

If  $M < |e|$  the solution is everywhere static and has a naked singularity at  $r = 0$ , as is in fact required by Einstein's theorem. If  $M > |e|$  the solution as given splits into three regions, and  $\xi$  is spacelike when  $r_- < r < r_+$ . There is an outer event horizon at  $r = r_+$  and an inner Cauchy horizon at  $r = r_-$ . Once the solution has been analytically extended as far as possible an infinite number of asymptotic regions appears. In the borderline case  $M = e$  the function  $V(r)$  has a double root. This case is known as the extremal Reissner-Nordström solution, and its Penrose diagram is dramatically different from that of the generic case. In particular there is only one horizon per asymptotic region. The timelike singularities mean that strong cosmic censorship is violated in both cases, but the weak censor

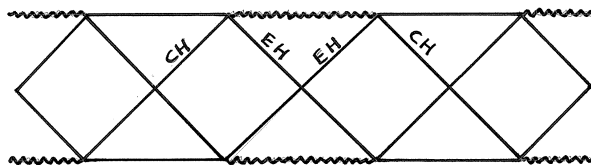


Figure 11: The Schwarzschild-de Sitter spacetime ( $e = 0$ ). There is an event horizon surrounding the black hole, and a cosmological horizon outside it.

is doing her job.

I give the Penrose diagrams without explaining the details of how to draw them—but then I could not explain it better than Walker already did.<sup>11</sup>

For  $e = 0$ ,  $M > 0$ ,  $\lambda > 0$  the Penrose diagram becomes significantly more involved than that of Schwarzschild. When all three parameters are non-zero we obtain something gloriously complicated. We find the location of the horizons by factorizing the quartic polynomial

$$r^2 - 2Mr + e^2 - \frac{\lambda}{3}r^4 = -\frac{\lambda}{3}(r - r_a)(r - r_b)(r - r_c)(r - r_d) . \quad (138)$$

One of the roots is for negative  $r$  and does not appear in the physical spacetime. As in the pure Reissner-Nordström case there are special cases when a pair of roots coincide.

This was not very pedagogical, but we may return to some of these examples later. Meanwhile, just enjoy the diagrams.

### *Null hypersurfaces*

The various solutions that we brought up have a static region, extending out to infinity in the asymptotically flat case. Hence the theory admits non-trivial equilibrium states, which is surprising in view of Einstein's theorem, but not in contradiction to it. The static region also has an inner boundary which is a null hypersurface with very special properties.

First some facts about null hypersurfaces in general. Locally every hypersurface is defined by setting some function of the coordinates to zero. The

---

<sup>11</sup>M. Walker, *Block diagrams and the extension of timelike two-surfaces*, J. Math. Phys. **11** (1970) 2280.

gradient of that function defines the normal vector of the hypersurface, and at each point of the hypersurface the tangent space contains all vectors orthogonal to the normal. If the normal vector is timelike the hypersurface is spacelike, and conversely. But it can happen that the normal vector is null, in which case it is orthogonal to itself—and the normal vector is then tangential to the hypersurface. Such a hypersurface is null. At every point of a null hypersurface there is a preferred null direction within the hypersurface, along which its null normal vector points.

Interestingly the preferred null vector field is geodetic. To see this, consider the equation  $f(x) = c$ , with  $c \in [-\epsilon, \epsilon]$  a constant. Locally this describes a one parameter family of hypersurfaces with normal vectors  $n_a = \nabla_a f$ . We assume that

$$f = 0 \quad \Rightarrow \quad n^2 = g^{ab} \nabla_a f \nabla_b f = 0 . \quad (139)$$

In words  $f = 0$  describes a null hypersurface, but  $f = c$  may not. We now compute

$$n^b \nabla_b n_a = n^b \nabla_b \nabla_a f = n^b \nabla_a \nabla_b f = n^b \nabla_a n_b = \frac{1}{2} \nabla_a n^2 . \quad (140)$$

Two cases arise. Either we are dealing with a one parameter family of null hypersurfaces, in which case  $n^2$  vanishes in a region and the normal vector field  $n^a$ —which then lies within the null hypersurfaces—is geodetic. Or else we have a null hypersurface only if  $c = 0$ , in which case that particular hypersurface is singled out by the equation

$$n^2 = g^{ab} \nabla_a f \nabla_b f = 0 . \quad (141)$$

At the hypersurface it follows that the gradient of  $f$  and the gradient of  $n^2$  point in the same direction, namely along the unique null direction on the hypersurface. Therefore eq. (140) says that the acceleration along the vector field  $n^a$  is aligned with the vector field itself. We can then make the acceleration vanish by means of a reparametrization of the parameter along the vector field, and again we conclude that there is a null geodesic directed along that null direction. The conclusion is that every null hypersurface is ruled by null geodesics.

The intrinsic metric on a null hypersurface is degenerate. In a way it resembles a Newtonian spacetime, in which distances can be measured either

in spacelike directions, or along a preferred time direction (here using the affine parameter along the null geodesics), while a proper notion of spacetime distance is missing. But the inner boundary of the Schwarzschild solution is a very special null hypersurface since it is ruled by a null Killing vector field. It is this property that singles it out as an equilibrium state of the theory, as we will see.

### *Killing horizons*

In all sufficiently small regions spacetime is close to flat. If spacetime has a symmetry, and if you look at it with a sufficiently strong magnifying glass, the Killing vector field will behave like some Killing vector field in Minkowski space. There are then three main cases to consider: translations, rotations, and boosts. There are also various linear combinations of these which we gloss over. The various cases are distinguished by the nature of their fixed points and by the nature of the hypersurfaces on which the norm squared of the Killing vectors vanish.

Translations have no fixed points, and their norms are always non-zero. Rotations do have fixed points—forming timelike 2-planes in Minkowski space. Boosts are more interesting. In Minkowski space, with its standard coordinate system, a typical boost is

$$\xi = T\partial_X + X\partial_T \quad \Rightarrow \quad \xi^2 = T^2 - X^2 . \quad (142)$$

There is a spacelike 2-plane of fixed points at  $T = X = 0$ . More is true; the flow lines are lightlike on a two sheeted null hypersurface

$$T = \pm X . \quad (143)$$

More than that, the flow lines are not only lightlike, they are null geodesics. The two sheets bifurcate at the fixed 2-plane. In general a null hypersurface where a Killing vector field becomes null is called a Killing horizon. The Schwarzschild solution also has a Killing horizon, but its bifurcation surface is a 2-sphere (represented by the central point of its Penrose diagram). The Reissner-Nordström-de Sitter solution has many Killing horizons.

We define the surface gravity  $\kappa$  of a Killing horizon as

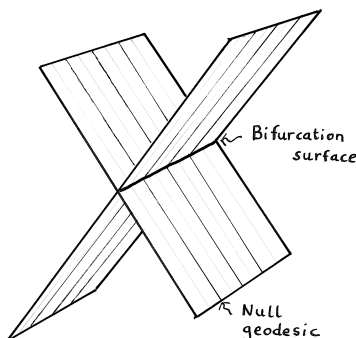


Figure 12: A bifurcate Killing horizon.

$$\nabla_a \xi^2 = -2\kappa \xi_a , \quad (144)$$

evaluated at the horizon itself. This equation will always hold, for some function  $\kappa$ , because we assume that the normal vector of the hypersurface defined by  $\xi^2 = 0$  is null, and we also know that the Killing vector  $\xi$  points along that same direction. It certainly can happen that a Killing vector field becomes null on some timelike hypersurface, but then the story ends because eq. (144) does not hold—there is no Killing horizon.

Let  $v$  be the Killing parameter along the flow lines of the Killing vector field, that is to say that

$$\xi^a \nabla_a v = 1 \quad \Leftrightarrow \quad \xi^a = \frac{dx^a}{dv} . \quad (145)$$

Now recall that on the Killing horizon there are null geodesics directed along these null flow lines. This permits us to interpret surface gravity as a measure of to what extent the Killing parameter differs from the standard affine parameter along a geodesic. To see this, we rewrite the defining equation a little;

$$\kappa \xi_a = -\xi^b \nabla_a \xi_b = \xi^b \nabla_b \xi_a . \quad (146)$$

The conclusion, a necessary one in view of what we already know about null hypersurfaces, is that within the horizon the Killing field is aligned with a geodesic vector field—and there is another preferred parameter along the generators, namely the affine parameter  $\sigma$ . We also note that the surface

gravity  $\kappa$  must be constant along each generator, obviously so because we can move in this direction using an isometry.

To find the relation  $\sigma = \sigma(v)$  between the two preferred parameters, set

$$\dot{x}^a \equiv \frac{dx^a}{d\sigma} = \frac{dv}{d\sigma} \xi^a = \frac{1}{\sigma'} \xi^a , \quad (147)$$

where the prime denotes differentiation with respect to the Killing parameter. A quick calculation then shows that

$$\dot{x}^b \nabla_b \dot{x}^a = \frac{1}{\sigma'^2} \left( \xi^b \nabla_b \xi^a - \frac{\sigma''}{\sigma'} \xi^a \right) . \quad (148)$$

We set this to zero. Comparing to eq. (146) this leads to

$$\frac{\sigma''}{\sigma'} = \kappa . \quad (149)$$

Ignoring two arbitrary integration constants the solution is

$$\sigma = \begin{cases} e^{\kappa v} & \text{if } \kappa \neq 0 \\ v & \text{if } \kappa = 0 . \end{cases} \quad (150)$$

We see that  $\kappa$  enters this relation in an essential way. At the bifurcation surface the affine parameter passes through zero while the Killing parameter  $v$  goes to  $-\infty$ .

The affine parameter, the Killing parameter, and the surface gravity are defined only up to arbitrary numerical factors. In asymptotically flat space-times the standard convention is to insist that the norm of the Killing field tends to one at infinity, and in any case to insist that the surface gravity is non-negative. This normalization is used for the Killing vector  $\partial_t$  in the Schwarzschild solution, but cannot be used for a boost in Minkowski space.

An explicit formula for the surface gravity is

$$\kappa^2 = -\frac{1}{2} \nabla_a \xi_b \nabla^a \xi^b . \quad (151)$$

This can be proved using the observation that  $\xi$  is hypersurface orthogonal on the horizon, implying that

$$\xi_{[a} \nabla_b \xi_{c]} = 0 \quad (152)$$

on the horizon. With this result in hand we go on to prove the important result that the surface gravity is constant on any bifurcate Killing horizon, and not only along each each generator separately. To do so we first observe the fact that  $\kappa$  must be constant along the Killing generators, so that it is enough to show that  $\kappa$  is constant on any cross section of the horizon. Let us choose the bifurcation surface for this purpose. Let  $s^a$  be a tangent vector to the bifurcation surface. Then we deduce that

$$\kappa s^a \nabla_a \kappa = -\frac{1}{2} s^c \nabla_c \nabla_a \xi_b \nabla^a \xi^b = \frac{1}{2} s^c R_{cabd} \xi^d \nabla^a \xi^b = 0 \quad (153)$$

on the bifurcation surface itself—because  $\xi^a$  vanishes there. We used the fact that for any Killing vector field

$$\nabla_c \nabla_a \xi_b = -R_{abcd} \xi^d, \quad (154)$$

which is easily shown to follow from the Killing equation and the Jacobi identity for the curvature.

Bifurcate Killing horizons are generic, but there is a special case where the Killing horizon consists of a single sheet. This is then said to be a degenerate Killing horizon, and is recognized by the fact that its surface gravity vanishes,  $\kappa = 0$  and  $v = \sigma$ . The extremal Reissner-Nordström solution provides an example. A more immediate example is any null plane in Minkowski space, because it is the Killing horizon of a null translation.

To summarize: The overall scale of the surface gravity is arbitrary since it can be changed by a constant renormalization of the Killing vectors, but it has an absolute zero attained by degenerate horizons. Also the surface gravity is the same all over the horizon. This is already enough to see that the surface gravity has properties reminiscent of the temperature of an object in equilibrium. A quantum field theory calculation first done by Hawking gives the interpretation

$$\kappa = 2\pi T_H \quad (155)$$

to the surface gravity of a Killing event horizon, where  $T_H$  is the Hawking temperature of an evaporating black hole. But we do not go into this here.

*Calculating  $\kappa$*



Keeping things as general as the Ansatz (133), and assuming that there is a Killing horizon at  $r = r_H$  so that  $V(r_H) = 0$ , we want to calculate its surface gravity. We do this using Eddington-Finkelstein coordinates, in which the Killing vector is

$$\xi = \partial_v \quad \Rightarrow \quad \xi_a = \nabla_a r . \quad (156)$$

Evidently then

$$\nabla_a \xi^2 = -\nabla_a V(r) = -V'(r) \nabla_a r = -2 \frac{V'(r)}{2} \xi_a . \quad (157)$$

This calculation shows first of all that the hypersurface  $V(r) = 0$  is null, and second—comparing to eq. (144)—it permits us to read off that

$$\kappa = \frac{V'(r_H)}{2} . \quad (158)$$

And the calculation is complete. The subscript on the argument reminds us that we must evaluate the expression at a zero of the function  $V(r)$ . For the event horizon in Schwarzschild we obtain

$$\kappa = \frac{M}{r_H^2} = \frac{1}{4M} . \quad (159)$$

A large black hole means a small surface gravity.

As long as the zero of  $V$  is a simple root the surface gravity comes out finite. If the root is repeated, so that  $V'(r_H) = 0$ , we have a degenerate Killing horizon with vanishing surface gravity. This is what happens for the extremal Reissner-Nordström black hole, see Fig. 10. Indeed, by definition a black hole is said to be extremal if its event horizon is a degenerate Killing horizon.

*What's in a name?*

The name we have given to  $\kappa$  remains obscure. It is based on an interpretation valid for static, but not for stationary, black holes. But this is the case to which we have restricted ourselves to. An observer following a Killing flow line with the unit tangent vector  $u^a = V^{-1/2} \xi^a$  is subject to the acceleration

$$a_a = u^b \nabla_b u_a = -\frac{1}{2V} \nabla_a \xi^2 = \frac{V'}{2V} \nabla_a r \quad \Rightarrow \quad a = \sqrt{a_a a^a} = \frac{V'}{2\sqrt{V}} . \quad (160)$$

Hovering just above the event horizon would be a strenuous affair since the acceleration diverges, but comparing to our formula for the surface gravity we see that

$$\kappa = \lim_{r \rightarrow r_H} (a\sqrt{V}) . \quad (161)$$

On the right hand side the diverging acceleration is multiplied with a redshift factor that tends to zero, so  $\kappa$  stays finite.

The argument that follows is delicate, and we go slowly through it. The energy of a stationary unit mass particle is

$$E = -u_a \xi^a = \sqrt{V} . \quad (162)$$

Reinserting the dimensionful factors we see that the energy of a particle at infinity equals  $mc^2$ , a familiar result.

We are interested in the work required to move a particle along some path in space. This is a differential form  $dW$ . Only shifts in the radial direction require work, so it must be that

$$dW = f_a dx^a = F dr . \quad (163)$$

Now work is force times distance, and the magnitude of the force acting on a stationary particle is the acceleration  $a$  computed above. Therefore, if we act with  $dW$  on a radial tangent vector of unit length, the result must be

$$dW(\sqrt{V}\partial_r) = F\sqrt{V} = a \quad \Rightarrow \quad dW = a \frac{dr}{\sqrt{V}} . \quad (164)$$

This gives the work expended locally when we move the particle in the radial direction.

But suppose that the particle hangs at the end of a massless inelastic string suspended from a rocket ship including a stationary observer. How much work  $W_2$  does the observer at  $r = r_2$  have to spend in order to perform an amount of work  $W_1$  on the particle at  $r = r_2$ ? It is part of the definition of the string that the lengths over which the two ends of the string move are

equal at  $r_2$  and  $r_1$ . But the amounts of work are not. If  $W_1$  is subsequently transformed into pure radiation and beamed back to the observer, this energy will be redshifted, so energy conservation actually requires that  $W_1 > W_2$ . The exact relation is given by introducing a redshift factor:

$$\sqrt{V(r_2)}W_2 = \sqrt{V(r_1)}W_1 . \quad (165)$$

The total work will be equal to force times distance. Since the distances are the same, the force applied by the observer is smaller, by the redshift factor, than the force acting on the particle:

$$F_2 = \sqrt{\frac{V(r_1)}{V(r_2)}}F_1 . \quad (166)$$

Suppose the observer is at infinity, and the particle is kept hovering at the horizon. The force acting on the particle will then be infinite, but the redshift factor will vanish, and the force exerted at infinity is

$$F_\infty = \sqrt{V(r)}a_{r=r_H} = \kappa . \quad (167)$$

Thus  $\kappa$  is the amount of force needed to hold the particle still at the event horizon, assuming that it is held at infinity by a massless inelastic string. “Surface gravity” is a fairly good name for that.

#### Exercises:

- Show that de Sitter space can be embedded in a Minkowski space of one dimension higher, and use this to foliate de Sitter space with spacelike hypersurfaces that are intrinsically flat.
- Derive eqs. (151) and (154).

## OPTICAL AND HYPERBOLIC GEOMETRY

### *Conformal transformations*

Two metric tensors  $g_{ab}$  and  $\hat{g}_{ab}$  are said to be related by a conformal transformation if there exists an everywhere non-vanishing function  $\Omega$  such that

$$\hat{g}_{ab} = \Omega^2 g_{ab} . \quad (168)$$

Note carefully that this is very different from (say) a homothety. No diffeomorphism is involved. The transformation leaves all points fixed and consists only of a rescaling of the metric (and possibly of the matter fields, if any, according to some definite rule).

A conformal transformation distorts lengths but leaves all angles between tangent vectors untouched. A further key property is that the path of a null geodesic according to  $g_{ab}$  is also the path of a null geodesic according to  $\hat{g}_{ab}$ . To see this, note that the affine connection transforms according to

$$\hat{\Gamma}_{bc}{}^a = \Gamma_{bc}{}^a + \frac{1}{\Omega} \left( \delta_b^a \Omega_{,c} + \delta_c^a \Omega_{,b} - g_{bc} g^{ad} \Omega_{,d} \right) . \quad (169)$$

It follows that

$$\ddot{x}^a + \hat{\Gamma}_{bc}{}^a \dot{x}^b \dot{x}^c = \ddot{x}^a + \Gamma_{bc}{}^a \dot{x}^b \dot{x}^c + \frac{1}{\Omega} g^{ad} \Omega_{,d} \dot{x}^2 - \frac{2}{\Omega} \dot{x}^b \Omega_{,b} \dot{x}^a . \quad (170)$$

In the null case,  $\dot{x}^2 = 0$ , one of the terms on the right hand side vanishes. The last term lies in the direction of  $\dot{x}^a$  itself. It follows that if  $x^a(\sigma)$  is a null geodesic according to  $g_{ab}$  it is a null geodesic according to  $\hat{g}_{ab}$  as well, although their affine parameters may differ.

Since the causal structure of spacetime is determined by its null geodesics this means that the causal structure is left invariant by a conformal transformation. This idea is employed whenever we draw a Penrose diagram. Moreover the interplay between conformal transformations and the Einstein equations underlies some of the deepest properties of general relativity, in particular its asymptotic properties and the possibility to define the notion of isolated systems within the theory. But for now we will only use it to play an interesting game with static spacetimes.

### *Optical space*

In a static spacetime the hypersurface forming timelike Killing field splits spacetime into space and time in a natural way. It will also enable us to define the optical geometry of space. To understand what that is, it is best to think about the example of the Schwarzschild solution. But in the following discussion we strike a compromise between concreteness and complete generality, and give the equations for a spherically symmetric static metric of the special form

$$ds^2 = -V(r)dt^2 + \frac{dr^2}{V(r)} + r^2(d\theta^2 + \sin^2\theta d\phi^2) , \quad (171)$$

for some function  $V(r)$ . Space is given by a hypersurface on which the Killing parameter  $t$  is constant and is equipped with the curved metric

$$dl^2 = \frac{dr^2}{V(r)} + r^2(d\theta^2 + \sin^2\theta d\phi^2) . \quad (172)$$

Once we have made the embedding of the equatorial plane of the Schwarzschild example into Euclidean space as Flamm's paraboloid (Fig. 2) we see that nothing remarkable has to happen where  $V(r) = 0$ . Nevertheless this is the boundary of space interpreted as a hypersurface in a static spacetime, so the spatial geometry is clearly missing something.

Any curve in a static spacetime can be projected down to a space curve in a natural way, so we can say that a particle or a photon moves along a space curve—just as we would in everyday life. But it is not true that particles follow spatial geodesics with respect to the spatial metric (172). Planets move on ellipses. Nor is it true that light moves along straight lines, unless we are in the special case  $g_{tt} = -1$ . This rather diminishes the intuitive appeal of this point of view.

Try again. Consider the conformally related metric

$$d\hat{s}^2 = \frac{1}{V(r)}ds^2 . \quad (173)$$

All null geodesics paths remain the same, and their projections down to space also stay the same. But  $\hat{g}_{tt} = -1$ , which means that we are in the special case where they are also geodesics with respect to the spatial metric

$$dl_{\text{opt}}^2 = \frac{dr^2}{V^2} + \frac{r^2}{V}(d\theta^2 + \sin^2\theta d\phi^2) . \quad (174)$$

We have adjusted our notion of “straight” to ensure that light travels along straight lines in space. Optical geometry can be used to study null geodesics as a problem in spatial geometry—and perhaps surprisingly for other purposes as well.

### *The neck and the horizon*

The first observation to make about the optical metric is that the event horizon, or more generally any Killing horizon that bounds the static region, has moved to infinite distance. Radial distance is given by

$$\Delta r_* = \int_{r_1}^{r_2} \frac{dr}{V(r)} , \quad (175)$$

and this integral diverges if  $r_1$  or  $r_2$  tends to a zero of  $V(r)$ . Optical space is infinite in both directions, outwards and inwards. The area of the 2-sphere at some constant value of  $r$  is

$$A = \frac{4\pi r^2}{V(r)} , \quad (176)$$

and it is clear that this radius diverges at any Killing horizon (where  $V = 0$ ) as well as at infinity (if  $V \rightarrow 1$  as  $r \rightarrow \infty$ , as is the case for Schwarzschild). Hence it necessarily has at least one minimum in between. Indeed

$$\frac{dA}{dr} = \frac{4\pi r}{V^2}(2V - V'r) . \quad (177)$$

For the Schwarzschild optical space it follows by insertion of  $V = 1 - 2M/r$  that there is such a “neck” at  $r = 3M$ . Clearly every Great Circle on the sphere at the neck is a geodesic with respect to optical space itself, which means that there are null geodesics circling the black hole—or the very compact star—at this radius. In spacetime the neck corresponds to a timelike 3-surface with the special property that if a null geodesic is tangent to the surface at a point then it is completely contained within the surface.

The existence of a neck in optical space is very important in understanding the physics of objects that are rotating close to the black hole.

The curvature scalar of the optical metric (174) is

$$R_{opt} = -\frac{3V'^2}{2} + 2VV'' + \frac{2V(V-1)}{r^2} + \frac{2VV'}{r} . \quad (178)$$

If we compare to eq. (158) for the surface gravity, and assume that  $V(r)$  is a reasonable function, it follows that

$$\lim_{r \rightarrow r_H} R_{opt} = -6\kappa^2 , \quad (179)$$

where  $\kappa$  is the surface gravity of the horizon at  $r = r_H$ , where  $V(r_H) = 0$ . The curvature of the optical geometry encodes an interesting feature of the event horizon in a nice and quite universal way, given the restriction to static black holes.

### *Embedding diagrams*

The two ends of optical space—the event horizon and spatial infinity—are quite unlike each other since one of them is flat and the other has negative curvature, unless  $\kappa = 0$  and the black hole is extremal. If we now try to embed the optical space as a surface of revolution in a flat space of one dimension higher in order to see what it looks like, we will run into a problem. The analog of Fig. 2 exists only partially.

To see this, use radial distance in the optical geometry as a coordinate, so that the metric becomes

$$dl_{opt}^2 = dr_*^2 + \tilde{r}^2(d\theta^2 + \sin^2\theta d\phi^2) , \quad \tilde{r}^2 = \frac{r^2}{V(r)} , \quad r = r(r_*) . \quad (180)$$

The coordinate  $r_*$  is defined by geodesic distance, eq. (175), and we came across it in the definition of the Eddington-Finkelstein coordinate  $v = t + r_*$ . It is known as the Regge-Wheeler tortoise coordinate; the name has to do with the fact that the event horizon is infinitely distant as far as Achilles is concerned. The function  $\tilde{r}(r_*)$  is the area radius of the round spheres in optical space.

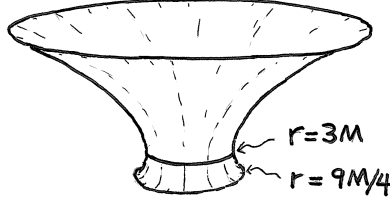


Figure 13: Optical space embedded, down to the Buchdahl limit, in Euclidean space.

Now suppose we want to embed an equatorial section ( $\theta = 0$ ) of optical space into Euclidean 3-space, with the metric

$$dl^2 = d\rho^2 + \rho^2 d\phi^2 + dz^2 . \quad (181)$$

We also insist that it should appear as a surface of revolution there, so the embedding must be given by  $\rho = \rho(r_*)$ ,  $z = z(r_*)$ , and the angles are to be identified. Then we must have

$$\rho = \tilde{r}(r_*) , \quad 1 = \left( \frac{d\rho}{dr_*} \right)^2 + \left( \frac{dz}{dr_*} \right)^2 \quad \Rightarrow \quad \left( \frac{dz}{dr_*} \right)^2 = 1 - \left( \frac{d\tilde{r}}{dr_*} \right)^2 . \quad (182)$$

Evidently this can work only if

$$1 \geq \left( \frac{d\tilde{r}}{dr_*} \right)^2 = \left( \frac{dr}{dr_*} \frac{d\tilde{r}}{dr} \right)^2 = \frac{1}{V} \left( V - \frac{rV'}{2} \right)^2 . \quad (183)$$

In the particular case of the Schwarzschild solution this inequality is

$$1 \geq \frac{(r - 3M)^2}{r(r - 2M)} \quad \Leftrightarrow \quad r \geq \frac{9}{4}M . \quad (184)$$

The embedding will work only down to this radius. At smaller radii the circumference of the surface grows so quickly that it cannot be fitted into Euclidean 3-space.

The problem is really that the optical space becomes more and more like a space of constant negative curvature as we approach the horizon. Already



Hilbert noticed that a surface of constant negative curvature cannot be globally embedded into flat 3-space. A space of negative curvature somehow contains too much space at large distances.

There is a nice connection to physics here. If the Schwarzschild spacetime surrounds a round star rather than a black hole the optical vacuum space should be matched to that of the star at some finite radius. It is known that the radius of a star made up of a perfect fluid—not a bad approximation for a neutron star—and having a regular centre must be larger than  $9M/4$ . This is known as the Buchdahl limit. The geometrical reason is that the optical space at the surface of the star has positive curvature, and then a glance at the embedding diagram shows that the Buchdahl radius corresponds to a limiting case in which the optical geometry of the star is flat. Whether stars whose radii are smaller than  $3M$  exist in nature is somewhat doubtful; it depends on the behaviour of matter at high densities.<sup>12</sup>

The embedding diagram is useful as far as it goes, since we can now use our intuition—nurtured by stretching threads along surfaces, and so on—to locate the geodesics of the surface, and thereby the null geodesics in spacetime. Perhaps I should remind you about how the sign of the intrinsic curvature of a surface embedded in Euclidean space is read off, namely by observing if the surface lies on one side of its tangent plane, or not. If it does the curvature is positive, if not negative. It follows that the surface shown in Fig. 13 has negative curvature. By the way, for a spacelike surface in Minkowski space this rule applies with the sign reversed—the hyperboloid  $x^2 + y^2 - z^2 = -1$  in Euclidean space has positive curvature, but a spacelike hyperboloid in Minkowski space has negative curvature.

### *The Poincaré ball*

Spaces of constant positive curvature are called spheres, and are of considerable interest. Spaces of constant negative curvature are equally or perhaps even more interesting, and we take time out to discuss 3-spaces of this kind. Already in the two dimensional case one can see that constant negative curvature is an interesting case: On a closed surface there will exist a metric

---

<sup>12</sup>L. Samuelsson, *Stellar Models in General Relativity*, PhD Thesis, Stockholm University, 2003.

of constant positive curvature if the topology is that of a 2-sphere, a flat metric if the topology is that of a torus, and a metric of constant negative curvature on every surface of genus higher than one. So negative curvature is infinitely more interesting than the others. At the same time, just as you can get a torus by identifying points in a flat plane, you can get a higher genus Riemann surface by identifying points in an infinite plane equipped with a metric of constant negative curvature. Here we will discuss the analogous three dimensional covering space of all 3-spaces with constant negative curvature. More detail can be found in the literature.<sup>13</sup>

The space we are interested can be presented in at least three different ways. It is useful to be able to flip back and forth between these for calculations, while singling out one of them for visualization. The first way is analogous to how we usually think of spheres. We define a 3-space as the hyperboloid

$$X^2 + Y^2 + Z^2 - U^2 = -1 \quad (185)$$

embedded in a four dimensional Minkowski space. Its metric is that induced on the hyperboloid by the Minkowski metric

$$ds^2 = dX^2 + dY^2 + dZ^2 - dU^2 . \quad (186)$$

This is why the space is also known as hyperbolic 3-space. For the two dimensional hyperbolic plane it follows from the rule of signs mentioned above that its intrinsic curvature is negative. Any Lorentz transformation in the embedding space transforms the hyperboloid into itself, and therefore gives rise to an isometry. There are enough symmetries to ensure that all points on the hyperboloid are connected by isometries, so the curvature must be constant. This space is not only spherically symmetric, it is spherically symmetric around every point.

The embedding coordinates are often convenient for calculations, say for computing geodesics and Killing vectors. The Poincaré ball is better for visualizing things. The intrinsic coordinates  $(x, y, z)$  on the hyperboloid are defined by stereographic projection.<sup>14</sup> Explicitly

---

<sup>13</sup>W. P. Thurston, *How to see 3-manifolds*, Class. Quant. Grav. **15** (1998) 2545.

<sup>14</sup>S. Holst: *Horizons and Time Machines*, PhD Thesis, Stockholm University, 2000.

$$X = \frac{2x}{1 - \rho^2}, \quad Y = \frac{2y}{1 - \rho^2}, \quad Z = \frac{2z}{1 - \rho^2}, \quad U = \frac{1 + \rho^2}{1 - \rho^2}. \quad (187)$$

The allowed range of the intrinsic coordinates is

$$\rho^2 \equiv x^2 + y^2 + z^2 < 1. \quad (188)$$

The intrinsic metric becomes

$$ds^2 = \frac{4}{(1 - \rho^2)^2} (dx^2 + dy^2 + dz^2). \quad (189)$$

Note that we can introduce the conformally related metric

$$d\hat{s}^2 = \frac{(1 - \rho^2)^2}{4} ds^2 = dx^2 + dy^2 + dz^2. \quad (190)$$

Using this metric it is legitimate to include the boundary of the ball in the picture—even though the conformal factor  $\Omega$  vanishes there the hatted metric still makes sense. This manoeuvre is known as conformal compactification, and is very important in general relativity. Flat space can also be conformally compactified, according to the procedure that turns the infinite complex plane into the compact Riemann sphere. In that case infinity is represented by a point. A key feature of hyperbolic space is that “there is a lot of space at infinity”. This can be seen by computing the ratio of the circumference and the radius of a circle, and causes its conformal boundary to be so different from that of flat space.

A third picture, often convenient for calculations, is the upper half space. We again use  $(x, y, z)$  for the intrinsic coordinates, but define them through

$$Y = \frac{y}{x}, \quad Z = \frac{z}{x}, \quad X + U = \frac{1}{x}, \quad X - U = -\frac{x^2 + y^2 + z^2}{x}. \quad (191)$$

The intrinsic metric becomes

$$ds^2 = \frac{1}{x^2} (dx^2 + dy^2 + dz^2). \quad (192)$$

This time the allowed range is

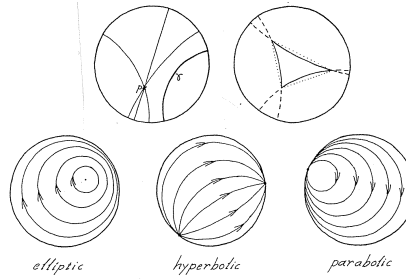


Figure 14: Geodesics (top) and Killing vector fields (bottom) in the hyperbolic plane. Pictures from Holst's PhD thesis.

$$x > 0 , \tag{193}$$

so this is the upper half space. The metric is manifestly conformally flat in both pictures, ball and half space, so all angles are given correctly in the pictures while distances are distorted—badly so near the conformal boundary (the surface of the ball), which is infinitely far away from every point in the interior as measured by the true metric.

In both pictures a geodesic appears as a segment of a circle (or straight line) meeting the conformal boundary at right angles. The angle sum of a triangle will always be less than  $\pi$ , and if its circumference is given its area is smaller than Euclidean intuition would suggest. See Fig. 14.

The isometries of hyperbolic space are Lorentz transformations of the flat Minkowski space in which the hyperboloid is embedded. Rotations have a line—that is a geodesic—of fixed points going through the ball, while Lorentz boosts have a pair of fixed points (one source and one sink) on the boundary. The flow lines are circles or (in the case of a boost) segments of circles. A nice detail is that there is one and only one flow line of every boost that is also a geodesic. It is interesting to observe that the isometries act as Möbius transformations of the conformal boundary—the conformal boundary is a sphere, which is the same as the complex plane with the point at infinity added. An equatorial section of the Poincaré ball—a Poincaré disk—is transformed into itself by a subgroup of Möbius transformations, isomorphic to the subgroup that takes the unit circle in the complex plane into itself.

*Some surfaces within the Poincaré ball*

Our immediate purpose is to understand how an equatorial section of the Schwarzschild optical geometry looks like when embedded in the Poincaré ball. For this we need to understand how a surface of constant intrinsic curvature looks like there. The answer is that it will look like a sphere. Let us consider a surface that looks like a sphere in coordinate space. It is given by the equation

$$(x - x_0)^2 + (y - y_0)^2 + (z - z_0)^2 = r_0^2 . \quad (194)$$

It should be kept in mind that the point  $(x_0, y_0, z_0)$  is not at the centre of the sphere—it is not situated at constant distance from the surface, and it may even lie outside hyperbolic space. There will be various cases corresponding to spheres lying inside or outside the ball, or intersecting the boundary either in circles or in single points. If we rewrite the equation in Minkowski coordinates, using eq. (187), we find that it becomes

$$k_\alpha X^\alpha = \sqrt{r_0^2 - k \cdot k} , \quad (195)$$

where we introduced the four vectors

$$X^\alpha = (X, Y, Z, U) \quad \text{and} \quad k_\alpha = (x_0, y_0, z_0, \frac{1}{2}(r_0^2 - x_0^2 - y_0^2 - z_0^2 - 1)) . \quad (196)$$

Therefore the sphere in the ball corresponds to the intersection of a hyperplane with the hyperboloid. If the hyperplane is spacelike the intersection will give rise to a sphere inside the ball, provided that a suitable condition holds. If the hyperplane is timelike there will always be an intersection, but only a segment of the sphere will lie in the ball. If the plane is null the sphere will intersect the boundary of the ball in a point, and the sphere will be inside the ball provided that a condition holds.

We would like to compute the intrinsic geometry of these spheres. We will use our freedom to flip back and forth between the various pictures. Consider first a sphere lying inside the ball. In the hyperboloid picture this corresponds to the intersection of the hyperboloid with a spacelike hyperplane, and since all metric properties are preserved by Lorentz transformation we lose no generality if we bring the hyperplane to the standard form

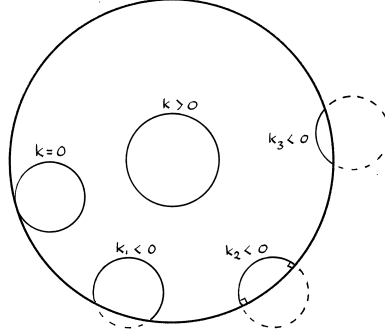


Figure 15: An equatorial section of the Poincaré ball, including some embedded spheres of varying intrinsic curvatures ( $k_3 < k_2 < k_1$ ). One of the embedded spheres (curvature  $k_2$ ) is totally geodesic.

$$U = c . \quad (197)$$

Provided that  $c > 1$  this corresponds to a sphere centered at the origin of the ball;

$$\rho^2 = \frac{c-1}{c+1} . \quad (198)$$

If we insert this condition in the line element for the ball we obtain the induced line element on the embedded sphere, namely

$$d\gamma^2 = \frac{4}{1-\rho^2}(d\rho^2 + d\Omega^2) = 2(c-1)d\Omega^2 . \quad (199)$$

Hence the intrinsic metric has constant positive curvature. The same is of course true for all spheres lying entirely in the ball—we can compute their curvatures by first going to Minkowski space and then bring their spacelike hyperplane to standard form by means of a Lorentz boost.

The curvature of a sphere touching the boundary in one point can be found by first working out its null hyperplane in Minkowski space and then rotating this plane to the standard form

$$X + U = c . \quad (200)$$

Next we use this condition in the upper half plane metric, where it corresponds to  $x = c$ . The induced line element is simply

$$d\gamma^2 = \frac{1}{c^2}(dy^2 + dz^2) . \quad (201)$$

Hence the intrinsic metric on the sphere is flat. Such spheres have a name—they are called horospheres, flat planes conformally compactified to a sphere by the addition of a single point from the conformal boundary of the Poincaré ball.

Finally, a sphere that has a segment inside the ball corresponds to a timelike hyperplane in Minkowski space. We bring it to the standard form

$$Z = c . \quad (202)$$

In the upper half plane this corresponds to  $z = cx$ . Inserting this condition in the line element and rescaling the coordinate  $x$  yields

$$d\gamma^2 = \frac{1}{x^2}(dx^2 + dy^2 + c^2 dx^2) = \frac{1 + c^2}{x'^2}(dx'^2 + dy^2) . \quad (203)$$

This is a surface of constant negative intrinsic curvature, given in upper half plane coordinates. By changing coordinates we can exhibit it as a Poincaré disk, with a conformal boundary sitting as a circle on the conformal boundary of the Poincaré ball. A particularly interesting case is  $c = 0$ , or more generally any timelike plane through the origin in embedding space. This corresponds to segments of spheres meeting the boundary of the ball at right angles. They are totally geodesic surfaces, which means that any geodesic in the surface is also a geodesic in the embedding space.

### *Embedding, once more*

We can now make another embedding diagram of an equatorial section of the optical space of the Schwarzschild solution. It has an asymptotically flat end, and another end where the curvature tends towards constant and negative. This is easily embedded in a Poincaré ball. Since the event horizon touches the conformal boundary of the ball in a circle it follows that it can be approximated by a segment of something that looks like a sphere in the

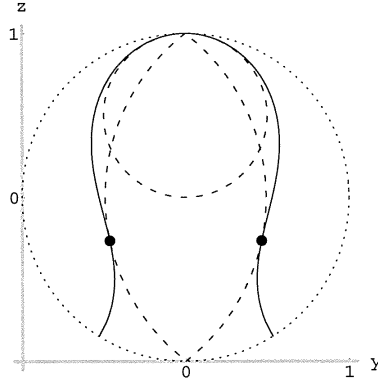


Figure 16: A section through our embedding diagram. Killing flow lines are shown dashed, to make it evident where the neck is sitting. Taken from M. A. Abramowicz et al., *Class. Quant. Grav.* **19** (2002) 3963.

picture, which given what we now know about such surfaces means that the intrinsic curvature becomes asymptotically constant and negative there.

Because the picture distorts distances we have to think a little to locate the neck. In the embedding space it is really a bottleneck: we ask for the radius of the largest sphere that can be pushed by means of an isometry through the interior of the embedded surface. In the picture this means that one has to find a Killing vector field with one flowline along the axis of revolution, and then work out where the flowlines are tangential to the embedded surface of revolution. This defines a circle representing the neck. To locate the Buchdahl radius  $r = 9M/4$ , where embedding into Euclidean space fails, we let a flat horosphere touch infinity at  $y = 0$  in Fig. 16, and then blow it up until it touches the surface.

### *Surfaces, totally geodesic surfaces, and the Gauss-Bonnet theorem*

We have used the term “totally geodesic surface” several times already. To make sure that its meaning does not escape you: this is a surface (or perhaps a hypersurface) such that any geodesic tangential to the surface stays in the surface when you extend it to arbitrary parameter values. In this case, and in this case only, there is a very simple relation between the Riemann



tensor  $R_{abcd}$  of the embedding space and the Riemann tensor  $\bar{R}_{ijkl}$  of the surface. The latter is simply a projection down to the surface of the former. In equations, if the intrinsic coordinates on the surface are  $x^i$ , and if the embedding is given by the parametric equations  $x^a = x^a(x^i)$ , we have

$$\bar{R}_{ijkl} = x^a_{,i} x^b_{,j} x^c_{,k} x^d_{,l} R_{abcd} . \quad (204)$$

In this equation  $x^a_{,i}$  evaluated at a point on the surface is just a matrix that projects an arbitrary tangent vector to a vector tangential to the surface. For surfaces that are not totally geodesic there are further terms on the left hand side.

Now recall that for two dimensional surfaces the Riemann tensor is determined by the Riemann scalar  $\bar{R}$ ,

$$\bar{R}_{ijkl} = \frac{\bar{R}}{2} (\gamma_{ik} \gamma_{jl} - \gamma_{il} \gamma_{jk}) = k (\gamma_{ik} \gamma_{jl} - \gamma_{il} \gamma_{jk}) , \quad (205)$$

where  $k = \bar{R}/2$  is known as the Gaussian curvature of the surface. This is also known as a sectional curvature of the embedding space. The idea is that at any point in a space of arbitrary dimension we can choose a two dimensional subspace of the tangent space and create a surface element by extending geodesics in these special directions. By construction this surface element will be totally geodesic, and its Gaussian curvature is then said to be a sectional curvature of the full space. This is a purely local construction: if you try to extend the geodesics to all parameter values you will typically find that they begin to intersect each other, which means that the totally geodesic surface element cannot be extended to a globally well behaved surface. In other words, totally geodesic surfaces are rare. Most spacetimes do not have any.

In a spherically symmetric spacetime an equatorial section is totally geodesic, and since every geodesic lies in some equatorial section one does not lose much understanding of geodesics by restricting oneself to an equatorial section. This is the first reason why our embedding diagrams work so well. The embedding diagrams for optical space are good for a second reason because a null geodesic in spacetime projects to a geodesic in optical space. This means that we can use our intuition for how geodesics within a surface behave to understand the behaviour of null geodesics in a four dimensional spacetime. We see at a glance that the neck is a totally geodesic surface in

optical space, which means that null geodesics tangent to this surface will circle the black hole for ever.

Sticking to surfaces for a while we recall Euler's formula for the number of vertices  $V$ , edges  $E$ , and faces  $F$  of a polyhedron:

$$V - E + F = 2 . \quad (206)$$

The faces of the polyhedron may be polygons with any number of vertices. If a polygon is divided into triangles the number of edges and faces will change in such a way that the formula remains valid, so we may just as well assume that all faces are triangles.

By projecting the faces onto a sphere we obtain a triangulation of the sphere. Any surface can be divided into regions that are diffeomorphic to triangles. This is said to be a triangulation of the surface. We adopt the rule that if the triangles intersect they do so either in one common edge or in one common vertex. In elementary topology it is shown that such a triangulation defines a topological invariant called the Euler number  $\chi$ . Euler's formula is then modified to

$$V - E + F = \chi . \quad (207)$$

The point is that for a given surface the Euler number comes out the same regardless of how the triangulation is done, provided that we follow the rule. It follows that the Euler number of a sphere is  $\chi = 2$ . To compute the Euler number of a torus it is best to begin by dividing it up into quadrangles, making sure that these have at most one vertex or one edge in common. To get a surface of higher genus one keeps adding handles (in the form of a torus with a face removed) to a given surface. In this way one finds that the torus has Euler number  $\chi = 0$  and a closed surface of genus  $g$  has  $\chi = 2 - 2g$ . The Euler invariant can as well be computed for surfaces that are not closed. In particular, a region of the plane bounded by a closed curve has the same topology as a sphere with a hole in it, and its Euler number is  $\chi = 1$  (just remove one face from the triangulation of the sphere). An annulus is topologically identical to a cylinder and to a sphere with two holes in it, and therefore it has  $\chi = 0$  (just remove two faces from the sphere).

At this point the Gauss-Bonnet theorem provides an interesting link between the local and the global geometry of a surface.<sup>15</sup> Suppose that we

---

<sup>15</sup>S. S. Chern, *From triangles to manifolds*, Amer. Math. Mon. **86** (1979) 339.

have a surface  $S$  bounded by a curve which is smooth, except perhaps at  $n$  “corners” where the tangent vector turns through an angle  $\delta_i$ . Then the statement is that

$$\sum_{i=1}^n \delta_i + \int_{\partial S} k_g ds + \int_S k dS = 2\pi\chi(S) . \quad (208)$$

Here  $k$  is the sectional curvature on the surface, and  $k_g$  is the curvature of the bounding curve—what we would refer to as the proper acceleration of the curve, had it been the timelike worldline of an observer.

Why is this true? Suppose first that the region bounded by the curve is simply connected ( $\chi = 1$ ). The statement is then that the tangent vector turns through the angle  $2\pi$  as we go around its boundary, but the turning is distributed among the three terms on the left hand side. If the region is flat ( $k = 0$ ) and its boundary a circle only the second term contributes—and the formula obviously holds since  $k_g$  is inversely proportional to the radius of the circle. If the boundary is a triangle only the first term contributes because the tangent vector turns only at the vertices. Moving on to geodetic triangles in a plane with arbitrary curvature  $k$  some of the turning is done by the third term. We observe that the angle  $\delta_i$  can be related to the interior angle at the vertex by  $\delta_i = \pi - \alpha_i$ . Remembering that  $k_g = 0$  and  $\chi = 1$  we immediately obtain

$$\sum_{i=1}^3 \delta_i + \int_S k dS = 2\pi \quad \Leftrightarrow \quad \sum_{i=1}^3 \alpha_i = \pi + \int_S k dS . \quad (209)$$

We see that the angle sum of a geodetic triangle is smaller or larger than  $\pi$  depending on the sign of the curvature. It is not difficult to verify this formula for the hyperbolic plane: use half plane coordinates and Stokes’ theorem to convert the right hand side to an integral along the boundary. Still there is something very remarkable about the Gauss-Bonnet formula, because its right hand side is purely topological while its left hand side is evaluated using a metric—and the point is that any metric that you can define on the surface will give the same result.

An immediate application concerns closed surfaces with genus  $g$ . In this case there is no boundary, so the Gauss-Bonnet theorem states that

$$\frac{1}{2} \int_S R dS = \int_S k dS = 2\pi\chi(S) = 4\pi(1 - g) . \quad (210)$$

It is perhaps worth noting that in two dimensions the integrand  $\sqrt{g}R$  can be written as a total divergence—but the formula is still true, because the quantity it is a total derivative of is not globally defined on the closed surface. It follows from eq. (210) that every metric on the sphere must be such that there is a point with  $k > 0$  somewhere. Similarly all Riemann surfaces of genus higher than 1 must have a point with  $k < 1$ . The theorem does not in itself suffice to prove that the metric can be chosen so that the curvature is constant, but this is true anyway.

### *Bending of light*

In a space of negative intrinsic curvature geodesics tend to diverge from each other. How is the negative curvature of optical space consistent with the way that the Sun bends light, and in fact tends to focus light?

We begin with the question if two geodesics emanating from the same point will cross each other again. If so they form a lune  $S$  with geodetic edges and two corners. Let us first assume that  $S$  is simply connected ( $\chi = 1$ ), in which case the Gauss-Bonnet theorem gives for the interior angles that

$$\alpha_1 + \alpha_2 = \int_S k dS . \quad (211)$$

But the left hand side is positive, so the lune can exist only if the curvature of the lune obeys  $k > 0$ , at least on average. This is consistent with what we know of spheres and of the Euclidean and hyperbolic planes—and it seems as if we have proved that geodesics in optical space cannot cross twice. But optical space has a hole in it. If the geodesics pass on different sides of the black hole the lune will have Euler number  $\chi = 0$ . If both geodesics pass outside the neck the hole in the lune can be bounded by the closed geodesic at  $r = 3M$ , and the equation becomes

$$\alpha_1 + \alpha_2 = 2\pi + \int_S k dS . \quad (212)$$

Now the Gauss-Bonnet theorem does allow the geodesics to cross. In this sense the bending of light around the black hole is a global rather than a local effect. Indeed it is even possible for a single geodesic to cross itself. Provided it also surrounds the circle at  $r = 3M$  the Gauss-Bonnet theorem gives for the angle of crossing that

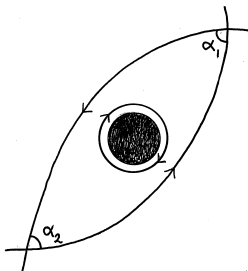


Figure 17: Two geodesics go around the photon sphere (another geodesic) and cross again, consistently with eq. (212). Incidentally, if nothing emits light below the photon sphere, the observer will see a black disk starting at  $r = 3M$ .

$$\alpha = 2\pi + \int_S k dS . \quad (213)$$

Again this is easy to satisfy even though  $k$  is negative.

It is possible to use the Gauss-Bonnet theorem for quantitative discussions of the bending of a single light ray by a black hole.<sup>16</sup> We surround the region of interest with a circle of such a large radius  $R$  that it can be regarded as sitting in Euclidean space. A geodesic passing outside the Sun—and outside the geodetic neck of optical space—meets this circle at right angles, and divides its circumference into two arcs of length  $(\pi \pm \delta)R$ , where the deflection angle is what we are trying to calculate. The geodesic divides the interior of the circle into two parts  $D_{\pm}$ . Applying eq. (208) to the part not containing the mass concentration at the center we find

$$\delta = - \int_{D_-} k dS . \quad (214)$$

To get an approximate answer we assume that the geodesic passes far enough from the Sun to be regarded as the straight line

$$r \sin \phi = b , \quad (215)$$

where  $b$  gives the distance of closest approach. To lowest order in  $1/r$  we have

---

<sup>16</sup>G. W. Gibbons and C. M. Warnick, *Universal properties of the near-horizon optical geometry*, Phys. Rev. **D79** (2009) 064031.

$$k \approx -\frac{2M}{r^3} \quad \Rightarrow \quad \delta = \int_0^\pi d\phi \int_{b/\sin\phi}^\infty dr \frac{2M}{r^2} = \frac{4M}{b} = \frac{4GM}{c^2 b} . \quad (216)$$

When this effect was first measured by Eddington he was interested in light rays just grazing the surface of the Sun. Since the radius and the mass of the Sun are related by  $R_\odot = 2.4 \times 10^5 \times 2M_\odot$  the approximations made are amply justified. The prediction for such a light ray is  $\delta = 1.7$  arc seconds.

### *Centrifugal forces*

Remarkably, the optical metric turns out to be very useful as a tool for understanding a wide range of at first sight counter-intuitive physical effects in static spacetimes. In particular, thinking in terms of the optical geometry enables one to define “centrifugal forces” in a surprisingly useful way. According to this definition the centrifugal force on a particle orbiting a static black hole is a velocity dependent force acting in the direction of  $\nabla_a \tilde{r}$ , where  $\tilde{r}$  is the area radius of the round spheres according to the optical geometry. In particular then there are no centrifugal forces acting on particles that are orbiting, at any speed, the Schwarzschild black hole at  $r = 3M$ . In a sense space is turned inside-out around the neck in the geometry. This is arguably the most interesting part of this story, but I have to refer elsewhere for it.<sup>17</sup>

### Exercises:

- Where is the neck in the optical geometry of the Schwarzschild-de Sitter spacetime?
- Show that the optical space of the extremal Reissner-Nordström solution admits a discrete conformal isometry interchanging the regions on both sides of its neck.

---

<sup>17</sup>M. A. Abramowicz and A. R. Prasanna, *Centrifugal-force reversal near a Schwarzschild black hole*, Mon. Not. R. astr. Soc. **245** (1990) 720.

- Sketch a proof of the Gauss-Bonnet theorem, or give a detailed discussion of as many special cases as suffices to convince you that it holds.

## WHAT IS THE MATTER?

### *The stress-energy tensor*

If we want a spherically symmetric spacetime to become dynamical we must include matter in Einstein's equation

$$R_{ab} - \frac{1}{2}g_{ab}R = 8\pi T_{ab} . \quad (217)$$

On the right hand side we have the symmetric stress-energy tensor, made up from the metric and from matter fields obeying equations guaranteeing that  $\nabla^a T_{ab} = 0$ . Given a stress-energy tensor and the world line of an observer we can identify local energy densities, local energy flows, and internal stresses in objects, as experienced by this observer. This is a purely local description, and the equivalence principle is called on to bring our special relativistic understanding of these notions into action.

Specifically, suppose that the world line of the observer has the unit tangent vector  $t^a$ . Introduce a tetrad of vector fields  $e_I^a$  such that

$$g_{ab}e_I^a e_J^b = \eta_{IJ} , \quad (218)$$

where  $\eta_{IJ}$  is the Minkowski metric. This is called a Lorentz frame, and we adapt it to our observer by requiring that  $e_0^a = t^a$ . The triplet of vector fields  $e_i^a$  are then spacelike. The local energy density relative to this Lorentz frame is now defined as

$$\rho = e_0^a e_0^b T_{ab} = T_{ab} t^a t^b , \quad (219)$$

the energy-momentum four vector density as

$$\pi_I = -e_I^a T_{ab} t^b , \quad (220)$$

and the spatial stress tensor as

$$S_{ij} = e_i^a e_j^b T_{ab} . \quad (221)$$

The component  $S_{ij}$  is the  $i$ -component of force across a unit area perpendicular to the  $j$ -direction inside the body.



We cannot be specific about the stress-energy tensor itself without specifying what kind of matter we want to model, but in order to agree with what we know about the behaviour of matter it must obey certain inequalities. Notably it is expected to obey the weak energy condition. This states that for every timelike vector  $t^a$  it is true that

$$T_{ab}t^at^b \geq 0 . \quad (222)$$

The local energy density—which we believe can be understood from the point of view of special relativity—is bounded from below. By continuity the inequality holds for all non-spacelike vectors. A stronger requirement is the dominant energy condition, which requires both that the weak energy condition holds and that the vector

$$P_a = -T_{ab}t^b \quad (223)$$

is non-spacelike and future pointing for every timelike vector  $t^a$ . This is closely related to causality (“local energy fluxes occur slower than light”), as we will come to appreciate later on.

A third requirement that is frequently imposed is the strong energy condition, which says that

$$\left(T_{ab} - \frac{1}{2}g_{ab}T^c_c\right)t^at^b \geq 0 \quad (224)$$

for every timelike  $t^a$ . Despite its name the strong energy condition does not imply the weak energy condition. Moreover the motivation for imposing it is that it helps in proving theorems about the behaviour of spacetime, rather than any strong expectation that matter must behave this way.

### *Timelike congruences and the Raychaudhuri equation*

We make a brief detour in order to see where the strong energy condition comes from. Consider a congruence of timelike curves, that is to say look at some region of spacetime such that one and only one of these curves pass through every given point in the region. In equations

$$x^a = x^a(\sigma; y^i) , \quad (225)$$

where  $\sigma$  is an affine parameter and the  $y^i$  are labelling the individual curves. It is useful to think of the congruence as the flow of a fluid, and then these labels form what is known as a Lagrangian coordinate system. A unit tangent vector of a curve is denoted  $u^a$ , and we use the abbreviation  $D = u^a \nabla_a$ . Now consider a vector field  $\eta^a$  that is Lie dragged along the congruence,

$$\mathcal{L}_{\vec{u}}\eta^a = 0 \quad \Leftrightarrow \quad D\eta^a \equiv u^b \nabla_b \eta^a = \eta^b \nabla_b u^a \equiv B^a_b \eta^b . \quad (226)$$

Because it commutes with  $u^a$  the vector field  $\eta^a$  can be thought of as pointing along some Lagrangian coordinate line. Intuitively it gives the separation between neighbouring fluid elements. The object

$$B_{ab} = \nabla_b u_a = u_{a;b} \quad (227)$$

(the old fashioned semicolon notation makes it easy to remember the ordering of the indices) evidently describes how  $\eta^a$  changes as it is dragged along a curve.

We now simplify matters by assuming that all the curves are geodesics. This means that  $D(u_a \eta^a) = 0$ , so we can take  $\eta^a$  to be ortogonal to  $u^a$  if we wish. Moreover it follows that

$$B_{ab} u^b = u^b B_{ba} = 0 , \quad (228)$$

so  $B_{ab}$  is a tensor that lives in the hypersurface elements orthogonal to the curves. We introduce a projector field  $h_{ab}$  projecting any element in a tangent space orthogonally down to such a hypersurface element;

$$h^a_b = \delta^a_b + u^a u_b , \quad h_{ab} u^b = 0 . \quad (229)$$

We use this projector to take the trace of  $B_{ab}$  and can then decompose  $B_{ab}$  into three irreducible parts,

$$B_{ab} = B_{(ab)} + B_{[ab]} = \frac{\theta}{3} + \sigma_{ab} + \omega_{ab} . \quad (230)$$

The trace part

$$\theta \equiv h^{ab} B_{ab} = h^{ab} \nabla_b u_a = \nabla_a u^a \quad (231)$$

is known as the expansion of the congruence. As its name indicates a non-zero expansion gives rise to a volume change in a comoving fluid element. The traceless part

$$\sigma_{ab} \equiv B_{(ab)} - \frac{\theta}{3} h_{ab} \quad (232)$$

is known as the shear of the congruence. A non-zero shear will cause a spherical fluid element to become an ellipsoid, with no change in volume. Finally

$$\omega_{ab} \equiv B_{[ab]} = \nabla_{[b} u_{a]} \quad (233)$$

is known as the twist or vorticity of the congruence and will cause the fluid element to rotate. The congruence is hypersurface forming if and only if its twist vanishes.

We want to know how expansion, twist, and shear change as we move along the congruence. For this purpose we derive that

$$DB_{ab} = -B^c{}_b B_{ac} + R_{cbad} u^c u^d \quad (234)$$

(This is easy to verify because the presence of the Riemann tensor on the right hand side tells you to begin by changing the order of the derivatives on the left hand side.) Taking the trace of this equation we derive the celebrated Raychaudhuri equation

$$\dot{\theta} \equiv D\theta = -\frac{1}{3}\theta^2 - \sigma_{ab}\sigma^{ab} + \omega_{ab}\omega^{ab} - R_{ab}u^a u^b \quad (235)$$

The presence of twist will increase the expansion, and this is reasonable if we think of the twist as giving rise to “centrifugal” forces. The presence of shear and expansion on the other hand will increase focusing. The twist changes according to

$$D\omega_{ab} = -\frac{2}{3}\theta\omega_{ab} - 2\sigma^c{}_{[b}\omega_{a]c} \quad (236)$$

If the twist is zero it stays zero, which means that if we start off a geodetic congruence in the direction of the normal of a hypersurface it will stay hypersurface orthogonal for as long as it remains a congruence—that is as long as the geodesics do not start to cross each other, which will happen if the expansion becomes negative infinite.

The evolution of shear is given by the symmetric trace-free part of eq. (234), viz.

$$\begin{aligned}
D\sigma_{ab} = & -\frac{2}{3}\theta\sigma_{ab} - \sigma_{ac}\sigma^c_b - \omega_{ac}\omega^c_b + \frac{1}{3}h_{ab}(\sigma_{cd}\sigma^{cd} - \omega_{cd}\omega^{cd}) + \\
& + C_{cbad}u^c u^d + \frac{1}{2}\bar{R}_{ab} , \quad \bar{R}_{ab} = (h_{ac}h_{bd} - \frac{1}{3}h_{ab}h_{cd})R^{cd} .
\end{aligned} \tag{237}$$

Here  $C_{abcd}$  is the Weyl tensor, i.e. the traceless part of the Riemann tensor. The lesson is that, generically, spacetime curvature will give rise to shear even if we start out the congruence without shear. This shear will then enter the Raychaudhuri equation (235) and cause the geodesics to attract each other.

Now we can understand what the strong energy condition says. Using Einstein's equation, condition (224) simply says that

$$R_{ab}u^a u^b \geq 0 . \tag{238}$$

In Hawking and Ellis this inequality is called the timelike convergence condition. If it holds the Raychaudhuri equation tells us that the expansion along a hypersurface forming geodesic congruence can only decrease. Indeed if  $\theta < 0$  to begin with the geodesics are bound to cross ( $\theta \rightarrow -\infty$ ) if they live long enough. This seemingly innocent statement is the starting point of Penrose's singularity theorems and Hawking's area increase theorem for black holes.

### *A separation of scales*

Back to matter. What is it? In principle the Standard Model gives a stress-energy tensor, but if we are interested in describing the Universe this is a poor choice. The matter content of the Universe is concentrated in atoms, and the relevance of elementary particle physics is largely confined to the interior of their nuclei. It simply determines the masses of the nucleons. Once we are clearly above the length scale of atoms and molecules even electromagnetic forces are of limited relevance since charges tend to average out. We describe everyday objects without any reference to their microscopic structure. This suppression of the internal degrees of freedom is not absolute, as it would be

were they confined to a black hole, but is nevertheless very effective—and it is precisely when this suppression is in force that gravity begins to dominate the scene. Hence the stress-energy tensor is usually regarded as made up from phenomenological fields taken from theories such as fluid dynamics or kinetic theory.

### *Dust*

Perhaps the simplest matter model one can think of is called dust. Its stress-energy tensor is given by

$$T_{ab} = \rho u_a u_b , \quad (239)$$

where  $\rho$  is some function and  $u^a$  is a timelike vector field of unit length which defines the local rest frame of the dust. To ensure the consistency of Einstein's equations we impose

$$\left\{ \begin{array}{l} u^a \nabla_a u^b = 0 \\ \nabla_a (\rho u^a) = 0 \end{array} \right\} \Rightarrow \nabla_a T^{ab} = 0 . \quad (240)$$

The function  $\rho$  must therefore be constant along a timelike geodesic vector field, and the motion of the dust defines a geodesic congruence. Physically it consists of particles in free fall. (In cosmology the particles would in fact be galaxies.) As long as  $\rho \neq 0$  the implication in (240) goes the other way too, but this is accidental. The weak, dominant, and strong energy conditions all agree that  $\rho \geq 0$ .

The idea to think of a congruence of curves as the flow of the fluid can now be justified. If the congruence is geodesic the fluid consists of freely falling dust. However, precisely because dust follows geodesics there is a problem with dust matter. When the expansion  $\theta$  of the congruence becomes negative infinite—as Raychaudhuri's equation tells us it will in generic circumstances—the geodesics cross each other and form caustics where the matter density diverges. In the spherically symmetric case such caustics are called shell crossing singularities—and are artefacts of the over-simplified matter model.

In the Vaidya solution we encountered a variant of this matter model where the vector  $t^a$  is null. It describes a pressureless radiation fluid, if you like incoherent electromagnetic radiation, and is colloquially referred to as null dust.

### *Perfect fluids*

We can go one step beyond dust and consider perfect fluids. They are “perfect” in the sense that there is neither heat conduction nor viscosity, and they have the stress-energy tensor

$$T_{ab} = (\rho + p)u_a u_b + p g_{ab} . \quad (241)$$

For the comoving observer this diagonalizes and becomes spatially isotropic. No special direction is singled out by the stress tensor, which is simply given by the scalar pressure  $p$ . As in the case of dust the field equations can be derived from the Bianchi identity  $\nabla^a T_{ab} = 0$ , but to complete the model we need to specify an equation of state  $p = p(\rho)$ .

The energy conditions provide some model independent constraints on the fluid. The weak energy condition implies that

$$\rho \geq 0 \quad \text{and} \quad \rho + p \geq 0 . \quad (242)$$

The first inequality follows when the arbitrary non-spacelike vector  $t^a$  in (222) is set equal to  $u^a$ , and the second when it equals a null vector of the form  $u^a + s^a$ , where  $s \cdot u = 0$ . The dominant energy condition (223) can be unravelled in a similar way, and implies

$$\rho \geq 0 \quad \text{and} \quad -p \leq \rho \leq p . \quad (243)$$

This is an obvious strengthening of the weak energy condition. Finally the strong energy condition (224) demands

$$\rho + 3p \geq 0 \quad \text{and} \quad \rho + p \geq 0 . \quad (244)$$

It is clear from Fig. 18 that this does not imply (nor is it implied by) the more physically motivated weak energy condition.

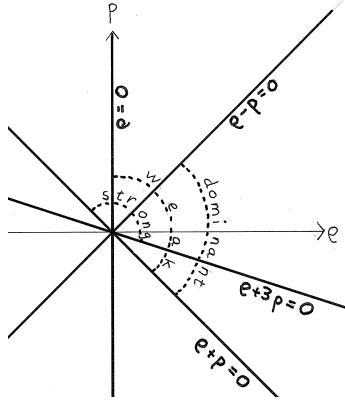


Figure 18: Three energy conditions imposed on a perfect fluid.

This matter model has many applications. Cosmology is one. In fact the assumption of spherical symmetry together with the Copernican principle—all points in space are equivalent—force perfect fluids on us. The fluids we encounter there have equations of state of the simple form

$$p = k\rho, \quad (245)$$

with  $k$  a constant. If  $k = 0$  we have dust (galaxies), if  $k = 1/3$  we have incoherent radiation (the cosmic microwave background), and if  $k = -1$  we can move the entire stress-energy tensor to the left hand side of Einstein's equations and regard it as a contribution from a cosmological constant, with a constant and negative pressure. In the case of radiation the trace of the stress-energy tensor vanishes, as it does for all electromagnetic fields. Furthermore it is quite reasonable to model stars as perfect fluids. A particularly clear cut case is that of cold neutron stars, for which both the energy density and the pressure are given as functions of the number density of the nucleons. This forces the equation of state to take the simple form  $p = p(\rho)$ , with no other variables entering. The calculation of that function is not an easy task however.

For perfect fluids there exists a kind of converse of Birkhoff's theorem, stating that the only static solution is spherically symmetric. Its proof is very much more difficult than that of Birkhoff's, and has been carried through

under some restrictions on the equation of state.<sup>18</sup>

Perfect fluids share one problem with the special case of dust matter, namely that shocks can develop and solutions become singular also if the equations are solved in flat space. This kind of singularities will appear in solutions of Einstein's equation as well, but they clearly signal a breakdown of the matter model and tend to obscure the issue of purely gravitational singularities.

### *Scalar fields and the Einstein-Vlasov equation*

A matter model that cannot be accused of creating spurious singularities is that of electromagnetic fields, but if spherical symmetry is imposed this is a non-dynamical kind of matter. One way out is to add a scalar field to the Einstein action. There definitely are spherically symmetric propagating wave solutions of the Klein-Gordon equation. Another possibility is to use the general relativistic version of the collisionless Boltzmann equation. We will not go into this in any detail, but it is worth recalling the Newtonian version of the equations. The matter field is a distribution  $f = f(t, x, v)$ , where  $x$  and  $v$  are phase space coordinates of the particles. The spatial density is

$$\rho(t, x) = \int f(t, x, v) d^3v . \quad (246)$$

By assumption the particles influence each other through gravitational forces only, and the Newton-Vlasov equations are

$$\frac{\partial f}{\partial t} + v^a \frac{\partial f}{\partial x^a} - \delta^{ab} \frac{\partial U}{\partial x^a} \frac{\partial f}{\partial v^b} = 0 \quad (247)$$

$$\Delta U = -4\pi\rho , \quad (248)$$

where  $\Delta$  is the flat space Laplacian and  $U$  is the gravitational potential. These equations play a large role in galactic dynamics, and much is known about them. Indeed there is a theorem stating that if one starts with initial data in the form of a  $C^1$  (once differentiable) function  $f_0(x, v)$  with compact

---

<sup>18</sup>R. Beig and W. Simon, *On the uniqueness of static perfect-fluid solutions in general relativity*, Commun. Math. Phys. **144** (1992) 373.



support (vanishing outside some finite region) then there exists a solution  $f(t, x, v)$  which is  $C^1$  for all times  $t$ .

But we can recover dust matter from the collisionless Boltzmann equation by setting

$$f_{\text{dust}} = \rho(x)\delta^{(3)}(v - v(x)) . \quad (249)$$

Since the equations are linear in  $f$  such distributions can be handled. However, one observes that there now exists solutions that develop singularities in the form of infinite densities in finite time. The theorem I referred to tells us that these singularities disappear if the delta-function is smoothed out a little in phase space. The conclusion is that dust matter brings in spurious singularities.

The relativistic version of the Newton-Vlasov equation exists, and has been much studied over the past twenty years or so.<sup>19</sup> (In this area of physics progress is steady but slow.) Whether the resulting Einstein-Vlasov equation has any direct physical application is not so clear, but as an ingredient in the study of Einstein's equation it has many advantages. It is plausible that any shell focussing singularity of the kind we encountered in the Vaidya solution will dissolve—in its causal future we would have one ingoing and one outgoing stream of null dust, and would be at liberty to concentrate on the purely gravitational part of the singularity. But we would have to study massive dust in order to apply this idea directly.

This concludes our menu of useful matters. Now what does matter do?

### *Stars*

It was Eddington who first dared to exploit to the full the idea that stars are balls consisting of a perfect gas. Assuming that no convection occurs stars are held up by internal pressure. This leads to the equation of hydrostatic support, which in its Newtonian version reads

$$\frac{dp}{dr} = -\frac{Gm\rho}{r^2} . \quad (250)$$

---

<sup>19</sup>A. D. Rendall, *Cosmic censorship and the Vlasov equation*, Class. Quant. Grav. **9** (1992) L99.

Here we assume that the star is spherical and non-rotating, and  $\rho = \rho(r)$  is the matter density. Finally  $m = m(r)$  is the mass contained inside the radius  $r$ , given by

$$m(r) = \int_0^r 4\pi\rho r^2 dr . \quad (251)$$

For a star such as the Sun the equation of state can be taken to be of the form  $p = p(\rho, T)$ , which brings in the temperature as a new variable. Additional equations involving the rate of energy production and the luminosity of the star are needed to close the system. A white dwarf on the other hand is well approximated as a degenerate Fermi gas at zero temperature. Both the density and the pressure can be expressed as functions of the number density of the fermions, and therefore the equation of state will be of the form  $p = p(\rho)$ . The same is true for neutron stars, but for the latter the gravitational field is so intense that general relativity theory plays a major role. Another way of saying this is that the Newtonian star models need to be amended only in a regime where the pressure is non-thermal, so that the problem simplifies at the same time as it becomes more difficult.

The metric is assumed to take the spherically symmetric form

$$ds^2 = -e^{2\Phi} dt^2 + \frac{dr^2}{1 - \frac{2m}{r}} + r^2 (d\theta^2 + \sin^2 \theta d\phi^2) . \quad (252)$$

The Einstein equations, including a perfect fluid stress-energy tensor, tell us that

$$G_t^t = 8\pi T_t^t \quad \Leftrightarrow \quad \frac{dm}{dr} = 4\pi\rho r^2 \quad (253)$$

$$G_r^r = 8\pi T_r^r \quad \Leftrightarrow \quad \frac{d\Phi}{dr} = \frac{m + 4\pi r^3 p}{r(r - 2m)} \quad (254)$$

$$\nabla_a T_r^a = 0 \quad \Leftrightarrow \quad \frac{dp}{dr} = -(\rho + p) \frac{d\Phi}{dr} . \quad (255)$$

The rest of the Einstein equations are then automatically satisfied. Eq. (255) will give us the explicit form of the metric once  $\rho$  and  $p$  are known.

In the Newtonian limit  $p$  can be ignored compared to  $m$  and  $\rho$ , and the function  $\Phi$  can be interpreted as the Newtonian potential—which is of course why the  $g_{tt}$  component of the metric was written in the form it was.

By comparing the relativistic equation to its Newtonian counterpart (250) we observe the striking feature that “pressure gravitates”: the pressure itself contributes to the right hand side, which means that an attempt to counteract a strong gravitational field with strong outward pressure will be self-defeating if the field is strong enough. A somewhat related fact is that the negative pressure from the cosmological constant causes the universe to expand faster, rather than the other way around.

The solution of eq. (253) is identical with its Newtonian counterpart. At first sight this is surprising, since one would expect the total amount of mass within radius  $r$  to be given as

$$m_{\text{m}}(r) = \int \rho dV = \int_0^r \frac{4\pi\rho r^2}{\sqrt{1-2m/r}} dr . \quad (256)$$

Actually this is quite reasonable—we can interpret  $E_{\text{b}} = m_{\text{m}} - m > 0$  as the gravitational binding energy if we like. So this is consistent with our interpretation of the Misner-Sharp mass function as the total energy inside a given area radius. For a neutron star this binding energy amounts to about 10 % of its rest mass—to be compared with the nuclear binding energy of the most tightly bound nucleus, that of iron, which is only about 1 % of the rest mass. Presumably this energy left the star in an explosion of considerable force.

Combining eqs. (254-255) we obtain the relativistic version of the equation of hydrostatic support,

$$\frac{dp}{dr} = -(\rho + p) \frac{m + 4\pi r^3 p}{r(r - 2m)} . \quad (257)$$

This is known as the Tolman-Oppenheimer-Volkov equation, and is a necessary and sufficient condition for equilibrium. Given an equation of state of the form  $p = p(\rho)$  we can proceed to solve the equation. The correct way to do this is to assume a central density  $\rho(0) = \rho_c$ , and integrate outwards. After discretization this can be left to a computer. The computer will be instructed to stop when it reaches a radius  $R$  such that  $p(R) = 0$ . We have then reached the surface of the star, and there we match the solution to the Schwarzschild vacuum.

### *An exact solution*

Before we cast a brief look at realistic neutron star models we follow Schwarzschild himself in considering stars with constant density  $\rho_0$ , or more precisely

$$\rho(r) = \begin{cases} \rho_0 & , \quad r \leq R \\ 0 & , \quad r > R \end{cases} . \quad (258)$$

This is totally unrealistic as a model of a star. In the Newtonian case it would make sense as a model of a moon made of water. Still the solution we are heading for does give some interesting insights, so we proceed with the calculation. In the interior of the star—we call it a star—we have

$$m(r) = \frac{4\pi}{3} \rho_0 r^3 . \quad (259)$$

The total mass of the star is

$$M = \frac{4\pi}{3} \rho_0 R^3 . \quad (260)$$

This is true both relativistically and non-relativistically.

In the Newtonian case the equation of hydrostatic support is

$$\frac{dp}{dr} = -\frac{m\rho}{r^2} = -\frac{4\pi}{3} \rho_0^2 r . \quad (261)$$

We solve it “backwards” by integrating inwards from the surface at  $r = R$ , remembering that  $p(R) = 0$ . The solution is

$$p(r) = \frac{2\pi}{3} \rho_0^2 (R^2 - r^2) \quad \Rightarrow \quad p(0) = \frac{2\pi}{3} \rho_0^2 R^2 = \left(\frac{\pi}{6}\right)^{\frac{1}{3}} M^{\frac{2}{3}} \rho_0^{\frac{4}{3}} . \quad (262)$$

There is nothing remarkable here.

Moving on to relativistic stars the equation of hydrostatic support becomes, upon inserting the simple expression for  $m(r)$ ,

$$\frac{dp}{dr} = -(\rho + p) \frac{m + 4\pi r^3 p}{r(r - 2m)} = -\frac{4\pi}{3} (\rho_0 + p)(\rho_0 + 3p) \frac{r}{1 - \frac{8\pi}{3} \rho_0 r^2} . \quad (263)$$

This is easily integrated. After a modest amount of algebra we arrive at the solution

$$p(r) = \rho_0 \frac{\sqrt{1 - 2M/R} - \sqrt{1 - 2Mr^2/R^3}}{\sqrt{1 - 2Mr^2/R^3} - 3\sqrt{1 - 2M/R}} . \quad (264)$$

The central pressure is

$$p(0) = \rho_0 \frac{\sqrt{1 - 2M/R} - 1}{1 - 3\sqrt{1 - 2M/R}} . \quad (265)$$

But this diverges if

$$\frac{2M}{R} = \frac{8}{9} < 1 . \quad (266)$$

This is known as the Buchdahl limit. Perfect fluid stars with constant density and regular centers cannot be made more compact than this. The result is important because it can be extended to derive upper bounds on the masses of neutron stars also under quite realistic assumptions about the equation of state.

It only remains to solve for the metric, and check that it can be joined to an exterior vacuum solution. Using our solutions for  $m(r)$  and  $p(r)$  eq. (254) becomes, upon examination,

$$\frac{d\Phi}{dr} = \frac{d}{dr} \ln \left( \sqrt{1 - 2Mr^2/R^3} - 3\sqrt{1 - 2M/R} \right) . \quad (267)$$

A proper choice of the integration constant ensures that the  $t$ -coordinates on both sides of the surface of the star agree. We have arrived at Schwarzschild's interior solution

$$ds^2 = -\frac{1}{4} \left( 3\sqrt{1 - 2M/R} - \sqrt{1 - 2Mr^2/R^3} \right)^2 dt^2 + \frac{dr^2}{1 - 2Mr^2/R^3} + r^2 (d\theta^2 + \sin^2 \theta d\phi^2) . \quad (268)$$

The spatial geometry is that of a round 3-sphere.

### *Neutron stars and their stability*

The most interesting stars from the point of view of relativity theory are the neutron stars. We have already argued that they can be regarded as perfect fluids held up by non-thermal pressure. A possible flaw in the argument is that they could turn solid. They are in fact expected to have a solid crust, but it seems quite likely that their interior are in a fluid state. They will typically rotate, but probably not by so much that their structure is seriously affected by this. So it should be possible to use the formulas we have at hand to describe them. The calculation of their equations of state  $p = p(\rho)$  is a question for nuclear physicists. A major source of uncertainty is that core densities will exceed the nuclear density ( $10^{17}$  kg/m<sup>3</sup>), so there is little guidance from experiment to act as a check on the calculated equations of state. Our earlier claim that Nature has matter organized into atoms, and that strong and weak interactions are irrelevant outside their nuclei, needs a little amendment here. The core of a neutron star is in itself a giant atomic nucleus, and partly unknown properties of the strong interaction are needed to calculate its behaviour. But it remains true that gravity is the only long-range force in the game.

Each equation of state will give rise to a one-parameter family of solutions of the Tolman-Oppenheimer-Volkov equation, parametrized by the central density  $\rho_c$  that we give to the computer. A sketch of the result, for an equation of state that is about as good as people have been able to make it, is given in Fig. 19. There are only two relevant segments on the curve, labelled “white dwarfs” and “neutron stars”, respectively. The segment in between these, as well as the continuation of the curve beyond its leftmost maximum, are physically irrelevant because they correspond to unstable solutions. There is an easy way to see this, called the Poincaré turning point method, which I will now explain. It enables us to see at a glance on the set of equilibrium states what states are stable, and what states are unstable. No calculations are necessary.

The obvious way to investigate stability is to perturb the equilibrium state, so that the fluid elements execute small movements. Such perturbations can be radial or tangential. The latter are strongly damped and can be ignored as far as the question of stability is concerned—although in a neutron star the damping is caused by gravitational waves, so from other points of view this is the interesting part. Radial perturbations can be expanded into

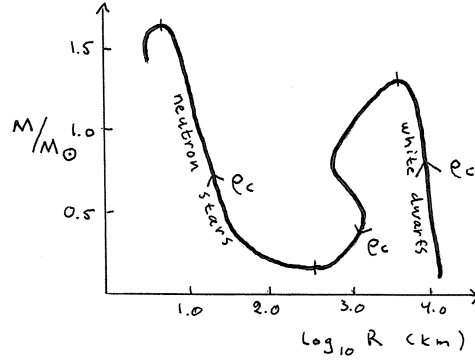


Figure 19: Possible equilibrium states of a cold static star, as computed by experts.

a discrete set of normal modes, of the form

$$\xi_n(r, t) = \xi_n(r)(Ae^{i\omega_n t} + Be^{-i\omega_n t}) . \quad (269)$$

The solution is stable if all the frequencies  $\omega_n$  are real, and unstable otherwise. We will have to make some assumptions about the spectrum of normal modes, namely

- i) the space part  $\xi_n(r)$  has an even or an odd number of zeroes depending on whether  $n$  is even or odd,
- ii) the normal frequencies are non-degenerate,  $\omega_0^2 < \omega_1^2 < \omega_2^2 < \dots$ , and there is no level crossing,
- iii) the curves representing  $\omega_n^2(\rho_c)$  are never tangent to the line  $\omega^2 = 0$ ,
- iv) the star is stable at low densities.

Actually anyone of these assumptions could fail, so the turning point method is not completely watertight.

We will move along the curve of equilibrium states in the direction of increasing density, and we ask what happens if a particular mode reaches  $\omega_n = 0$  for some  $\rho_c$ . This is then a time independent displacement of  $\rho$ , and therefore turns one equilibrium state into another one. This can only happen at constant energy  $M$ , so we reach the important conclusion that changes in stability occur if and only if the curve of equilibrium states passes through an extremum, where its slope is horizontal. In Fig. 20 I have distorted the calculated curve a bit, to ensure that there are many such points  $(a, b, \dots, h)$ . Now consider the modes  $\xi_n(t, r)$  in some more detail. The centre of the star

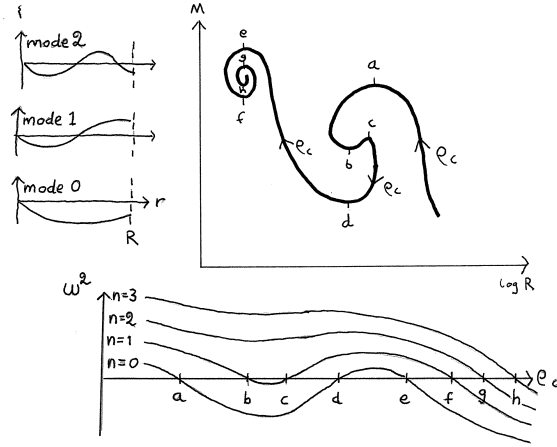


Figure 20: A slightly distorted equilibrium series for stars. To the left we see the typical behaviour of some normal modes, and at the bottom we see how they change between oscillatory and growing as we move along the series.

is not moved by the pulsation, so we must have  $\xi(0) = 0$ , and if we are moving in the direction of increasing central density the star must be moving inwards in the neighbourhood of its centre, hence  $\xi(r) < 0$  for small values of  $r$ . But assumption i) then implies that the radius of the star is decreasing if the mode is even, and increasing if the mode is odd. The conclusion is that an even mode is passing through zero at the points  $a, d, e, g$ , and an odd mode is passing through zero at  $b, c, f, h$ . Assumption iv) then forces us to conclude that the star becomes unstable at  $a$  because its lowest frequency normal mode passes through zero there. Assumptions ii) and iii) assure us that things proceed in an orderly fashion, so as we follow the curve of equilibrium states we see that there must be two unstable modes between  $b$  and  $c$ , one unstable mode between  $c$  and  $d$ , no unstable mode between  $d$  and  $e$ , and so on. The spectrum of the normal modes must behave as sketched in Fig. 20. One unstable mode is enough to kill the star, so stability holds only before  $a$  and between  $d$  and  $e$ .

The Poincaré turning point method has many applications besides this one, and since it gives something almost for nothing is well worth remembering.



### Mass bounds

Perhaps the most interesting feature of Fig. 19 is that there is a maximum mass above which no stable neutron star exists. The precise value of this mass cannot be determined by relativity theory alone, since Einstein's vacuum equation—with the cosmological term, irrelevant here, set to zero—is scale invariant.

Let us assume not only an equation of state of the form  $p = p(\rho)$ , but also that  $\rho \geq 0$ ,  $p \geq 0$ , and

$$\frac{dp}{d\rho} > 0 . \quad (270)$$

This is needed for microscopic stability—were this not true compression of the star would lead directly to collapse on small scales. We also assume that the equation of state is known up to some fiducial density  $\rho_0$ , which we take to be the nuclear density  $\rho_0 = 2.9 \cdot 10^{17} \text{ kg/m}^3$ . This gives a scale to the problem. Inside the radius  $r_0$  where this density is reached lies a core of unknown constitution. However, given that the pressure decreases with radius it follows directly from (270) that the density does too. From this we derive an inequality for the mass  $M_0$  of the core,

$$M_0 = \int_0^{r_0} 4\pi r^2 \rho \, dr \geq \frac{4\pi}{3} r_0^3 \rho_0 . \quad (271)$$

On the other hand we have the Buchdahl bound

$$\frac{2M_0}{r_0} < \frac{8}{9} . \quad (272)$$

Equality would be reached only for an incompressible core. In a plot of  $M_0$  against  $r_0$  the allowed region must lie above the cubic curve defined by the first bound, and below the straight line defined by the second. The largest allowed  $M_0$  occurs where the two curves intersect. In this way we end up with a bound on  $M_0$  which is

$$M_0 \leq \frac{4}{9\sqrt{3\pi}} \frac{1}{\sqrt{\rho_0}} = \frac{4}{9\sqrt{3\pi}} \frac{c^3}{G\sqrt{G\rho_0}} = 6.7 M_\odot . \quad (273)$$

(The Sun's mass is  $2.0 \cdot 10^{30} \text{ kg}$ .) To this we must add the mass of the envelope of the star, which is calculable (and not very large) since the equation of

state is known below  $\rho_0$ . On the other hand the bound we have derived is not optimal.<sup>20</sup> By making further assumptions the bound on the total mass of the neutron star can be brought down to about  $3 M_\odot$ . Anything heavier than this, and compressed to such small radii, must be a black hole—unless Nature has some very unexpected trick up her sleeve.

Typical neutron stars have a radius of around 12 km and weigh in at around 1.4 solar masses. The heaviest specimen known so far weighs  $1.97 \pm 0.04 M_\odot$ . It has been possible to determine its mass that precisely because it is part of a binary system with an unusually massive white dwarf companion. Its orbital plane is seen almost edge on so that the Shapiro time delay of the pulsar signals can be used to infer the mass of the companion with precision.<sup>21</sup> Note that an equation of state describing a star mostly composed of nucleons results in higher masses than the “soft” (compressible) equations of state derived from more exotic matter models involving hyperon or kaon condensates. Some models of the latter kind are therefore now excluded. Come to think of it the equation of state that gave Fig. 19 is in some need of amendment too.

### Exercises:

- Decipher Lemma 4.3.1 and the Conservation Theorem in Hawking and Ellis: the dominant energy condition is needed for causality.
- Study the optical geometry of Schwarzschild’s interior solution, and how it appears in the embedding diagram.

---

<sup>20</sup>J. B. Hartle, *Bounds on the mass and moment of inertia of non-rotating neutron stars*, Phys. Rep. **46** (1978) 201.

<sup>21</sup>P. B. Demorest, T. Pennucci, S. M. Ransom, M. Roberts, and J. W. T. Hessels, *A two-solar-mass neutron star measured using Shapiro delay*, Nature **467** (2010) 1081.

## THE TOLMAN-BONDI SOLUTION

### *Normal coordinates*

Geodesics can be used to set up coordinate systems in a systematic way. Riemannian normal coordinates are based on geodesics emanating from some special point whose neighbourhood one wants to study. Gaussian normal coordinates are based on a congruence of geodesics emanating from some special hypersurface in the direction of its normal. In relativity that hypersurface is typically spacelike, and the congruence then consists of timelike geodesics. The Eddington-Finkelstein coordinates on the other hand are adapted to a congruence of null geodesics.

Typically a significant amount of work is needed to set up coordinate systems of this type. We will go through this for a congruence of radially infalling timelike geodesics in the Schwarzschild spacetime. We first solve the geodesic equation, and then turn these geodesics into coordinate lines with proper time as the coordinate along them. At first there is no suggestion that there is a fluid flow associated with this congruence, but we will get there eventually—by which time we are no longer dealing with a vacuum spacetime.

### *Free fall in Schwarzschild*

Because of the Killing vector  $\partial_t$  there are two conserved charges for a radial geodesic, so the equations for a geodesic at fixed  $\theta, \phi$  read

$$-V(r)\dot{t}^2 + \frac{\dot{r}^2}{V(r)} = -1, \quad V(r)\dot{t} = E; \quad V(r) = 1 - \frac{2M}{r}. \quad (274)$$

We first consider a congruence of geodesics reaching a maximal area radius at some given time  $t$ . It is then convenient to introduce a new constant  $R$  through

$$E^2 = V(R) = 1 - \frac{2M}{R} \quad \Rightarrow \quad \dot{r}^2 = V(R) - V(r). \quad (275)$$

It follows that  $\dot{r} = 0$  when  $r = R$ , so the constant  $R$  equals the maximal area radius reached by the given geodesic. There it stops and falls back again.

It is straightforward to solve the geodetic equations. We have

$$d\tau = -\sqrt{\frac{R}{2M}} \frac{\sqrt{r}dr}{\sqrt{R-r}} . \quad (276)$$

We do the substitution  $r = R \cos^2 \frac{\eta}{2}$ , and obtain the solution—a cycloid—in parametric form,

$$\begin{aligned} r(\eta) &= \frac{R}{2}(1 + \cos \eta) \\ \tau(\eta) &= \sqrt{\frac{R^3}{8M}}(\eta + \sin \eta) . \end{aligned} \quad (277)$$

The clock was set so that  $r = R$  at proper time  $\tau = 0$ . We observe that the the time it takes to go from maximum radius to the singularity at  $r = 0$  is

$$\Delta\tau = \pi\sqrt{\frac{R^3}{8M}} . \quad (278)$$

It remains to solve for  $t(\tau)$ . Again in parametric form a solution is

$$t(\eta) = 2M \left[ \sqrt{\frac{R}{2M} - 1} \left( \eta + \frac{R}{4M}(\eta + \sin \eta) \right) + \ln \left[ \frac{\sqrt{\frac{R}{2M} - 1} + \tan \frac{\eta}{2}}{\sqrt{\frac{R}{2M} - 1} - \tan \frac{\eta}{2}} \right] \right] \quad (279)$$

where  $r > 2M$  was assumed (since  $\tan \eta/2 = \sqrt{R/r - 1}$ ). If  $r < 2M$  just switch the sign inside the logarithm. Also, an integration constant was adjusted to ensure that maximum radius is reached at  $t = 0$ . This geodetic congruence passes the hypersurface  $t = 0$  in the direction of its normal.

Other radial congruences exist. We may insist that  $\dot{r} \rightarrow 0$  at infinity, in which case the geodesics “fall” with the escape velocity everywhere. We then choose  $E = 1$  and find that the proper time needed to fall from some given  $r = r_1$  to some arbitrary  $r$  is

$$\tau = -\int_{r_1}^r \frac{\sqrt{r}dr}{2M} = \frac{4M}{3} \left( \left( \frac{r_1}{2M} \right)^{\frac{3}{2}} - \left( \frac{r}{2M} \right)^{\frac{3}{2}} \right) . \quad (280)$$

We also find, up to an integration constant,

$$t = \int^r \frac{d\tau}{dr} \frac{dr}{V(r)} = -2M \left[ \frac{2}{3} \left( \frac{r}{2M} \right)^{\frac{3}{2}} + 2\sqrt{\frac{r}{2M}} + \ln \frac{\sqrt{\frac{r}{2M}} - 1}{\sqrt{\frac{r}{2M}} + 1} \right] . \quad (281)$$

This time the solution is fully explicit.

### *Coordinates adapted to a congruence*

We now use the geodetic congruences we have found to build Gaussian normal coordinate systems. One coordinate will be the proper time along the geodesics, and three coordinates will be used to label the geodesics. We begin with the “marginally bound” congruence where the geodesics move with the escape velocity. They are labelled by  $\theta$ ,  $\phi$ , and the  $r_1$  occurring in eq. (280), but it is convenient to trade  $r_1$  for the new coordinate

$$R = \frac{4M}{3} \left( \frac{r_1}{2M} \right)^{\frac{3}{2}} . \quad (282)$$

The proper time  $\tau$  will also be used as a coordinate, and eq. (280) can then be inverted to read

$$r = (2M)^{\frac{1}{3}} \left( \frac{3}{2}(R - \tau) \right)^{\frac{2}{3}} . \quad (283)$$

The event horizon is at  $r - \tau = 4M/3$  and the singularity at  $r - \tau = 0$ .

Taking partial derivatives we compute that

$$r_{,R} = -r_{,\tau} = \sqrt{\frac{2M}{r}} = \sqrt{1 - V(r)} . \quad (284)$$

The integration constant in eq. (281) will be some function of  $R$ , so we set

$$t = -2m \left[ \frac{2}{3} \left( \frac{r}{2M} \right)^{\frac{3}{2}} + 2\sqrt{\frac{r}{2M}} + \ln \frac{\sqrt{\frac{r}{2M}} - 1}{\sqrt{\frac{r}{2M}} + 1} \right] + g(R) . \quad (285)$$

Then

$$t_{,\tau} = \frac{\partial t}{\partial r} \frac{\partial r}{\partial \tau} = \frac{1}{V(r)} , \quad t_{,R} = \frac{\partial t}{\partial r} \frac{\partial r}{\partial R} + g_{,R} = -\frac{1}{V(r)} + g_{,R} . \quad (286)$$

Now we are in a position to transform the line element to the new coordinates. A straightforward calculation gives, for the part orthogonal to the round spheres, that

$$\begin{aligned} ds^2 &= -V(r)(t_{,\tau}d\tau + t_{,R}dR)^2 - \frac{(r_{,\tau}d\tau + r_{,R}dR)^2}{V(r)} = \\ &= -d\tau^2 + 2(1 - g_{,R})d\tau dR + \frac{1 - V - (1 - Vg_{,R})^2}{V(r)}dR^2 . \end{aligned} \quad (287)$$

Evidently it is convenient to choose  $g(R) = R$ . Then we arrive at the Schwarzschild metric in the Lemaître coordinate system,

$$\begin{aligned} ds^2 &= -d\tau^2 + \frac{2MdR^2}{r} + r^2(d\theta^2 + \sin^2\theta d\phi^2) = \\ &= -d\tau^2 + r_{,R}^2 dR^2 + r^2(d\theta^2 + \sin^2\theta d\phi^2) . \end{aligned} \quad (288)$$

The function  $r = r(\tau, R)$  is given by eq. (283). The coordinate  $\tau$  has a clear meaning as the proper time along radial geodesics, and the coordinate system is perfectly regular at the event horizon.

We now turn to the other radial congruence, which is time symmetric since all geodesics reach their maximum area radius at  $t = 0$ . Again we have a coordinate  $R$  that labels the geodesics, but this time the function  $r = r(\tau, R)$  is only known in parametric form, and this makes the calculation quite tricky. The function  $t = t(\tau, R)$  is also implicitly known, from eq. (279).

What we have explicitly is a function  $r = r(\eta, R)$ , which has a different functional form from  $r = r(\tau, R)$ . Using the notation that is standard in thermodynamics we can show that

$$r_{,\tau} \equiv \left( \frac{\partial r}{\partial \tau} \right)_R = -\sqrt{V(R) - V(r)} \quad (289)$$

$$r_{,\eta} \equiv \left( \frac{\partial r}{\partial \eta} \right)_R = \left( \frac{\partial \tau}{\partial \eta} \right)_R \left( \frac{\partial r}{\partial \tau} \right)_R = -\frac{R}{2} \sin \eta . \quad (290)$$

The calculation that follows would look clearer if thermodynamical notation were used throughout, but unfortunately it would also look clumsy. So, with the understanding that from now and until further notice all derivatives with respect to  $R$  are taken at constant  $\eta$ , we have (ignoring the sphere part of the metric)

$$\begin{aligned} ds^2 = & -V(r)dt^2 + \frac{dr^2}{V(r)} = - \left( V(r)t_{,\eta}^2 - \frac{r_{,\eta}^2}{V(r)} \right) d\eta^2 - \\ & -2 \left( V(r)t_{,\eta}t_{,R} - \frac{r_{,\eta}r_{,R}}{V(r)} \right) d\eta dR + \left( \frac{r_{,R}^2}{V(r)} - V(r)t_{,R}^2 \right) dR^2 . \end{aligned} \quad (291)$$

If we take the trouble to derive, starting from eq. (279), that

$$t_{,R} = \frac{1}{\sqrt{V(R)}} \left( r_{,R} + \frac{r_{,\tau}r_{,R}}{V(r)} \right) , \quad (292)$$

we can rewrite the line element as

$$\begin{aligned} ds^2 = & -\tau_{,\eta}^2 d\eta^2 - 2\tau_{,\eta}\tau_{,R} d\eta dR + \left( \frac{1}{V(R)} (r_{,R} - r_{,\tau}\tau_{,R})^2 - \tau_{,R}^2 \right) dR^2 = \\ & = -d\tau^2 + (r_{,R} - r_{,\tau}\tau_{,R})^2 \frac{dR^2}{V(R)} . \end{aligned} \quad (293)$$

We are almost there. Using thermodynamical notation we have the identity

$$\left( \frac{\partial r}{\partial R} \right)_\tau = \left( \frac{\partial r}{\partial R} \right)_\eta - \left( \frac{\partial r}{\partial \tau} \right)_R \left( \frac{\partial \tau}{\partial R} \right)_\eta . \quad (294)$$

The time has come to switch and regard the area radius as a definite function  $r = r(\tau, R)$ . We know this function only in the parametric form given by eqs.

(277), but it does exist. In this way we arrive at the Schwarzschild metric in the form

$$ds^2 = -d\tau^2 + \frac{r_{,R}^2 dR^2}{1 - \frac{2M}{R}} + r^2 (d\theta^2 + \sin^2 \theta d\phi^2) . \quad (295)$$

Derivatives of  $r$  with respect to  $R$  are to be taken at constant  $\tau$ , which again has a clear meaning as the proper time along radial geodesics.

This coordinate system fails at  $R = 2M$ , that is if we try to start out the geodesics at the bifurcation sphere in the event horizon. We can handle this with a trick due to Einstein and Rosen, and to Novikov. We define a new radial coordinate  $R'$  through

$$R = 2M(1 + R'^2) , \quad 1 - \frac{2M}{R} = \frac{R'^2}{1 + R'^2} . \quad (296)$$

This is just a relabelling of the geodesics, but we can extend the range of  $R'$  to the entire real axis. The metric is

$$ds^2 = -d\tau^2 + \frac{(1 + R'^2)r_{,R'}^2 dR'^2}{R'^2} + r^2 (d\theta^2 + \sin^2 \theta d\phi^2) , \quad (297)$$

where  $r = r(\tau, R')$  is again given in parametric form. These coordinates cover the entire Schwarzschild manifold.

### *The Tolman-Bondi solution*

We now modify the Schwarzschild spacetime to include a freely falling dust. To do so we will rely on Synge's method a second time. We make the Ansatz

$$ds^2 = -d\tau^2 + \frac{r_{,R}^2}{1 - K} dR^2 + r^2 (d\theta^2 + \sin^2 \theta d\phi^2) , \quad (298)$$

where  $K$  and  $r$  are functions of  $R$  and  $\tau$ . As usual the Misner-Sharp mass function  $m$  is defined using the area radius as

$$g^{ab} \nabla_a r \nabla_b r = 1 - \frac{2m}{r} . \quad (299)$$

It follows that



$$r_{,\tau}^2 = \frac{2m}{r} - K . \quad (300)$$

Next we compute the Einstein tensor  $G_{ab}$  and see if we can obtain a sensible  $T_{ab}$  in this way. As long as  $r_{,R} \neq 0$  we find that  $G_{\tau R}$  vanishes if and only if  $K$  is a function of  $R$  only, so we assume this. The vanishing of  $G_{RR}$  is then (as long as we also require  $r_{,\tau} \neq 0$ ) equivalent to the condition that the mass function  $m$  is a function of  $R$  only. This amounts to a restriction on the function  $r = r(\tau, R)$ , and it is the only restriction since the vanishing of  $G_{\theta\theta}$  is now automatic. The remaining component  $G_{\tau\tau}$  does not vanish, but we can use it to define a dust density  $\rho$ . In conclusion the Einstein equations including dust reduce to eq. (300), together with

$$K_{,\tau} = 0 \quad (301)$$

$$m_{,\tau} = \frac{r_{,\tau}}{2}(2rr_{,\tau\tau} + r_{,\tau}^2 + K) = 0 \quad (302)$$

$$8\pi\rho = \frac{2m_{,R}}{r^2 r_{,R}} . \quad (303)$$

Here we used Synge's method to identify the stress-energy tensor, and obtained a quite reasonable answer, provided the free functions are chosen in such a way that  $\rho \geq 0$ . The mass function  $m$  depends only on  $R$  because it measures the active gravitational mass inside a shell of dust labelled by  $R$ . This is a "comoving" coordinate system.

The only equation we need to integrate in order to obtain a Tolman-Bondi solution in explicit form is eq. (300). Given that  $m = m(R)$  this is straightforward. If  $K = 0$  we have the marginally bound case, and the solution is

$$r_{,\tau} = -\sqrt{\frac{2m(R)}{r}} \quad \Rightarrow \quad r = \left(\frac{9m(R)}{2}\right)^{\frac{1}{3}} (\tau_0(R) - \tau)^{\frac{2}{3}} . \quad (304)$$

If  $K > 0$  the dust cloud is gravitationally bound, and admits the parametric solution

$$r = \frac{m}{K}(1 + \cos \eta) \quad (305)$$

$$\tau = \tau_0(R) + \frac{m}{K^{3/2}}(\eta + \sin \eta) . \quad (306)$$

In both cases the function  $\tau_0(R)$  is determined by the initial conditions.

This is known as the Lemaitre-Tolman-Bondi solution, and is the only explicitly known infinite dimensional class of asymptotically flat solutions of Einstein's equations. (The Vaidya solution is not asymptotically flat since the matter density and the curvature are non-zero at past null infinity.) It contains three free functions,  $m(R)$ ,  $K(R)$ , and  $\tau_0(R)$ . There is however some gauge freedom left in the system, since we can reparametrize  $R \rightarrow R' = R'(R)$  using any monotonic function  $R'$ . If we set  $m = M$ , a constant, we recover the Schwarzschild solution in various gauges.

In general the Tolman-Bondi model describes a spherically symmetric but inhomogeneous cloud of dust collapsing towards the centre (or expanding from the centre). One can think of the dust cloud as consisting of concentric shells of dust labelled by the coordinate  $R$ . If  $r_{,R} = 0$  the shells cross, the density diverges, and a shell crossing singularity arises. The Kretschmann scalar is

$$R_{abcd}R^{abcd} = \frac{12m_{,R}^2}{r^4 r_{,R}^2} - \frac{32mm_{,R}}{r^5 r_{,R}} + \frac{48m^2}{r^6} . \quad (307)$$

Indeed there are curvature singularities whenever  $r_{,R} = 0$ . In a certain sense these are mathematically harmless (since the Einstein equations can still be solved in a distributional sense there), and anyway the matter model cannot be trusted at arbitrarily high densities. Moreover they can be avoided by a judicious choice of initial data. The singularity at  $r = 0$  is a shell focussing singularity. It is unavoidable, and poses a serious question for cosmic censorship.

#### *Friedmann as a special case*

At fixed  $R$ , that is for a round shell of dust, eq. (300) is in fact one of Friedmann's equations, and the dust filled Friedmann models are examples of Tolman-Bondi spacetimes. To make this explicit we set

$$r = Ra(\tau) , \quad K(R) = kR^2 . \quad (308)$$

The choice of  $K$  is just a gauge choice. The metric becomes

$$ds^2 = -d\tau^2 + a^2 \left( \frac{dR^2}{1 - kR^2} + R^2 (d\theta^2 + \sin^2 \theta d\phi^2) \right) . \quad (309)$$

This is a metric of the Friedmann form. Eq. (300) implies that

$$m = \frac{aR^3}{2} (a_{,\tau}^2 + k) . \quad (310)$$

Eq. (303) then gives

$$\frac{8\pi}{3} \rho = \frac{a_{,\tau}^2 + k}{a^2} = \frac{2m}{a^3 R^3} . \quad (311)$$

The dust density is a function of  $\tau$  only, and we follow this up with eq. (302),

$$\frac{8\pi}{3} \rho a^3 = a_m = \text{constant} \quad \Rightarrow \quad m = \frac{a_m}{2} R^3 . \quad (312)$$

Finally we rewrite eq. (310) as

$$a_{,\tau}^2 + k = \frac{a_m}{a} . \quad (313)$$

If  $k = 0$  the contracting solution is

$$a = \left( \frac{9a_m}{4} \right)^{\frac{1}{3}} (\tau_0 - \tau)^{\frac{2}{3}} . \quad (314)$$

If  $k = 1$  we can get the solution in the parametric form

$$\begin{aligned} a(\eta) &= \frac{a_m}{2} (1 + \cos \eta) \\ \tau(\eta) &= \frac{a_m}{2} (\eta + \sin \eta) . \end{aligned} \quad (315)$$

We adjusted an integration constant to ensure that the expansion is maximal at  $\tau = 0$ . In particular  $r(0, R) = a(0)R = a_m R$ , so it is natural to choose the scale by setting  $a_m = 1$ .

It is worth noting that the metric for the  $k = 1$  Friedmann model can be written

$$ds^2 = a^2(\eta) \left( -d\eta^2 + d\chi^2 + \sin^2 \chi (d\theta^2 + \sin^2 \theta d\phi^2) \right) , \quad R = \sin \chi . \quad (316)$$

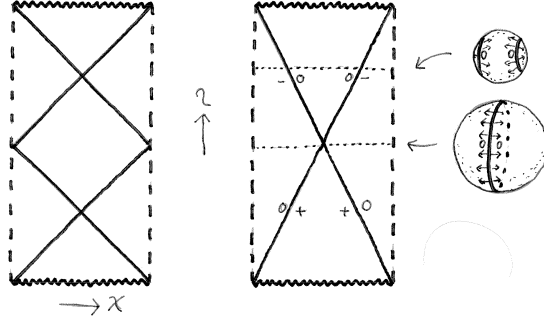


Figure 21: From left to right a Penrose diagram of the  $k = 1$  Friedmann model, another Penrose diagram showing the  $r = 2m$  hypersurface (with respect to an origin at one of the poles), and two spatial slices (one dimension suppressed) showing the marginally trapped spheres at some given moment in  $\eta$ .

Hence this spacetime is conformal to a region of the static Einstein universe, whose spatial geometry—once we have extended the range of  $\chi$  to go from 0 to  $\pi$ —is that of a round 3-sphere. The parameter  $\eta$  has an interpretation as “conformal time”. The Penrose diagram is interestingly different from that of de Sitter space, since a light ray has just time to go once around the 3-sphere during the life of such a universe. It is also of interest to look at the hypersurface

$$r - 2m = aR - a_m R^3 = \frac{a_m R}{2} (\cos \eta + \cos 2\chi) = 0 . \quad (317)$$

This is a timelike hypersurface, given in these coordinates by

$$\eta = \pm(2\chi - \pi) . \quad (318)$$

The round spheres foliating this hypersurface have interesting properties. If a flash of light is emitted orthogonally from a sphere we would expect the outgoing wave front to grow in area, and the ingoing wave front to shrink. However, when we are in the contracting phase ( $\eta > 0$ ) one finds that the Universe is shrinking at such a rate that the wave-fronts going out from the round spheres in this hypersurface keep their area constant. Round spheres of even larger radii are trapped, meaning that both in- and outgoing wave-fronts shrink in area. In the expanding phase we find spheres that are anti-trapped, in the sense that both wave-fronts grow in area. Since the 3-sphere

is a homogeneous space these statements hold for every sphere at constant  $\eta$ , provided its radius is big enough.

*Polishing the gravitationally bound solution*

We now restrict ourselves to gravitationally bound solutions possessing a moment of time symmetry, so we set  $\tau_0(R) = 0$  in the parametric solution (306). Note that

$$\tau_0(R) = 0 \quad \Rightarrow \quad r_{,\tau}(0, R) = 0 . \quad (319)$$

The moment of time symmetry is then at  $\tau = 0$ .

We have restricted the model a little. The next step is not a restriction at all. We are free to choose the radial coordinate—which just labels the dust shells—such that

$$r(0, R) = R \quad \Rightarrow \quad K(R) = \frac{2m(R)}{R} . \quad (320)$$

Then only one free function remains, and the solution takes the form

$$ds^2 = -d\tau^2 + \frac{r_{,R}^2 dR^2}{1 - \frac{2m(R)}{R}} + r^2 d\Omega^2 , \quad (321)$$

where

$$r = \frac{R}{2}(1 + \cos \eta) \quad (322)$$

$$\tau = \sqrt{\frac{R^3}{8m}}(\eta + \sin \eta) , \quad (323)$$

and a calculation using this parametric solution verifies that

$$\begin{aligned} r_{,R} = \left( \frac{\partial r}{\partial R} \right)_{\tau} &= \frac{1}{2}(1 + \cos \eta) + \frac{1}{4} \left( 3 - \frac{Rm'}{m} \right) \frac{\sin \eta (\eta + \sin \eta)}{1 + \cos \eta} = \\ &= \frac{r}{R} + \frac{\tau}{2} \left( \frac{3}{R} - \frac{m'}{m} \right) \sqrt{\frac{2m}{r} - \frac{2m}{R}} . \end{aligned} \quad (324)$$

The metric has a curvature singularity at

$$r = 0 \quad \Rightarrow \quad \eta = \pi \quad \Rightarrow \quad \tau = \pi \sqrt{\frac{R^3}{8m}} . \quad (325)$$

It takes a finite amount of proper time for any dust shell to reach the singularity.

### *A dust cloud of finite extent*

To make our dust cloud look more like a collapsing star we would like it to have a finite extent. This is very easily arranged. We assume that the surface of the star is at  $R = R_0$ , and that the mass function is

$$m(R) = \begin{cases} m(R) & R < R_0 \\ M & R > R_0 . \end{cases} \quad (326)$$

We would like to argue that an arbitrary mass function is allowed in the interior. The surface of the cloud is a timelike hypersurface with the intrinsic metric

$$dq^2 = -d\tau^2 + r^2 d\Omega . \quad (327)$$

This can be calculated in two ways: by taking the limit from the inside, and by taking the limit from the outside. We insist that these two procedures agree. Therefore  $\tau$  must be continuous across the surface, and this is ensured by the very reasonable condition

$$m(R_0) = M . \quad (328)$$

We seem to have a problem left, because the spacetime metric will not have continuous first derivatives across the surface of the cloud. However, the rules for matching solutions of Einstein's equations together across hypersurfaces tell us that it is enough if the intrinsic metric and extrinsic curvature of the hypersurface are continuous. Because our coordinate system is perfectly adapted to describe the surface of the cloud the second condition reduces to the requirement that

$$K_{ij} = \frac{1}{2} n^R q_{ij,R} \quad (329)$$

be continuous, where

$$n_a = \frac{r_{,R}}{\sqrt{1 - \frac{2m}{R}}} \nabla_a R \quad (330)$$

is the unit normal vector of the hypersurface. It is easily checked that this holds—if only because the discontinuous function  $r_{,R}$  cancels out when we compare the two limits.

### *Oppenheimer-Snyder collapse*

The Oppenheimer-Snyder solution is the special case when the collapsing dust cloud is described by a  $k = 1$  Friedmann model and a Schwarzschild exterior. Historically it was very important in fixing ideas about gravitational collapse. The first observation to make about it is that the proper time needed for a dust shell to reach the singularity at  $r = 0$  is, according to eq. (325) and eq. (312) for the Friedmann mass function with the scale set by  $a_m = 1$ ,

$$\tau = \pi \sqrt{\frac{R^3}{8m}} = \frac{\pi}{2} . \quad (331)$$

The dust shells reach the singularity in unison. This is not unexpected, and we can use Newtonian intuition to see why. The outer shells have a longer way to go, but are subject to larger acceleration than the inner shells. In a homogeneous cloud the mass  $m$  inside radius  $r$  obeys  $m \propto r^3$ , and due to spherical symmetry the force per unit mass obeys  $F \propto m/r^2 \propto r$ . Hence the equation of motion is  $\ddot{r} \propto r$ , and the result follows because the period of a harmonic oscillator is independent of its amplitude.

We know that the hypersurface at  $t = 0$  in Schwarzschild looks like a paraboloid with a neck at the event horizon, and this is to be matched to a dust-filled spherical cap. From this it is evident that the matching must be done in such a way that the paraboloid is joined to less than a hemisphere if the matching surface lies in the exterior of the Schwarzschild solution, that

is at some  $\chi = \chi_0 < \pi/2$ . If the matching is made inside the black hole, to a timelike hypersurface in the other asymptotic region, it must be made at some  $\chi_0 > \pi/2$ . The latter configuration is sometimes called a Bag of Gold, but we choose the former here.

### *Cosmic censorship revisited*

I did not finish the Oppenheimer-Snyder solution. The next and final point to be made would be to point out that the inhomogeneous models work rather differently—and that they have received very satisfactory treatments in the literature.<sup>22</sup>

---

<sup>22</sup>D. M. Eardley and L. Smarr, *Time functions in numerical relativity: Marginally bound dust collapse*, Phys. Rev. **D19** (1979) 2239; D. Christodoulou, *Violation of cosmic censorship in the gravitational collapse of a dust cloud*, Commun. Math. Phys. **93** (1984) 171.



## THE GÖDEL UNIVERSE

### *Einstein and Gödel*

A universe filled with galaxies is described by a solution of Einstein's equations with a stress-energy tensor for dust. In the Einstein universe, the gravitational attraction of the dust is balanced by a repulsive force stemming from a positive cosmological constant. The result is a static universe. The Gödel universe is in some sense the counterpart of the Einstein universe, but with a negative cosmological constant. To ensure that the universe remains stationary the attractive forces are balanced by a global rotation. The Einstein and Gödel universes are in fact the only perfect fluid solutions of Einstein's equations in which the mass density is non-zero, the fluid four velocity is geodetic with zero expansion and shear, and the manifold is simply connected. The main point that Gödel wanted to make is that the latter solution proves that relativity theory admits spacetimes without any notion of absolute time lapsing objectively, lending support to Parmenides, Kant, and other philosophers who consider change as an illusion or an appearance due to our special mode of perception.<sup>23</sup>

### *The solution*

The Gödel universe has topology  $\mathbf{R}^4$ , and can be covered by a single coordinate system. The metric is

$$ds^2 = 4a^2 \left[ -2 \left( dt + \frac{r^2 d\phi}{1-r^2} \right)^2 + \frac{1}{(1-r^2)^2} (dr^2 + r^2 d\phi^2) + dx_3^2 \right] , \quad (332)$$

where

$$0 < r < 1 , \quad 0 \leq \phi < 2\pi , \quad -\infty < t, x_3 < \infty . \quad (333)$$

---

<sup>23</sup>K. Gödel, *A remark about the relationship between relativity theory and idealistic philosophy*, in P. A. Schilpp: *Albert Einstein: Philosopher-Scientist*, Open Court, Lassalle, Illinois, 1949.

The direction coordinatised by  $x_3$  is evidently somewhat trivial and will be ignored henceforth. Hence we will in effect be studying a  $2 + 1$  dimensional spacetime.

There is a timelike Killing vector field  $\partial_t^a$ . The set of its orbits—in physical terms, the set of galactic world-lines—forms a hyperbolic plane which in these coordinates is described as a Poincaré disk. As we will see the isometry group is  $SO(1, 2) \times \mathbf{R} \times \mathbf{R}$ . Any pair of points can be related by an isometry, which means that this is a homogeneous spacetime which looks the same from every point. Once the  $dx_3^2$ -term is deleted, and if we change the coefficient in front of the first term from 2 to 1, the metric describes three dimensional anti-de Sitter space in a coordinate system adapted to an everywhere non-vanishing timelike Killing vector field with a “helical” structure. Hence the Gödel spacetime can be obtained by stretching anti-de Sitter space along this Killing vector field, but we will not pursue this aspect here.

The Gödel metric solves Einstein’s equations including a negative cosmological constant and matter in the form of dust. To be precise about it

$$8\pi\rho = \frac{1}{a^2} \ , \qquad \lambda = -\frac{1}{2a^2} \ , \qquad (334)$$

where  $\rho$  is the dust density and the fluid velocity is directed along the  $t$  coordinate lines. It is therefore natural to “view” this spacetime from the “galaxy” situated on the  $t$ -axis. The geodesic congruence described by the vector field  $\xi = \partial_t$  is rotating. Indeed

$$\omega_{ab} \equiv \nabla_{[a}\xi_{b]} \quad \Rightarrow \quad \omega_{r\phi} = -8a^2 \frac{r}{(1-r^2)^2} \ , \qquad (335)$$

with the remaining components vanishing. Hence

$$\omega \equiv \frac{1}{2}\omega_{ab}\omega^{ab} = \frac{1}{a^2} \ . \qquad (336)$$

It is this vorticity that opens up the possibility of closed timelike curves in this spacetime. More immediately it means that the fluid flow is not hypersurface orthogonal. It is still true that setting  $t$  to a constant describes a hypersurface, but it has unexpected properties. To see this, write out the metric as

$$ds^2 = -2dt^2 + \frac{4r^2}{1-r^2}dtd\phi + \frac{dr^2}{(1-r^2)^2} + \frac{r^2(1-2r^2)}{(1-r^2)^2}d\phi^2 + dx_3^2 . \quad (337)$$

Now set  $t$  to a constant. When  $r \geq 1/\sqrt{2}$  this hypersurface fails to be spacelike. This shows that the local notion of time relevant to individual galaxies cannot serve as a cosmic time.

### *Isometries and geodesics*

From now on we will set the scale using  $4a^2 = 1$ . We also set  $x_3$  to a constant. To understand a spacetime we must understand its symmetries, if any, and its geodesics. To begin with we want to exhibit the isometry group in finite form. For transformations along the  $t$ -axis this is clear. For the  $SO(2,1)$  group, introduce the complex coordinate

$$z = x + iy = re^{i\phi} . \quad (338)$$

The three dimensional metric then takes the form

$$ds^2 = -2 \left( dt + \frac{i}{2} \frac{zd\bar{z} - \bar{z}dz}{1-r^2} \right)^2 + \frac{dzd\bar{z}}{(1-r^2)^2} . \quad (339)$$

Both terms in the metric are left invariant by

$$z \rightarrow z' = \frac{\alpha z + \beta}{\bar{\beta}z + \bar{\alpha}} , \quad |\alpha|^2 - |\beta|^2 = 1 \quad (340)$$

$$t \rightarrow t' = t + \frac{i}{2} \ln \frac{\bar{\alpha} + \bar{\beta}z}{\alpha + \beta\bar{z}} . \quad (341)$$

When projected down to the Poincaré disk this is a Möbius transformation, taking circles to circles (or straight lines). Note the accompanying time shift.

The geodesic equations can be integrated. Using the conserved quantities associated to the Killing vector fields  $\partial_t^a$  and  $\partial_\phi^a$  we obtain

$$\dot{t} + \frac{r^2 \dot{\phi}}{1-r^2} = k_1 \quad (342)$$

$$\frac{r^2}{1-r^2} \left[ 2 \left( \dot{t} + \frac{r^2 \dot{\phi}}{1-r^2} \right) - \frac{\dot{\phi}}{1-r^2} \right] = k_2 . \quad (343)$$

Since spacetime is homogeneous it is enough to solve for geodesics through the origin, so we set  $k_2 = 0$  without loss of generality. We also know that

$$\frac{1}{(1-r^2)^2} \left[ 2 \left( (1-r^2)\dot{t} + r^2\dot{\phi} \right)^2 - \dot{r}^2 - r^2\dot{\phi}^2 \right] = \epsilon , \quad (344)$$

where  $\epsilon = 1$  for timelike, 0 for null, and  $-1$  for spacelike geodesics.

From the symmetries present we suspect that geodesics will appear as circles when projected down to the Poincaré disk.<sup>24</sup> We can see that

$$\dot{r}^2 = (1-r^2)^2 \left[ 2k_1^2(1-2r^2) - \epsilon \right] . \quad (345)$$

Hence null geodesics starting from the origin are circles extending out to  $r = 1/\sqrt{2}$ , timelike geodesics project to smaller circles, and spatial geodesics to larger circles.

For null geodesics starting from the origin we obtain

$$\frac{dt}{d\phi} = \frac{1-2r^2}{2(1-r^2)} . \quad (346)$$

There is a caustic at the critical radius  $r = 1/\sqrt{2}$ , where null geodesics are stationary in  $t$ . Explicit integration gives

$$r = \frac{1}{\sqrt{2}} \sin(\phi - \phi_0) \quad \Leftrightarrow \quad \sqrt{x^2 + y^2} = \frac{y}{\sqrt{2}\sqrt{x^2 + y^2}} \quad (347)$$

$$t = \phi - \frac{1}{\sqrt{2}} \arctan \frac{\tan(\phi - \phi_0)}{\sqrt{2}} + \text{constant} . \quad (348)$$

Indeed, when projected down to the Poincaré disk, null geodesics are circles of radius  $1/2\sqrt{2}$ , and their envelope is a circle with radius  $1/\sqrt{2}$ . Thus each galaxy is surrounded by a particle horizon beyond which null geodesics do not reach. The light cone of the origin has a caustic on the particle horizon, forming a circle at

---

<sup>24</sup>For explicit integration (using half plane coordinates) see W. Kundt, *Trägheitsbahnen in einem von Gödel angegebenen kosmologischen Modell*, Z. Phys. **145** 611 (1956), and J. Pfarr, *Time travel in Gödel's space*, Gen. Rel. Grav. **13** 1073 (1981).

$$r = \frac{1}{\sqrt{2}} , \quad t = \frac{\pi}{2} \left( 1 - \frac{1}{\sqrt{2}} \right) . \quad (349)$$

At the caustic

$$\frac{dt}{d\phi} = 0 . \quad (350)$$

After encountering the caustic the light cone reconverges to a single point on the  $t$ -axis. Such reconvergence signals a singularity, unless there is a breakdown of the causal structure. Indeed there will be trapped surfaces occurring as cross-sections of the reconverging light cone.

### *Gödel circles*

There are no closed timelike geodesics in this spacetime. But there are closed Killing flow lines, corresponding to the Killing field

$$\xi = \xi^a \partial_a = \partial_\phi . \quad (351)$$

They are called Gödel circles, and their tangent vectors have length squared equal to

$$||\partial_\phi||^2 = \frac{r^2(1 - 2r^2)}{(1 - r^2)^2} . \quad (352)$$

Beyond the “critical radius” at  $r = 1/\sqrt{2}$  the Gödel circles are timelike. Since they are also closed they are closed timelike curves, abbreviated CTCs.

Introduce a tangent vector of unit length along the Gödel circles, namely

$$u^a = \frac{1 - r^2}{r\sqrt{|2r^2 - 1|}} \xi^a . \quad (353)$$

Using the Killing vector property  $\nabla_b \xi_a = \nabla_a \xi_b$ , it is easy to verify that the acceleration vector is

$$a_a \equiv u^b \nabla_b u_a = \frac{1 - 3r^2}{r(1 - r^2)|2r^2 - 1|} \nabla_a r . \quad (354)$$

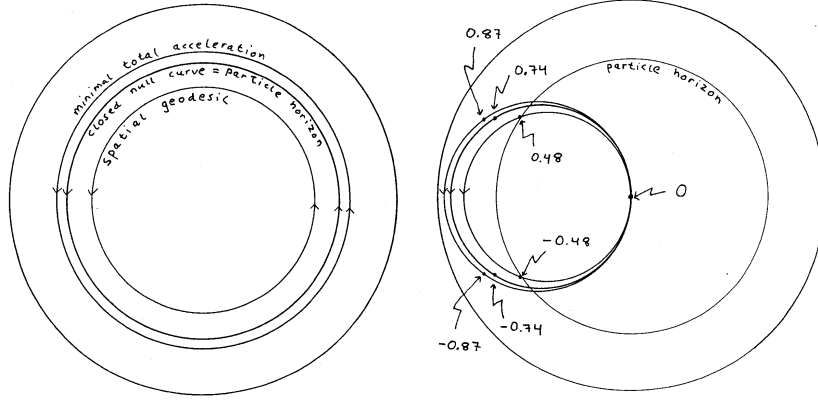


Figure 22: Gödel circles in the Poincaré disk formed by the galactic world-lines. The circles are shown first at  $t = 0$ , and then going through the origin. The time shift in eq. (341) is relevant here; the numbers are the minimal and maximal values of  $\tau = \sqrt{2}t$ .

Written in this way this equation is valid for both the timelike and the spacelike cases. The acceleration is then given by

$$a = \sqrt{|a^2|} = \frac{|3r^2 - 1|}{r|2r^2 - 1|} . \quad (355)$$

Two values of  $r$  stand out, namely  $r = 1/\sqrt{3}$  for which the Gödel circle is a spacelike geodesic, and  $r = 1/\sqrt{2}$  for which it is a closed null curve. The CNC is precisely the caustic discussed above; all the CTCs must pass behind the particle horizon.

### *Time travel*

To any curve  $\gamma$  we can associate a dimensionless number TA, its total acceleration, defined by

$$\text{TA}(\gamma) \equiv \int_{\gamma} a ds . \quad (356)$$

If the curve is timelike this quantity has a physical interpretation in terms of the mass ratio for an ideal rocket following the curve. To see this, define

the vector

$$J^a = -\dot{x}^b \nabla_b (m \dot{x}^a) , \quad m = m(\tau) > 0 . \quad (357)$$

It represents the energy-momentum of the rocket exhaust, and must therefore be future directed timelike or null. Then

$$||J||^2 = m^2 a^2 - (\dot{x}^a \nabla_a m)^2 \leq 0 . \quad (358)$$

This translates to

$$a \leq -\frac{\dot{m}}{m} \quad \Rightarrow \quad \int_1^2 a ds \leq -\int_1^2 \frac{\dot{m}}{m} = \ln m_1/m_2 . \quad (359)$$

Hence

$$m > 0 \quad \Rightarrow \quad \frac{m_2}{m_1} \leq e^{-\text{TA}} . \quad (360)$$

If  $m(\tau)$  is the time dependent mass of the rocket, this is indeed a bound on its performance.

For the Gödel circles the total acceleration is

$$\text{TA} = \int_0^{2\pi} a \left| \frac{ds}{d\phi} \right| d\phi = 2\pi \frac{|3r^2 - 1|}{(1 - r^2)\sqrt{|2r^2 - 1|}} . \quad (361)$$

It is seen that TA diverges when  $r \rightarrow \infty$  and also when  $r \rightarrow 1/\sqrt{2}$  which is when the Gödel circle becomes null. A calculation shows that TA has a minimum when

$$r = \frac{1}{\sqrt{\sqrt{3}}} . \quad (362)$$

Its value at the minimum is

$$\text{TA}_{\min} = 2\pi\sqrt{9 + 6\sqrt{3}} \approx 27.669 . \quad (363)$$

Malament has argued—but not proved—that this is the minimal total acceleration achieved by any smooth CTC in the Gödel universe.<sup>25</sup> Note the

---

<sup>25</sup>D. Malament, *Time travel in the Gödel universe*, in P. D. Asquith and P. Kitcher (eds.): Proc. of the PSA **2**, Chicago 1985.

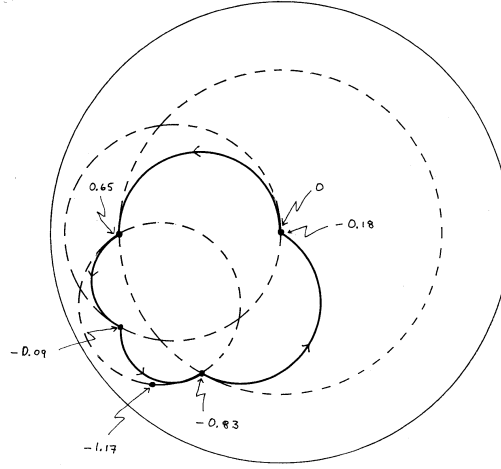


Figure 23: Sending a signal back in time, using null geodesics and three relay stations. Particle horizons are shown dashed. The numbers are values of  $\tau = \sqrt{2}t$ .

analogy to the problem of minimizing the total curvature of a plane curve—the solution to this problem is a circle of arbitrary radius.

Assuming Malament’s conjecture to be correct the optimal mass ratio for a rocket that takes us back in time is bounded by

$$\frac{m_2}{m_1} \leq 10^{-12} . \quad (364)$$

Such a rocket would hardly start out as a test particle, and time travel would not be realistic even if the Gödel solution was. Gödel himself felt that precisely this practical limit on the feasibility of time travel means that such a space-time structure of the real world cannot be excluded *a priori*, while Einstein expressed some doubts on this point.

Still, if a Gödel universe is filled with helpful beings one might consider sending signals to one’s past, using null geodesics that are resent in different directions by the beings. It is clear that at least three foreign civilisations must be involved: the first one resends the signal so that it passes beyond the particle horizon, and the last one sends it back to us. Closer examination shows that only one further civilisation needs to be involved, so between the four of us we could do some interesting things.



### *Space-time pictures*

It is instructive to see what happens with the light cones as we move out from the origin. In the picture that results from our choice of coordinates they are tipping over at the same time as they expand in the positive  $\phi$ -direction. More precisely one finds for the light cones that

$$dr = 0 \quad \Rightarrow \quad \frac{\sqrt{2}dt}{rd\phi} = \frac{\pm 1 + \sqrt{2}r}{1 - r^2} \quad (365)$$

$$d\phi = 0 \quad \Rightarrow \quad \frac{\sqrt{2}dt}{dr} = \frac{\pm 1}{1 - r^2} . \quad (366)$$

When  $r \rightarrow 1$  the light cones degenerate to two dimensional half spaces—this spacetime does not admit any conformal compactification. Interestingly the picture drawn in Hawking and Ellis is not quite right. The tilting null cones in the picture should be widened a bit so that they include the timelike world-lines of the galaxies—as was pointed out only much later.<sup>26</sup> Still, it is a beautiful picture.

### Exercises:

- Introduce the differential forms

$$\begin{aligned} d\omega^0 &= dt - \frac{r^2 d\phi}{1 - r^2} , & \omega^1 &= \frac{1}{1 - r^2} (\cos \tau dr - r \sin \tau d\phi) , \\ \omega^2 &= \frac{1}{1 - r^2} (\sin \tau dr + r \cos \tau d\phi) , & \tau &= 2t + \phi . \end{aligned} \quad (367)$$

Write the Gödel metric in terms of them. Check that  $d\omega^0 = -2\omega^1 \wedge \omega^2$ ,  $d\omega^1 = 2\omega^2 \wedge \omega^0$ ,  $d\omega^2 = 2\omega^0 \wedge \omega^1$ . Adapt the notation to fit Wald's eqs. (3.4.26-28), and compute the Riemann and Einstein tensors. Why is it so easy?

---

<sup>26</sup>I. Ostváth and E. Schücking, *Gödel's trip*, Am. J. Phys. **71** (2003) 801.